2010

Optimum Design of Cable-Stayed Bridges

Mahmoud M. Hassan
Western University, eng_mahmoud_hassan@hotmail.com

OPTIMUM DESIGN OF CABLE-STAYED BRIDGES

(Spine title: Optimum Design of Cable-Stayed Bridges)

(Thesis Format: Integrated-Article)

By

Mahmoud Mohamed Hassan

Graduate Program in Engineering Science
Department of Civil and Environmental Engineering

A thesis submitted in partial fulfillment
of the requirements for the degree of
Doctor of Philosophy

School of Graduate and Postdoctoral Studies
The University of Western Ontario
London, Ontario, Canada
July, 2010

Your file Votre référence
ISBN: 978-0-494-73364-6
Our file Notre référence
ISBN: 978-0-494-73364-6

The University of Western Ontario

School of Graduate and Postdoctoral Studies

CERTIFICATE OF EXAMINATION

Supervisors	Examiners
Dr. El Damatty A.A.	Dr. Rashwan, Shokry
	Dr. Hong, Hanping
Supervisory Committee	
	Dr. Asokanthan, Samuel
	Dr. Sennah, Khaled

The thesis by

Mahmoud Mohamed Ibrahim Hassan

entitled:

Optimum Design of Cable-Stayed Bridges

is accepted in partial fulfillment of the
for the requirements of the degree of
Doctor of Philosophy

Date_____

_____
Chair of the Thesis Examination Board

ABSTRACT

Owing to their excellent structural characteristics, aesthetic appearance, low maintenance cost, and efficient use of structural materials, cable-stayed bridges have gained much popularity in recent decades. Stay cables of a cable stayed bridge are post-tensioned to counteract the effect of the bridge dead load. The solution for an optimum distribution of post-tensioning cable forces is considered one of the most important and difficult tasks in the design of cable-stayed bridges. A novel approach that utilizes the finite element method, B-spline curves, and real coded genetic algorithm to determine the global optimum post-tensioning cable forces is developed. The effect of geometric nonlinearity on the determination of the post-tensioning cable forces is assessed. The study is further extended to develop the first surrogate polynomial functions that can be used to evaluate the post-tensioning cable forces in semi-fan cable stayed bridges. The developed post-tensioning functions are then used to investigate the optimal geometric configurations, which lead to the most uniform distribution of the post-tensioning cable forces. Details of an optimization code developed in-house specifically to optimize the design of composite cable-stayed bridges with semi-fan cable arrangement are then reported. The optimization design code integrates a finite element model, the real coded genetic algorithm, the post-tensioning polynomial functions, and the design provisions provided by the Canadian Highway Bridge Design Code. An extensive parametric study is then conducted using this optimization code to develop a database for the optimum design of semi-fan cable-stayed bridges. The database covers bridge lengths ranging from *250 m* to *700 m*. It describes the variations of the optimum design parameters, such as the main span length,

height of the pylon, number of stay cables, and cross-sectional dimensions with the total length of the bridge.

KEYWORDS: Cable-Stayed Bridge, Semi-Fan Cable-Stayed Bridge, Finite Element, Real Coded Genetic Algorithms, Genetic Algorithms, B-spline Function, Post-Tensioning Cable Forces, Optimization, Optimum Design, Preliminary Design, Cost minimization, Design Constraints.

CO-AUTHORSHIP

This thesis has been prepared in accordance with the regulation for an Integrated-Article format thesis stipulated by the School of Graduate and Postdoctoral Studies at the University of Western Ontario and has been co-authored as:

Chapter 2: Determination of Optimum Post-Tensioning Cable Forces of Cable-Stayed Bridges

The numerical modelling work was conducted by M. M. Hassan under close supervision of Dr. A. A. El Damatty and Dr. A. O. Nassef. Drafts of Chapter 2 were written by M. M. Hassan and modifications were done under close supervision of Dr. A. A. El Damatty and Dr. A. O. Nassef. A paper co-authored by M. M. Hassan, Dr. A. O. Nassef, and Dr. A. A. El Damatty was submitted to the *Journal of Engineering Structures.*

Chapter 3: Surrogate Function of Post-Tensioning Cable Forces for Semi-Fan Cable-stayed Bridges

All the analytical work was conducted by M. M. Hassan under close supervision of Dr. A. A. El Damatty and Dr. A. O. Nassef. Drafts of Chapter 3 were written by M. M. Hassan and modifications were done under close supervision of Dr. A. A. El Damatty and Dr. A. O. Nassef. A version of this work co-authored by M. M. Hassan, Dr. A. O. Nassef, and Dr. A. A. El Damatty will be submitted to the *Journal of Engineering Structures, ASCE.*

Chapter 4: Optimal Design of Semi-Fan Cable-Stayed Bridges

All the analytical work was conducted by M. M. Hassan under close supervision of Dr. A. A. El Damatty and Dr. A. O. Nassef. Drafts of Chapter 4 were written by M. M. Hassan and modifications were done under close supervision of Dr. A. A. El Damatty and Dr. A. O. Nassef. A version of this work co-authored by M. M. Hassan, Dr. A. A. El Damatty, and Dr. A. O. Nassef will be submitted to the *Journal of Computers and Structures*.

Chapter 5: Database for the Optimum Design of Semi-Fan Cable-Stayed Bridges

All the analytical work was conducted by M. M. Hassan under close supervision of Dr. A. A. El Damatty and Dr. A. O. Nassef. Drafts of Chapter 5 were written by M. M. Hassan and modifications were done under close supervision of Dr. A. A. El Damatty and Dr. A. O. Nassef. A version of this work co-authored by M. M. Hassan, Dr. A. A. El Damatty, and Dr. A. O. Nassef will be submitted to the *Journal of Engineering Structures, ASCE.*

DEDICATION

To my late father

To **my beloved mother**

To my beloved wonderful wife, **Sherin**

To my beloved kids, **Menna**, **Hana**, and **Ahmed.**

For patiently enduring and sharing these years of hard work

ACKNOWLEDGEMENT

I would like to express my appreciation and sincere gratitude to my research supervisors, Dr. El Damatty, A. A. and Dr. Nassef, A. O. Their interest, valuable guidance and encouragement throughout the course of this thesis are gratefully acknowledged. Dr. El Damatty's engineering experience, foresight, support, input, encouraging words and energy have always been appreciated. Dr. Nassef's optimization experience, comments and suggestions are truly appreciated.

I am obliged to the Egyptian Ministry of Higher Education and Scientific Research, Egypt, for the financial and in-kind support provided to this research work. Also, I deeply appreciate the SHARCNET supercomputer facility and staff at the University of Western Ontario, Canada.

Above all, I wish to express my sincere gratitude to my family, especially, mother, sisters and brother for their understanding, encouragement, continuous prayers and guidance throughout this study. Also, I am indebted to my family-in-law for their continuous support and encouragement.

I would like to dedicate this thesis to my sincere wonderful patient wife, Sherin, dear daughters Menna and Hana, and dear son Ahmed, for their love, encouragement, great scarifies, and fruitful care during the period of this study.

TABLE OF CONTENTS

LIST OF TABLES

LIST OF FIGURES

LIST OF APPENDICES

LIST OF SYMBOLS

Symbol	Units	Description
A	m^2	Area of the cross-section of a member
A_d	m^2	Area of the deck
A_s	m^2	The area of the steel reinforcement
B	m	Width of the deck
B_{FB}	m	Width of the bottom flange
B_{FT}	m	Width of the top flange
B_p	m	Width of the pylon
C_{cable}	\$/ton	Unit price of steel cables
$C_{concrete}$	$\$/m^3$	Unit price of concrete
C_D	-	Drag shape coefficient
C_M	-	Torsional shape coefficient
C_N	-	Lift shape coefficient
C_{fDeck}	kN	Factored compressive force in the deck.
C_{rDeck}	kN	Factored compressive resistance of the deck
C_{steel}	\$/ton	Unit price of structural steel
D	m	Diameter of stay cables
d	m	Width of the pylon
E	MPa	Elastic modulus of the material
E_c	MPa	Modulus of elasticity of concrete
E_{ds}	MPa	Modulus of elasticity of the deck
E_{eq}	kN/m^2	Equivalent modulus of elasticity of stay cables
E_s	MPa	Elastic modulus of structural steel
E_{sc}	kN/m^2	Modulus of elasticity of stay cables
$F(\mathbf{x})$	--	Objective function
F_{FB}	-	Factor defining the thickness of the bottom flange
F_{FT}	-	Factor defining the thickness of the upper flange
F_{fPylon}	kN	Factored axial force in the pylon

F_{fw}	kN	Factored compressive force in the web component at ultimate limit state
$F_{(M_f, N_f)Deck}$	-	Distance to the (M_{fDeck}, C_{fDeck})
$F_{(M_r, N_r)Deck}$	-	Distance to the interaction diagram
$F_{(M_f, N_f)Pylon}$	-	Distance to the (M_{fPylon}, P_{fPylon})
$F_{(M_r, N_r)Pylon}$	-	Distance to the interaction diagram
F_{rPylon}	kN	Critical buckling load of the pylon
f_y	MPa	Yield strength of reinforcement steel
F_y	MPa	Yield strength of structural steel
F_{W1}	kN	Factor defining the thickness of the web
F_{yw}	kN	Axial compressive force at yield stress
g	-	Design constraint
H	m	Total height of the pylons' tops above the bridge deck
h	m	Wind exposure depth
h_B	m	Height of the upper strut cross beam above the bridge deck
H_G	m	Height of main girder
h_T	m	Distance is equal to number of stay cables times 2.0 m
H_P	m	Depth of the pylon
I_{dv}	m^4	Vertical moment of inertia of the deck
I_{dh}	m^4	Transverse moment of inertia of the deck
$[k_T]_b$	kN/m	Tangent stiffness matrix of a frame element
$[k_E]_b$	kN/m	Elastic stiffness matrix of a *3-D* frame element
$[k_G]_b$	kN/m	Geometric stiffness matrix of a *3-D* frame element
L	m	Total length
M	m	Main span length
M_{fDeck}	kN.m	Factored bending moment in the deck.
m_F	-	Modification factor used when more than one design lane is loaded
M_{fPylon}	kN.m	Factored bending moment in the pylon

M_{rDeck}	kN.m	Factored moment resistance of the composite section
M_{rPylon}	kN.m	Factored moment resistance of the pylon
N	-	Number of stay cables in each single plane
n_{Lane}	-	Number of lanes
p	-	Degree of the basic function
P_{fPylon}	kN	Factored compressive force in the pylon
P_{rPylon}	kN	Factored compressive resistance of the pylon
S	m	Side span length
T	kN	Tension in stay cable
T_{cCable}	kN/m^2	Ultimate tensile strength of stay cables
t_{FB}	m	Thickness of the bottom flange
T_{fCable}	kN	Factored tensile force in the stay cable
T_{fDeck}	kN	Factored tensile force in the deck
t_{FT}	m	Thickness of the top flange
T_{max}	kN	Maximum cables tensile force
t_p	m	Thickness of the pylon
T_{rDeck}	kN	Factored tensile resistance of the deck
t_s	m	Thickness of concrete deck slab
t_w	m	Thickness of girder web.
T_{uCable}	kN	Minimum tensile resistance of stay cables
V_{fDeck}	kN	Factored shear force
V_{rDeck}	kN	Factored shear resistance of the web steel main girder
V_{cables}	m^3	Volume of stay cables
V_{steel}	m^3	Volume structural steel
V_c	m^3	Volume of concrete
w_{cs}	kN/m	Weight per unit length of the cable
W	kN	Wind load
$\gamma_{Asphalt}$	kN/m^3	Unit weight of asphalt
γ_c	kN/m^3	Unit weight of concrete
γ_{scable}	kN/m^3	Unit weight of concrete stay cables

γ_{steel}	kN/m^3	Unit weight of structural steel
γ_1	-	Ratio of main span length to total length of bridge = (M/L)
γ_2	-	Ratio of height of upper strut cross beam to bridge length (h_B/L).
γ_3	-	Ratio of width of top flange to height of main girder (B_{FT}/ H_G)
γ_4	-	Ratio of width of bottom flange to height of main girder (B_{FB}/ H_G)
γ_5	-	Ratio of the bridge length to (1000m) = (L/1000)
δ	m	Vertical deflection of the deck
δ_{max}	m	Maximum deflection of the bridge deck
v_s	-	Steel Poisson's ratio
v_c	-	Concrete Poisson's ratio
ε	-	Convergence tolerance

CHAPTER 1

INTRODUCTION

1.1 General

Although the concept of a bridge partially suspended by inclined stays dates back to the seventeenth century, the concept and practical applications of cable-stayed bridges started to attract the attention of structural engineers after the construction of the first modern cable-stayed bridge, the Swedish Strömsund Bridge in 1955, (Podolny and Scalzi, 1986). Cable-stayed bridges are elegant, economical and efficient structures, consisting of three major components: the deck, the pylons, and the stay cables, which stretch down diagonally from the pylons to support the deck, as shown in Fig. 1.1 (Gimsing, 1997). Such structures provide a solution for the range of medium to long-span bridges, and offer varieties to designers regarding not only the choice of construction materials, but also the geometric arrangements. Compared with suspension bridges, cable-stayed bridges are stiffer and require less material, especially for stay cables and abutments. The recent advances in the design and construction methods and the availability of high strength steel cables are opening a new era for cable-stayed bridges with main span lengths exceeding a value of *1000 m.*

1.2 Arrangement of Stay Cables

Harp, fan, and semi-fan arrangements are the most common forms of stay cables arrangements, shown in Fig. 1.1 (Troitsky, 1988). The harp layout appears to be less suitable for large span bridges, as it needs a taller pylon and produces large forces in the

stay cables. In the fan pattern, increasing the number of the stay cables increases the weights of the anchorages and makes them difficult to accommodate. Therefore, the fan patterns are suitable only for moderate spans with a limited number of stay cables. A semi-fan pattern is considered to be the best choice, as it provides an intermediate solution between the harp and fan patterns. The semi-fan pattern combines the advantages and avoids the disadvantages of both patterns. The semi-fan pattern has been chosen for a large number of modern cable-stayed bridges, e.g. the world's longest cable stayed bridge main span, the Sutong Bridge in China (main span 1088 m), shown in Fig. 1.2.

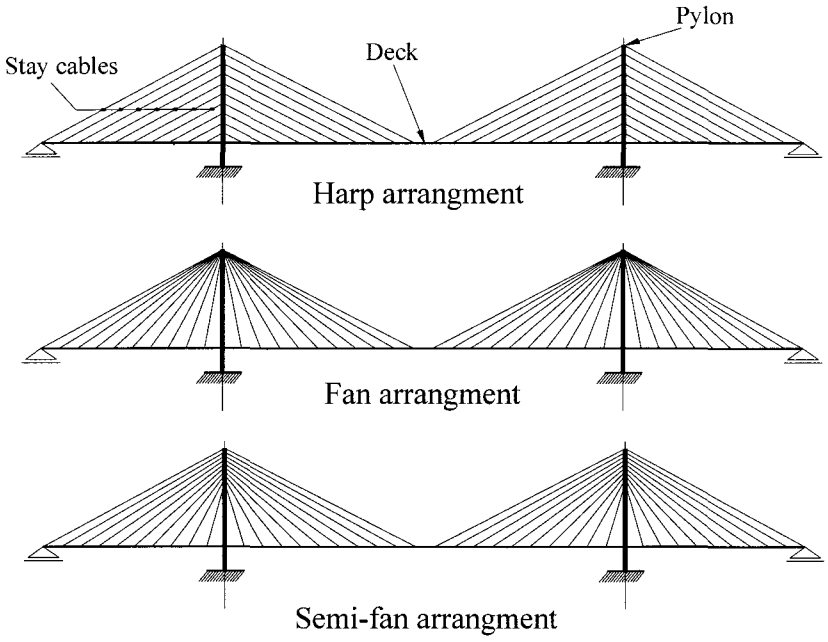

Fig. 1.1 Cable arrangements in cable-stayed bridges

Fig. 1.2 Sutong Cable-Stayed Bridge (http://www.panoramio.com/photo/9112135).

1.3 Deck Cross-Section

One of the popular systems used in the design and construction of cable-stayed bridges is the composite steel-concrete deck. In this system, the deck consists of two structural steel edge girders connected by transverse steel floor beams and supporting a precast reinforced concrete slab, as shown in Fig. 1.3. The advantages of such composite decks are as follows:

1. The concrete roadway slab is cheaper than the steel orthotropic deck.
2. The precast slab minimizes the redistribution of the compression forces onto the steel girders resulting from shrinkage and creep.
3. High resistance against rotation can be achieved by anchoring the stay cables to the outside steel main girders.

4. The construction of the relatively light steel girders can be done easily before adding the heavy concrete slab.
5. The dead weight of the composite deck is far below that of a concrete deck.

As a result, the composite deck was used in a large number of cable-stayed bridges, such as the Quincy Bayview Bridge, Annacis Island Bridge, and Qingzhou Bridge, located in USA, Canada, and China, respectively, (Troitsky, 1988) and (Ren and Peng, 2005).

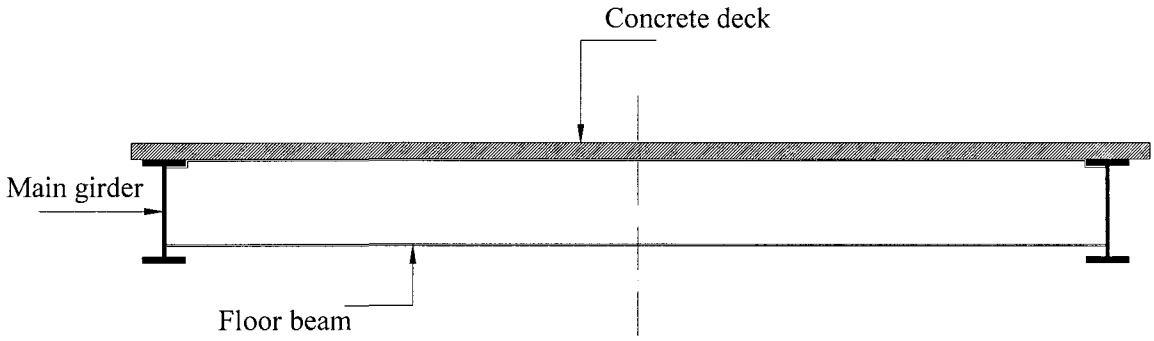

Fig. 1.3 Composite deck.

1.4 Post-Tensioning Cable Forces

In cable-stayed bridges, inclined stay cables are post-tensioned in order to counteract the effect of the deck dead load. The post-tensioning cable forces are applied to minimize both the vertical deflection of the deck and the lateral deflection of the pylons along the longitudinal direction of the bridge. Under the combined effect of dead and post-tensioning cable forces, the bending moment along the deck becomes equivalent to that of a beam resting on a series of continuous rigid supports located at the cable-deck connections and the pylons behave as pure axial members. The post-tensioning cable forces control the distribution of internal forces and affect the overall design of the bridge. As a result, the selected set of post-tensioning cable forces represents a design

parameter that can be tailored to achieve an effective design for the bridge. Determining the optimum distribution of post-tensioning cable forces is considered one of the most difficult tasks in the design of cable-stayed bridges. The new trend towards very long-span cable-stayed bridges requires using a large number of stay cables. This significantly increases the bridge redundancy, and complicates the determination of the optimum post-tensioning cable forces (Lee *et al.,* 2008). Mathematically, the problem of evaluation of the optimum post-tensioning cable forces might not have a unique solution (Sung *et al.,* 2006).

Four methods were developed in the literature to determine the post-tensioning cable forces in cable-stayed bridges. These methods are based on either minimizing the vertical deflections of the bridge deck to a convergence tolerance value or obtaining a bending moment diagram along the deck, as though the deck is resting on simple rigid supports at the cable locations. The zero displacement method was proposed by Wang *et al.* [1993] to determine post-tensioning cable forces and the initial profile of a cable-stayed bridge under the action of dead load. The method starts by assuming zero tension forces in the stay cables. Based on an assumption of zero deflections in the deck, the equilibrium position of the cable-stayed bridge under dead load action is obtained iteratively. Although the first determined configuration satisfies the equilibrium conditions, it does not lead to zero deflections. Therefore, the cable forces determined in the previous step are used as initial cable forces, and a new equilibrium is determined. The above process is repeated until the convergence tolerance is achieved at selected locations of the deck. The zero displacement method suffers from a slow convergence and requires a significant amount of computational effort (Kim and Lee, 2001).

In the research done by Negrão and Simões [1997] and Simões and Negrão [2000], the post-tensioning cable forces are determined by minimizing a convex scalar function. This function combines dimensions of cross-sections of the bridge, overall structural geometry and post-tensioning cable forces. The gradient based non-linear programming techniques used in this study may linger in local optima. In addition, the method is quite sensitive to the constraints, which should be imposed very cautiously to obtain a practical output (Chen *et al.,* 2000). Due to numerical difficulties and very high computational cost, this method does not account for the large displacements and (P-Δ) effects.

Chen *et al.* [2000] proposed a method that utilizes the concept of force equilibrium for the determination of a scheme of post-tensioning cable forces. In this method, the cable forces are considered as independent variables for achieving target bending moments along the deck. The target moments are determined by replacing all cables that support the deck by rigid simple supports. A set of coefficients, that represent bending moments at cable-deck connections caused by a unit load in each cable location, are then calculated. A rough estimate of the cable forces can be obtained by considering the equilibrium of the previous stage. The calculated cable forces are used to update the deck bending moments, which are then used to calculate the updated cable forces. The last two steps are repeated until the deck bending moments converge to the target bending moment values. In this method, it is difficult to control bending moments at deck-pylon junctions and pylon sections. In addition, incorrect selections of the target moments can lead to singularities in the system of equations.

Janjic *et al.* [2003] suggested the unit load method (ULM). A desired bending moment distribution at specific degrees of freedom (at the cable-deck connections) is used to

obtain the optimum cable forces in this method. The bending moments at these specific degrees of freedom (DOFs) are first calculated due to a unit load case for each stay cable. The bridge is also analyzed under the action of the dead load. A system of linear equations can be established with one equation for each DOFs. This system of equations can be directly solved for the unknown cable forces that are used to achieve the desired moment distribution. The selection of DOFs is one of the challenges in this method, as it may lead to singularities in the equations system. The case of unequal cable forces on both sides of the pylon is an example of this situation. According to Lee *et al.* [2008], the ULM may get locked in a local minimum. Therefore, ULM needs to be improved by introducing additional constraints to avoid getting stuck in one of these local minima.

1.5 Optimal Design of Cable-stayed Bridges

Owing to the typical high cost of cable-stayed bridges, the tendency of increasing the bridges' spans, and the inflation in construction material prices, the optimization of the design of cable-stayed bridges is becoming quite important. Achieving an optimum design solution for such structures is a challenging task due to several reasons. Cable-stayed bridges are large, sophisticated, and highly statically indeterminate structures (Troitsky, 1988). Their behaviour is influenced by the following forms of geometric nonlinear effects: beam-column (P-Δ), cable sagging, and large displacements (Nazmy and Abdel-Ghaffar, 1990). The behaviour of such structures is affected by the interaction between a large number of design parameters, such as main span length, height of the pylon, number of stay cables, pylon type, deck material, and the dimensions of various components of the bridge (Walther *et al.*, 1988). The proper set of post-tensioning forces

required to off-set the effect of the bridge dead load adds extra design variables. A Cable-stayed bridge should be designed to meet the strength and serviceability requirements imposed by the design codes to ensure that all elements of the bridges satisfy the safety and functionality criteria. In summary, the design optimization of a cable-stayed bridge is a challenging exercise due to the high structural redundancy, large number of design variables, strict design constraints imposed by design codes, sensitivity to the geometric nonlinear effects, and robust influence of post-tensioning cable forces. All these make traditional design methods and available optimization packages incapable of obtaining the optimum design of this kind of bridges.

Several design optimization algorithms for cable-stayed bridges are available in the literature. Simões and Negrão [1994] presented the entropy-based optimization algorithm to optimize the cost of cable-stayed bridges. The locations of the stay cables along the main girders and the pylons, as well as the cross-section dimensions of the deck, pylons, and stay cables were considered as design variables. In this method, an initial configuration is required to initiate the optimization process. In addition the post-tensioning cable forces are not included in the analysis and both the number of stay cables and main span length are assumed to be constant.

Long *et al.* [1999] used the internal penalty function algorithm to optimize the cost of cable-stayed bridges having composite superstructures. The geometric nonlinear effects were included in this study. The geometric parameters of the bridges, including the pylon height, the main span length, and the number of stay cables, were given pre-assigned values. The design variables included only the dimensions defining the cross section of various elements of the bridges. The effect of the post-tensioning cable forces was not

taken into account. In addition, an initial feasible design was needed in order to start the optimization algorithm.

Simões and Negrão [2000] employed a convex scalar function to minimize the cost of a box-girder deck cable-stayed bridge. This function combines the cross sectional dimensions of the bridge and the post-tensioning cable forces. Maximum and minimum allowable stresses in stay cables and deflections of the deck were the three constraints considered in the method. The study uses the gradient based non-linear programming technique, which may linger in local optima. The pylon height and the main span length were not considered within the design variables. Additionally, an initial starting point was required to start the optimization technique.

Lute *et al.* [2009] demonstrated the capability of support vector machine (SVM) to reduce the computational time of a genetic algorithm (GA) for optimizing cable-stayed bridges. The results demonstrated the efficiency of the genetic algorithm (GA) for such an application. However, a limited number of simple constraints, which are not based on a standard code and are not sufficient to assess the strength of the bridges, were imposed in this study. The number of stay cables was treated as a pre-set constant and the effect of post-tensioning cable forces was neglected.

1.6 Research Objectives

The main objectives of the current research are summarized in the following points:

1. Develop a new method, combining finite element analysis, B-spline curves, and an optimization technique to determine the optimum post-tensioning cable forces for cable-stayed bridges under the action of dead load.

2. Develop surrogate polynomial functions that can be used to evaluate the post-tensioning cable forces in semi-fan cable stayed bridges under the action of dead load.
3. Develop an optimization algorithm that integrates a finite element model, the real coded genetic algorithm, the post-tensioning functions, and proper design methodologies to optimize the design of semi-fan cable-stayed bridges.
4. Develop a database for the optimum design of three-span composite cable-stayed bridges with semi-fan cable arrangement.

1.7 Organization of the Thesis

This thesis has been prepared in "Integrated-Article" format. Each chapter includes its own bibliography. In the present chapter, a review of the studies and approaches related to the evaluation of post-tensioning cable forces and the optimization of cable-stayed bridges is provided. The objectives of the study are then described. The following four chapters address the thesis objectives. Conclusively, in Chapter 6, relevant findings of the study together with suggestions for further research work are included.

In Chapter 2, a novel method to determine the optimum post-tensioning cable forces under the action of the dead load is developed. An extensive literature review for available methods to evaluate post-tensioning cable forces is conducted. The advantages of the proposed new method over other post-tensioning methods available in the literature are presented. The numerical model, combining finite element analysis, B-spline curves, and real coded genetic algorithm is presented. The validity of this proposed method is checked by evaluating the post-tensioning cable forces for a real cable-stayed bridge. The

effect of the geometric nonlinearities on the determination of the post-tensioning cable forces is assessed.

In Chapter 3, surrogate polynomial functions that can be used to obtain the post-tensioning cable forces for semi-fan cable-stayed bridge are developed. Parameters affecting the post-tensioning cables forces are investigated. Estimation of regression coefficients in the post-tensioning polynomial functions is conducted. The accuracy the regression models is assessed. The post-tensioning functions are validated by applying the evaluated post-tensioning cable forces on several cable-stayed bridges. The optimum geometric configurations that lead to the most uniform distribution of post-tensioning cable forces are investigated.

In Chapter 4, an optimization algorithm that integrates a finite element model, real coded genetic algorithm, post-tensioning polynomial functions, and design methodologies is developed specially to optimize the design of semi- fan cable-stayed bridges. The advantages of the proposed optimization algorithm over the previous optimization techniques available in the literature are presented. Various components of the proposed optimization algorithm, including the design variables, design constraints, objective function, finite element model, post-tensioning polynomial functions, load consideration, and the optimization technique, are demonstrated. The Quincy Bayview Bridge, located in Illinois, USA, as an example of three-span composite cable-stayed bridges, is selected as a case study. The effects of all design variables on the cost of the cable-stayed bridge are explored separately. The optimal design of the bridge is obtained, while varying all these design variables.

In Chapter 5, a database for the optimum design of cable-stayed bridges is developed. The study focuses on the optimization of three-span composite bridges with a semi-fan cable arrangement. The database describes the variations of the optimum design parameters, including the main span length, height of the pylon, number of stay cables, and cross-sectional dimensions of all elements with the total length of the bridge. The database is presented in the form of design tables and curves. The study covers bridge lengths ranging from *250* m to *700* m.

In Chapter 6, the main conclusions drawn from the study as well as the recommendations for future researches are given.

1.8 References

1. Podolny W, Scalz, J. Construction and Design of Cable-stayed Bridges. John Wiley and Sons, New York; 1986.
2. Gimsing NJ. Cable supported bridges: Concepts and design. John Wiley& Sons Ltd; 1997.
3. Troitsky MS. Cable-stayed bridges: theory and design. 2nd Ed. Oxford: BSP; 1988.
4. Ren WX, Peng, XL. Baseline finite element modeling of a large span cable-stayed bridge through field ambient vibration tests. Comput. Struct 2005; 83(8-9):536-550.
5. Lee TY, Kim YH, Kang SW. Optimization of tensioning strategy for asymmetric cable-stayed bridge and its effect on construction process. J Struct Multidisc Optim 2008;35:623–629.
6. Sung YC, Chang DW, Teo EH. Optimum post-tensioning cable forces of Mau-Lo His cable-stayed bridge. J Engineering Structures 2006;28:1407-1417.

7. Wang PH, Tseng TC, Yang CG. Initial shape of cable-stayed bridges. J Comput Struct 1993; 46:1095-1106.
8. Kim KS, Lee H S. Analysis of target configurations under dead loads for cable-supported bridges. Comput.Struct. 2001;79:2681-2692.
9. Negrão JHO, Simões LMC. Optimization of cable-stayed bridges with three-dimensional modelling. J Comput Struct 1997;64:741-758.
10. Simões LMC, Negrão JHJO. Optimization of cable-stayed bridges with box-girder decks. J Adv. Eng. Software 2000; 31:417-423.
11. Chen DW, Au FTK, Tham LG, Lee PKK. Determination of initial cable forces in prestressed concrete cable-stayed bridges for given design deck profiles using the force equilibrium method. J Comput Struct 2000;74:1–9.
12. Janjic D, Pircher M, Pircher H. Optimization of cable tensioning in cable-stayed bridges. J Bridge Eng ASCE 2003;8:131–137.
13. Nazmy AS, Abdel-Ghaffar A. Three-dimensional nonlinear static analysis of cable-stayed bridges. Computers and Structures 1990;34(2):257-271.
14. Walther R., Houriet B., Isler W., Moia P., Klein JF. Cable-stayed bridges. Thomas Telford Ltd., Thomas Telford House, London; 1988.
15. Simões LMC, Negrão JHJO. Sizing and geometry optimization of cable-stayed bridges. J Computer & structure 1994; 52:309-321.
16. Long W, Troitsky, MS, Zielinski ZA. Optimum design of cable stayed bridges, J Structural Engineering and Mechanics 1999; 7, 241-257.
17. Lute V, Upadhyay A, Singh KK. Computationally efficient analysis of cable-stayed bridge for GA-based optimization. Eng Appl Artif Intell 2009;22(4-5):750-758.

CHAPTER 2

DETERMINATION OF OPTIMUM POST-TENSIONING CABLE FORCES OF CABLE-STAYED BRIDGES*

2.1 Introduction

Since the construction of the first modern cable-stayed bridge, the Swedish Strömsund Bridge in 1955, cable-stayed bridges have become one of the most popular types of bridges worldwide. These bridges provide an economical solution for the range of medium to long span bridges, and possess excellent structural characteristics, technical advantages and aesthetic appearance (Gimsing, 1997). Typical Cable-stayed bridges consist of three major components: the deck, the erected pylons, and the stay cables, which stretch down diagonally from the pylons to support the deck.

Cable-stayed bridges are large, complicated and highly statically indeterminate structures. The use of a large number of stay cables has become common in modern cable-stayed bridges, as this leads to slender main girders that require less flexural stiffness. Typically, the stay cables are post-tensioned and the magnitudes of the tension forces vary among various cables. The selected set of post-tensioning cable forces represents a design parameter that can be tailored to achieve an effective design for the bridge.

A set of post-tensioning cable forces can be applied such that the transverse deflections of both the deck and the pylon are minimized under the effect of the own weight of the structure. This will reduce the bending moment acting along the longitudinal direction of the deck due to dead loads, leading to a reduction in the material and the weight of the

* A version of this chapter has been submitted to the *Journal of Engineering structures*

structure. Additionally, the reduction of the lateral displacement of the pylon along the longitudinal direction of the bridge decreases the secondary moment acting on the pylon associated with the (P-Δ) effect. However, as the number of the stay cables increases, the evaluation of the proper set of post-tensioning forces becomes a challenging exercise.

There are four main methods used to determine the post-tensioning cable forces in cable-stayed bridges, namely (1) the zero displacement method, (2) the optimization method, (3) the force equilibrium method, and (4) the unit load method.

The zero displacement method was proposed by Wang *et al.* [1993] to determine post-tensioning cable forces and the initial profile of a cable-stayed bridge under the action of the dead load. The method takes into account nonlinearities due to large displacement, (P-Δ), and cable sag effects. The method starts by assuming zero tension forces in the stay cables. Based on an assumption of zero deflections in the deck, the equilibrium position of the cable-stayed bridge under dead load action is obtained iteratively. Although the first determined configuration satisfies the equilibrium conditions, it does not lead to zero deflection. Therefore, the cable forces determined in the previous step are used as initial cable forces, and a new equilibrium is determined again. The previous process is repeated until the convergence tolerance for selected nodes of the deck is achieved.

In the optimization method Negrão and Simões [1997] and Simões and Negrão [2000], the post-tensioning cable forces are determined by minimizing a convex scalar function. This function combines dimensions of cross-sections of the bridge, overall structural geometry, and post-tensioning cable forces. Maximum and minimum allowable stresses in stay cables and deflections of the deck are the three constraints imposed in the method.

The gradient based non-linear programming techniques used in this study may linger in local optima. In addition, it is very sensitive to the constraints, which should be imposed very cautiously to obtain a practical output (Chen *et al*, 2000). Due to very high computational cost and numerical difficulties in implementing sensitivity analysis for geometrical nonlinearities, this method does not account for the large displacements and (P-Δ) effects.

A method that utilizes the concept of force equilibrium for the determination of a scheme of post-tensioning cable forces was proposed by Chen *et al.* [2000]. In this method, the cable forces are considered as independent variables for achieving target bending moments along the deck. The target moments are determined by replacing all cables that support the deck by rigid simple supports. A set of coefficients, that represent bending moments at cable-deck connections caused by a unit load in each cable location, are then calculated. A rough estimate of the cable forces can be obtained by considering the equilibrium of the previous stage. The calculated cable forces are used to update the deck bending moments, which are then used to calculate the updated cable forces. The last two steps are repeated until the deck bending moments converge to the target bending moment values. In this method, it is difficult to control bending moments at deck-pylon junctions and pylon sections. In addition, incorrect selections of the target moments can lead to singularities in the system of equations.

The unit load method (ULM) is suggested by Janjic *et al.* [2003]. The method takes into account the effect of the three sources of geometric nonlinearities. In this method, a desired bending moment distribution at specific degrees of freedom (cable-deck connections) is used to obtain the optimum cable forces. The bending moments at these

specific DOFs are first calculated due to a unit load case for each stay cable. The bridge is also analyzed under the action of the dead load. A system of linear equations can be established with one equation for each DOFs. This system of equations can be directly solved for the unknown cable forces that can be applied to achieve the desired moment distribution. Selection of DOFs is one of the most critical precautions of this method, as it may lead to singularities in the equation system. The case of unequal cable forces on both sides of the pylon is an example of this situation. According to Lee *et al.* [2008], the ULM may get locked in a local minimum. Therefore, ULM needs to be improved by introducing additional constraints to avoid getting stuck in one of these local minima.

2.2 Research Significance

In this study, a new method to determine the optimum distribution of post-tensioning cable forces under the action of dead load is developed. The objective of this method is to minimize both the vertical deflection of the deck and the lateral deflection of the pylons. The new approach combines the finite element method, the B-spline function, and a modern optimization algorithm. The advantages of the proposed method over previous methods can summarized as follows:

1. Singularity problems encountered in the equation systems of the classical techniques can be avoided by formulating the problem of finding post-tensioning cable forces as an optimization problem.
2. In the standard post-tensioning optimization approaches, the cable forces are considered as discrete design variables. With the increase in the number of stay cables, the number of design variables becomes quite large leading to potential

numerical problems. In the current method, B-spline curves are used to represent the distribution of cable forces along the deck length. Parameters defining the shape of the B-spline curves are considered as the design variables. The number of these parameters is significantly less than the number of stay cables. This decreases the number of design variables in the optimization process. Decreasing the number of design variables reduces the complexity of the optimization search space, as well as the computational time required to get the optimum solution. Moreover, it improves the performance of the optimization technique by increasing the probability of finding the global optimum solution. Therefore, the proposed method is very efficient with modern long cable-stayed bridges that contain large numbers of stay cables.

3. Most of the previous post-tensioning optimization techniques are based on achieving one of two conditions. The first condition involves limiting the vertical deflections of the bridge deck to a convergence tolerance value. The other condition is fulfilled by obtaining a bending moment diagram along the deck, as though the deck is resting on simple rigid supports at the cable locations. In some cases, the desired-conditions of the deck may be achieved at the expense of either high bending moments in the pylons, exceeding the imposed limits, or very large cable forces with non-uniform distribution. Therefore, there is a strong need to account for the behaviour of the pylon in the optimization procedure. The objective function in the current method minimizes transverse deflections of the deck and pylons' tops, simultaneously. As a result, bending moment distributions along both the deck and the pylon are minimized.

4. Designing modern long cable-stayed bridges (main span more than *1000 m*) is characterized by using a large number of stay cables. Hence, the solution to the optimum post-tensioning cable forces is not unique, i.e., there is a large set of candidate solutions within a large search space, which may have many hills and valleys. In addition, the problem can have multiple minima due to the intersection of the constraints with the objective function. In the current method, a global optimization method, the Genetic Algorithm (GA), is used to optimize the shape of post-tensioning functions, since it is capable of finding the global minimum of the optimization problem.

2.3 Description of the Bridge

The geometry of the cable-stayed bridge chosen for this study is similar to that of the Quincy Bayview Bridge, located in Illinois, USA (Wilson and Gravelle, 1991). The original bridge has *56* cables, however, in the current example, this number is increased to *80* cables in order to demonstrate the efficiency of the new method for a large number of stay cables. The total length of the main channel span is *285.6 m*, with two side spans of *128.1 m*. Therefore, the total length of the bridge is *541.8 m*, as shown in Fig. 2.1(a). The deck superstructure is supported by double planes of helically wrapped stay cables in a semi-fan type arrangement. The cross-section of the bridge deck (Fig. 2.1(b)) consists of a precast concrete deck having a thickness of *0.23 m* and a width of *14.20 m*. Two steel main girders are located at the outer edge of the deck. These girders are interconnected by a set of equally spaced floor steel beams. The distance between each pair of floor steel beams is *9.0* meters. The vertical moment of inertia (I_{dv}), the transverse moment of inertia

(I_{dh}), the cross-section area (A_d), and the modulus of elasticity (E_{ds}) of the deck are *0 704* m^4, *14.2* m^4, *0.602* m^2, and *2x10*^{8} *kN/m*^{2}, respectively. All the deck section properties are based on transferring the concrete slab to an equivalent steel plate. The cables are assumed to have constant cross-sectional areas of *0.0176* m^2. The modulus of elasticity (E_{cs}), the ultimate tensile strength (T_{cCable}), and the weight per unit length (w_{cs}) of the cables are *2.1 x 10*^{8} *kN/m*^{2}, *1.6 x 10*^{6} *kN/m*^{2}, and *1.36 kN/m*, respectively.

The pylons consist of two concrete legs, interconnected with a pair of struts. The upper strut cross beam connects the upper legs, and the lower strut cross beam supports the deck. The lower legs of the pylon are connected by a *1.22 m* thick wall, which is placed as a web between the two legs, as shown in Fig. 2.1(c). The modulus of elasticity for the concrete (E_c) is *2.5 x 10*^{7} *kN/m*^{2}.

2.4 Description of the Numerical Model

The proposed numerical model involves interaction between three numerical schemes: finite element modeling (FEM), B-spline function, and Genetic Algorithm (GA). A brief description of these three numerical schemes, as they apply to the developed numerical tool, is provided in this section. The interaction between various components of the model and the sequence of analysis are then described.

2.4.1 Finite Element Formulation

The superstructure of a cable-stayed bridge consists of three components having different levels of rigidities: (a) deck, (b) pylon and (c) cables. The three components of the bridge are modeled using three-dimensional line elements. A three-dimensional nonlinear frame

element is used to model the deck and the pylon, while a three-dimensional nonlinear cable element is used to simulate the cables.

2.4.1.1 Modeling of Cables

Under the action of its own weight and axial tensile force, a cable supported at its end will sag into a catenary shape. The axial stiffness of a cable will change nonlinearly with cable tension and cable sagging. The equivalent modulus approach developed by Ernst [1965] is the most adopted method for cable modeling in cable-stayed bridges. In this approach, each cable is replaced by one truss element with equivalent cable stiffness. The equivalent tangent modulus of elasticity used to account for the sag effect can be written as:

$$E_{eq} = \frac{E_{cs}}{1 + \frac{(w_{cs} L)^2 AE}{12T^3}} \tag{2.1}$$

where E_{eq} is the equivalent modulus of elasticity; E_{cs} is the cable material effective modulus; L is horizontal projected length of a cable; w_{cs} is the weight per unit length of the cable; A is the cross-sectional area of the cable; and T is the tension in the cable.

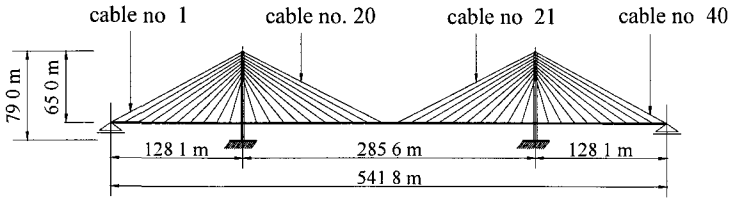

(a) Cables number and geometry of the bridge.

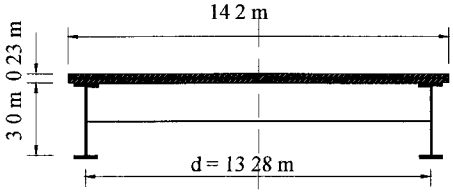

(b) Cross section of the bridge deck.

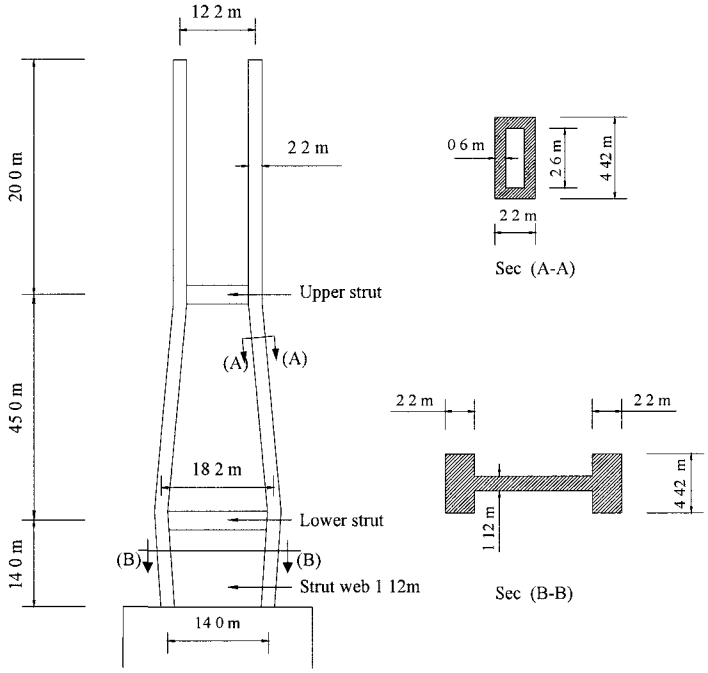

(c) Elevation view of the bridge pylon.

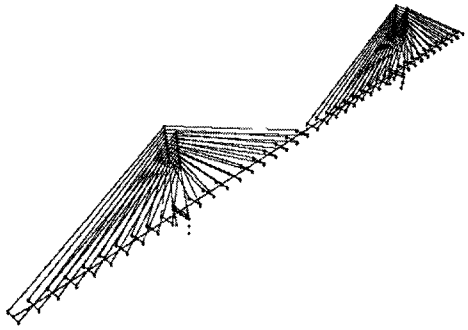

(d) Finite element model.

Fig. 2.1 Geometry and finite element model.

2.4.1.2 Modeling of Pylons and Girders

The local tangent stiffness matrix of a frame element $[k_T]_b$ that takes into account the (*P-Δ)* and large displacement effects is given by:

$$[k_T]_b = [k_E]_b + [k_G]_b \tag{2.2}$$

where $[k_E]_b$ is the elastic stiffness matrix of a *3-D* frame element (Weaver and Gere, 1980) and $[k_G]_b$ is the geometric stiffness matrix of a *3-D* frame element (Nazmy and Abdel-Ghaffar, 1990).

The deck is modeled using a single spine passing through its shear center. The translational and rotational stiffness of the deck are calculated and assigned to the frame elements of the spine. The cable anchorages and the deck spine are connected by massless, horizontal rigid links to achieve the proper offset of the cables from the centerline of the deck (Wilson and Gravelle, 1991). The finite element model (FEM) of the bridge is shown in Fig. 2.1(d).

2.4.2 Representation of the Post-tensioning Cable Forces by B-spline Function

Observations on the distributions of the post-tensioning cable forces, obtained by Simões and Negrão [2000], Chen *et al.* [2000], and Lee *et al.* [2008], along the span of a cable-stayed bridge show that they follow an arbitrary polynomial function, which can be represented by an p^{th} order polynomial

$$f = a_1 x^n + a_2 x^{n-1} + a_3 x^{n-2} + a_4 x^{n-3} + \ldots\ldots + a_p \tag{2.3}$$

where f is the post-tensioning cable function, and x is the length along the bridge span. If such a function is used, the independent variables employed in the optimization technique are the coefficients a_i. However, there are many limitations and disadvantages that arise

when using power polynomial functions. It is hard to predict the proper range of values of such coefficients a_i for a specific optimization problem. The optimum function (f) has often a complicated shape that should be described by high order polynomials with a large number of coefficients. Furthermore, the coefficients a_i impart very little geometric insight about the shape of the post-tensioning function (Piegl and Tiller, 1997).

In this study, B-spline curves are selected to represent the post-tensioning functions. B-spline curves are piecewise polynomials that remedy all the shortcomings associated with the power polynomial curves. They can be used to describe complex curves with lower-degree polynomials. Moreover, they have local control property that allows the user to modify a specific part of a curve and leaves the rest of the curve unchanged. B-spline curves are adequate for most of shape optimization problems (Piegl and Tiller, 1991), and (Pourazady and Xu, 2000).

A p^{th} degree B-spline curve $C(u)$, shown in Fig. 2.2 (a), is defined as follows

$$C(u) = \sum_{i=0}^{n} N_{i,p}(u) P_i \qquad 0 \le u \le 1 \tag{2.4}$$

where u is the independent variable, and P_i are the control points. The polygon formed by the control points P_i is called the control polygon. $N_{i,p}(u)$ are the p^{th} degree B-spline basis functions given as:

$$N_{i,0}(u) = \begin{cases} 1 & if \ \ u_i \le u \le u_{i+1} \\ 0 & otherwise \end{cases} \tag{2.5-a}$$

$$N_{i,p}(u) = \frac{u - u_i}{u_{i+p} - u_i} N_{i,p-1}(u) + \frac{u_{i+p+1} - u}{u_{i+p+1} - u_{i+1}} N_{i+1,p-1}(u) \tag{2.5-b}$$

and it is defined on nonperiodic and nonunifrom knot vector

$$U = \left\{ \underbrace{0, \quad ,0}_{p+1}, u_{p+1}, \quad , u_{m-p-1}, \underbrace{1, \quad ,1}_{p+1} \right\} \tag{2.6}$$

The degree of the basic function p, number of knots = $(m+1)$, and the number of control points = $(n+1)$ are related by the formula $m = n + p + 1$.

Fig. 2.2(a) shows a B-spline curve constructed using four control points. In general, slight variations in the location of the control points change the shape of the B-spline function significantly. Therefore, the control points represent the design variables used in the current study. Shape optimizations of post-tensioning cable functions are carried out through varying the location of these control points.

Determining the location of a point on a B-spline curve at a certain value u can be briefly summarized by the following steps:

1- Assign the number of the control points $(n+1)$, the degree of the function (p), and then calculate the number of knots $(m+1)$.

2- Define coordinates of the B-spline control points.

3- Calculate the nonzero basis functions.

4- Multiply the values of the nonzero basis function with the corresponding control points.

2.4.3. Designs Variables, Objective function, and Design constraint

The x and y-coordinates of the B-spline control points are the design variables (P_i in Fig. 2.1(b)), which define the shape of the B-spline curve representing the distribution of the post-tensioning cable forces. In Fig. 2.2(b), cables number i,j,k and l are mapped to their respective post-tensioning force values on the B-spline curves for exemplary purpose. In the present study, the upper and lower bounds for the x-coordinates are the span length

and zero, respectively, i.e. (span length $\geq x \geq 0$). The upper and lower bounds for the y-coordinates are a preset value for the maximum cables tensile force (T_{max}) and zero, respectively, i.e. ($T_{max} \geq y \geq 0$). Four B-spline curves are used to model the post-tensioning functions for a typical two-pylon semi-fan cable-stayed bridge, as show in Fig. 2.2(b). In the case of single-pylon cable-stayed bridge, two B-spline curves will be used, as it is a special case of the two-pylon cable-stayed bridge. The method can be also used also for cable-stayed bridges with different cable configurations.

The objective function (F) to be minimized is set as the square root of the sum of the squares (SRSS) of the vertical deflection of the nodal points of the deck and the squares of the lateral deflection of the top points of all pylons, i.e.:

$$F = \sqrt{(\delta_1^{\,2} + \delta_2^{\,2} + ...)_{deck} + (\delta_{1p}^{\,2} + \delta_{2p}^{\,2} + ...)_{Pylon}} \tag{2.7}$$

where:

$\delta_1, \delta_2, ...$ = vertical deflection of the nodes of the deck spine

$\delta_{1p}, \delta_{2p}, ...$ = lateral deflections of the pylons' tops

Subject to the following constraint:

$$\left| \frac{maximum\ vertical\ deflection\ of\ the\ deck\ (\delta_{max})}{length\ of\ main\ span\ (M)} \right| \leq \varepsilon \tag{2.8}$$

where ε is a convergence tolerance, which is set equal to 10^{-4}.

It should be noted that minimization of the maximum deflection along the deck and the pylons' tops could have been used as an objective function. However, the use of the SRSS smoothes out the objective function and does not induce false local optima. In addition, the applied constraint ensures that the ratio between the vertical deflection at any point of the deck and the length of the main span does exceed a small tolerance value

(ε). This constraint is required to achieve a smooth bending moment distribution along the deck.

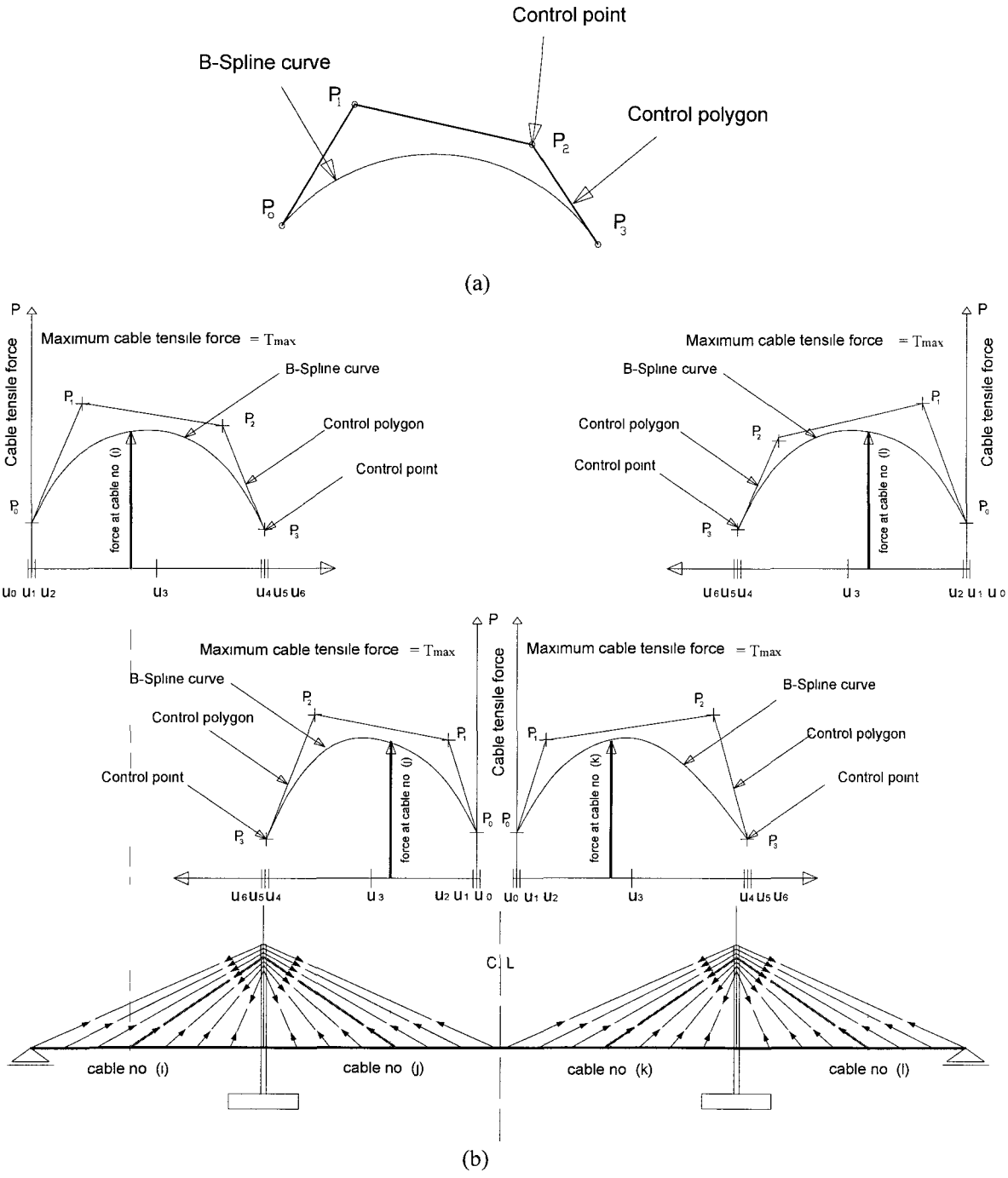

Fig. 2.2 Representation of the cable forces by B-spline curves.

2.4.4 The Optimization Technique

In spite of the apparent simplicity of the post-tensioning shape function, the search space of this function is expected to be complex and may contain several local minima due to the high redundancy of cable-stayed bridges, and the intersection of the constraint with the objective function. If the function has one optimum value, direct search methods are more appropriate to be used for optimization since they are not computationally-intensive, otherwise a global optimization technique is needed to reach a near globally optimum solution. In order to check whether the objective function exhibits local optima or not, a direct search technique can be repeated with different starting search points. If the search reaches different final solutions, then it can be concluded that the objective function is multi-modal i.e. has several local optima.

2.4.4.1 Checking the Objective Function for Multiple Optima

The objective function is checked for the existence of multiple optima by starting a direct search algorithm from different starting points. Three algorithms are tried. These are Broyden-Fletcher-Goldfarb-Shanno (BFGS), Sequential Quadratic Programming (SQP), and Nelder-Mead (NM), respectively (Rao, 2009).

(BFGS) and (SQP) methods turn to be not able to move from the starting points indicating the probable presence of discontinuities in the post-tensioning objective functions. Therefore, their results are immaterial and are not reported. The Nelder-Mead method is tried by repeating the optimization problem at five random starting points. Four control points are assumed to model the post-tensioning function in this analysis. Coordinates of the selected B-spline control points are tabulated in Table 2.1. The final

distributions of the post-tensioning cable forces obtained from these analyses are shown in Fig. 2.3. The final post-tensioning results are not identical and strongly depend on the starting point choice. Such results prove that the post-tensioning objective function has multiple local minima, making direct search methods inefficient to find the global optimum since they get trapped in the closest local minima. As a result, a global optimization method is needed. Since the control points of the post-tensioning functions are continuous in nature, the optimization method should be more suited to continuous variables. Based on the above, real coded genetic algorithm is chosen in the current study to optimize the shape of the post-tensioning cable forces function.

Table 2.1 Values of independent variables for initial search points used in the direct search

	Coordinates of B-spline control points
Case (1)	$(0, 0.5T_{max})$, $(0.25L, 0.5T_{max})$, $(0.75L, 0.5T_{max})$, $(L, 0.5T_{max})$
Case (2)	$(0, T_{max})$, $(0.25L, T_{max})$, $(0.66L, T_{max})$, (L, T_{max})
Case (3)	$(0, T_{max})$, $(0.4L, T_{max})$, $(0.8L, T_{max})$, (L, T_{max})
Case (4)	$(0, 0.5T_{max})$, $(0.4L, 0.5T_{max})$, $(0.8L, 0.5T_{max})$, $(L, 0.5T_{max})$
Case (5)	$(0, 0.5T_{max})$, $(0.25L, 0.5T_{max})$, $(0.66L, 0.5T_{max})$, $(L, 0.5T_{max})$

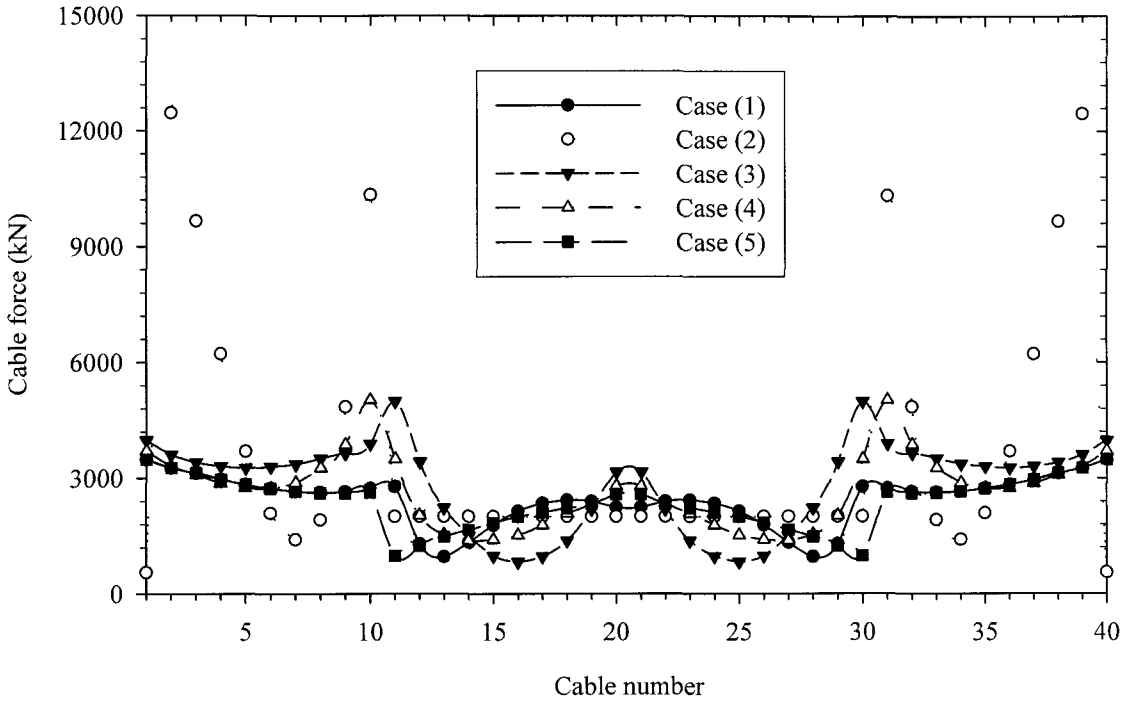

Fig. 2.3 Post-tensioning cable forces obtained by direct search for various starting points given in Table 2.1.

2.4.4.2 Real Coded Genetic Algorithms

In recent decades, the global optimization genetic algorithms (GAs), which are based on the theory of biological evolution and adaptation, have been adopted to solve many structural optimization problems (Gen and Cheng, 2000) and (Gen and Cheng, 1997). (GAs) are made from a population, other than a single point. Due to the non-deterministic transition rules, operators, and the multi-points search, (GAs) have more potential to obtain the global optimization solutions, compared with many traditional search methods (Goldberg, 1989).

The real coded genetic algorithm (RCGA) is a variant of genetic algorithms that are suited for the optimization of multiple-optima objective functions defined over

continuous variables. The algorithm operates directly on the design variables, instead of encoding them into binary strings, as in the traditional genetic algorithms. A complete description of (GAs) techniques and their variants can be found in Davis [1991]. The following section describes how the real coded genetic algorithm is adapted to the problem at hand to find the optimum post-tensioning cable forces.

2.4.5 Optimum Post-tensioning Cable Forces Algorithm.

The analysis sequence combining the finite element model, B-spline function, and real coded genetic algorithm (RCGA) for finding the optimum post-tensioning cable forces distribution under dead load is given as follows:

1. Develop a three dimensional finite element model of the cable-stayed bridge according to the geometry and physical properties of the bridge, as described in Section (2.4.1).
2. Create an initial population of the design variables, which are the x and y-coordinates of the B-spline control points, randomly selected by (GA) algorithm between the lower and upper bounds of each design variable. Each search point in the population is used to create a candidate function for the post-tensioning cable forces, as described in Section (2.4.2).
3. Use the post-tensioning function to evaluate the forces at all cables. Apply these forces to the *3-D FEM* together with the own weight of the bridge and analyze the structure to obtain the nodal deflections. The corresponding objective function (F) is then calculated using Eq. (2.7)

4. Sort the initial population in ascending order according to the value of the objective function (F) such that the first ranked candidate "post-tensioning function" has the minimum value for (F).
5. Generate, using the (GA), a new population by applying the crossover and mutation operators on the high ranked post-tensioning functions evaluated at step 4. These operators direct the search towards the global optimum solution. A description of these GA operators is provided in the next section.
6. Replace the previous population with the newer one containing the new candidate functions, in addition to the best candidate function found so far (elitist selection).
7. Repeat steps *3* to *6* until the convergence tolerance, described by Eq. (2.8), is achieved.
8. Deliver the candidate post-tensioning function obtained at step 7 as the final solution.

The procedure described above is summarized in the flow chart shown in Fig. 2.4.

2.4.6 Genetic Operators

The mutation operators allow the (GA) to avoid local minima by searching for solutions in remote areas of the objective function landscape. In the current study, the operators used are boundary mutation, non-uniform mutation, and uniform mutation. The first operator searches the boundaries of the independent variables for optima lying there, the second is random search that decreases its random movements with the progress of the search, and the third is a totally random search element. The crossover operators produce new solutions from parent solutions having good objective function values.

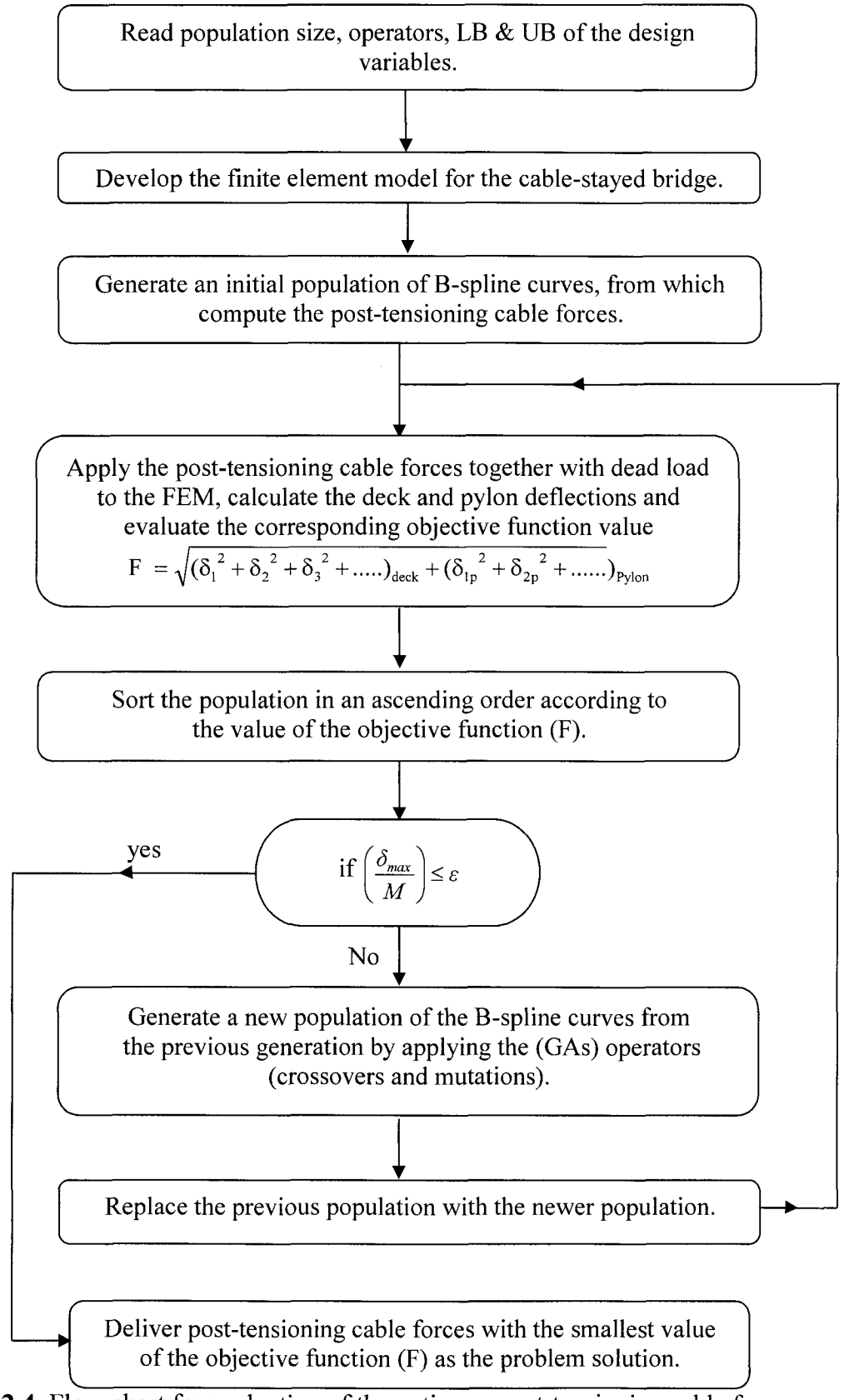

Fig. 2.4 Flow chart for evaluation of the optimum post-tensioning cable forces.

In the current study, this translates into producing new post-tensioning function from pairs of post-tensioning functions. The crossover operators used are the arithmetic, uniform and heuristic crossovers. The first produces new solutions in the functional landscape of the parent solutions. The second one is used to create a new solution randomly from two parents, while the last one extrapolates the parent solutions into a promising direction. Details of such operators are given by Michalewicz and Fogel [2004].

The above operators are applied on each population with the following values.

1) Population size = *100* solution instances (candidate post-tensioning curves).

2) 4 instances undergo boundary mutation.

3) 4 instances undergo non-uniform mutation.

4) 4 instances undergo uniform mutation.

6) 2 instances undergo uniform crossover.

7) 2 instances undergo heuristic crossover.

8) 2 instances undergo arithmetic crossover.

2.5 Results of the Analyses

A set of analyses is carried out by applying the developed optimization procedure to the considered bridge. The analyses involve varying a number of parameters in order to assess the effect of:

1. Number of control points.
2. Selection of design variables.
3. Top deflection of the pylons.

4. The three sources of geometric nonlinearities.

2.5.1 Optimum Number of Control Points

Reducing the number of design variables narrows down the search space and speeds up the convergence to the global solution. Therefore, it is very important to choose the least number of coordinates of the control points without compromising the flexibility of the B-spline curve. The bridge geometry and the number of stay cables are the factors affecting the shapes of post-tensioning functions. For each particular cable-stayed bridge, a preliminary study should be conducted by repeating the optimization procedure using different number of design variables. For the current example, the maximum deflection values obtained from analyses involving three, four, five, and six control points are *0.017* m, *0.0031 m*, *0.0031 m*, and *0.0030 m*, respectively. The results indicate that the maximum deflection of the deck is reduced with the increase in the number of used control points. However, beyond four control points this reduction becomes almost negligible. Therefore, it can be concluded that four control points are sufficient to represent the post-tensioning functions of the current bridge.

2.5.2 Advantages of Optimizing Shapes of Post-tensioning Functions

To illustrate the direct benefits of optimizing shapes of post-tensioning function instead of cable forces, the described numerical model is used to determine the optimum post-tensioning cable forces for the considered bridge for two cases:

- Case (A): the coordinates of the B-spline control points of the post-tensioning functions are considered as the design variables. Since the x-coordinates of the first

and last control points are equal to zero and the span length, respectively, i.e. ($x_1 = 0$, and x_4 = span length), as shown in Fig. 2.2, this analysis involves twelve design variables.

- Case (B): the values of the force in each stay cable, as discrete values, are considered as the design variables. Due to symmetry, twenty design variables are included in this analysis.

Fig. 2.5(a) shows that the post-tensioning cable forces obtained from Case (A) is more uniform and smoother than the one obtained from Case (B). Consequently, the difference between the maximum values of the positive and negative bending moments along the deck in Case (A) is small. However, such a difference is quite large for Case (B), as shown in Fig. 2.5(b). Fig. 2.5(c) shows that Case (A) requires a smaller number of generations to converge to the optimal solution compared to Case (B), i.e. the computational time required to arrive at the optimal post-tensioning cable forces in Case (A) is much less than the time required in Case (B). The maximum vertical deflections of the deck obtained by Case (A) and Case (B) are *0.0031 m* and *0.0143 m*, respectively.

It is obvious from the above that optimizing the shapes of the post-tensioning functions decreases the number of the design variables, which significantly enhances the convergence speed, the accuracy of final solutions, and the performance of the optimization technique. Additionally, optimizing the shapes of the post-tensioning functions makes the design variables not related to the number of stay cables. As previously mentioned, the proposed method is efficient with modern long cable-stayed bridges that contain large numbers of stay cables.

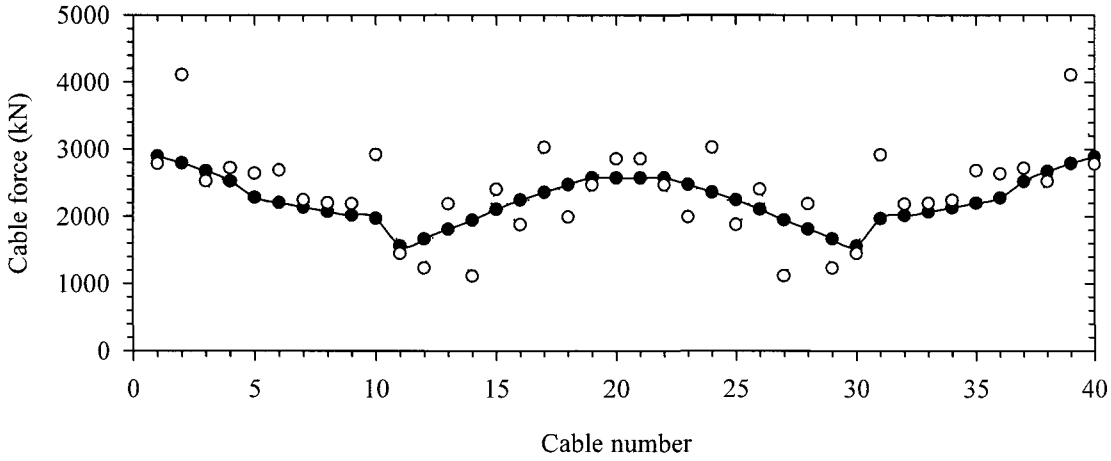

(a) Post-tensioning cable forces.

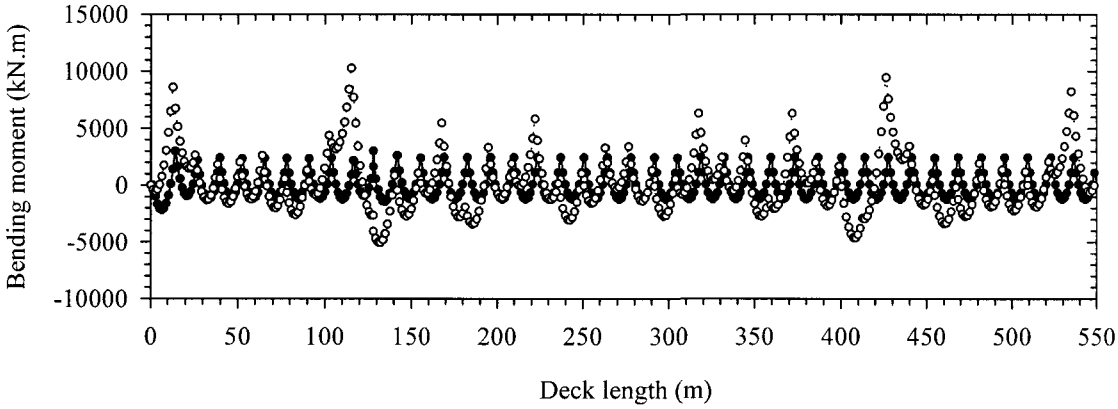

(b) Bending moment of the deck.

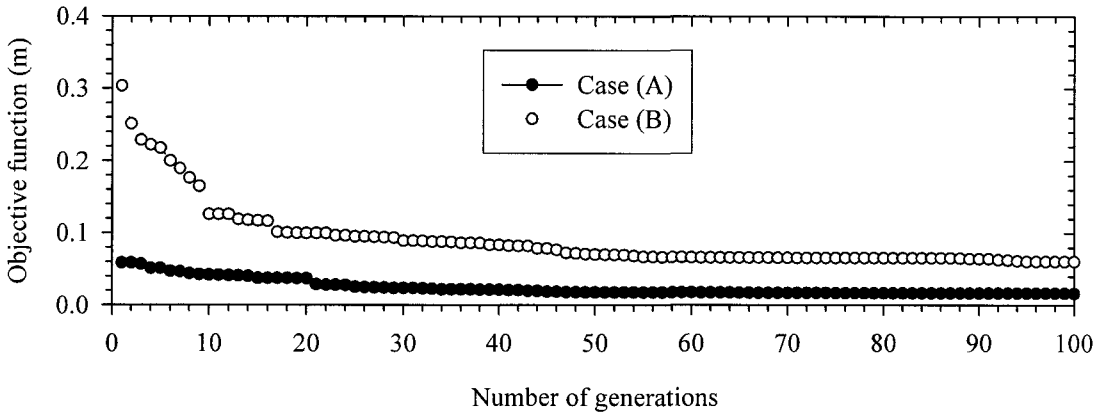

(c) Objective function values for cases (A) and (B).

Fig. 2.5 Effect of decreasing the number of design variables.

2.5.3 Lateral Deflection of the Pylon's Top

In order to demonstrate the importance of minimizing the lateral deflection of the pylons' top, the cable-stayed is analyzed using two different objective functions:

- The first objective function (Obj-1) is defined by Eq. (2.7), which is based on minimizing deflections of both the deck and the pylon.
- The second objective function (Obj-2) is based on optimizing the deflections of the deck only and it is defined as

$$F = \sqrt{(\delta_1^{\,2} + \delta_2^{\,2} + ...)_{deck}} \tag{2.9}$$

where:

$\delta_1, \delta_2, ...$ = vertical deflection of the nodes of the deck spine

Subject to the same constraint defined by Eq. (2.8).

Fig. 2.6(a) shows that the maximum vertical deflection of the deck, without post-tensioning cable forces, is *0.518 m*. After the application of the obtained post-tensioning cable forces resulting from (Obj-1) and (Obj-2), the maximum vertical deflection is reduced to *0.0031* and *0.0035* m, respectively. Both objective functions are able to achieve the convergence tolerance of the deck. The lateral displacements of the pylon's tops along the longitudinal direction of the bridge are found to be *0.1634 m* when subjected to dead load without post-tensioning cable forces as shown in Fig. 2.6 (b).

After the application of the obtained post-tensioning cable forces resulting from (Obj-1) and (Obj-2), these displacements are reduced to *0.0082* and *0.0832 m*, respectively. The (Obj-1) solution gives *95%* reduction in the lateral displacement of the pylon's tops, in comparison with only *50%* reduction obtained by (Obj-2).

Fig. 2.6(c) shows that the absolute bending moment at the pylon base is *24,879 kN.m* without post-tensioning cable forces. After applying the post-tensioning cable forces resulting from (Obj-1) and (Obj-2), the bending moments of the pylon bottom are reduced to *2,174 kN.m* and *14,582 kN.m*, respectively. The (Obj-1) gives *91 %* reduction in the moment at the pylon base, in comparison with *41 %* reduction obtained by (Obj-2).

Fig. 2.6(d) shows the obtained post-tensioning cable forces for one half of the bridge. Due to symmetry, the other half of the bridge will have the same post-tensioning cable forces. The post-tensioning cable forces distribution obtained from (Obj-1) is more uniform than the one obtained from (Obj-2), as shown in Fig. 2.6(d). The maximum difference between the cable forces obtained from (Obj-1) is *1400 kN*, while this difference is *4300 kN* for (Obj-2).

Although both objective functions are able to achieve the convergence tolerance of the deck, there is a significant reduction in the values of the pylon deflection and moment resulting from (Obj-1) compared to the values resulting from (Obj-2). This reduction makes the behaviour of the pylon close to that of a pure axial member, and facilitates the design of the pylon.

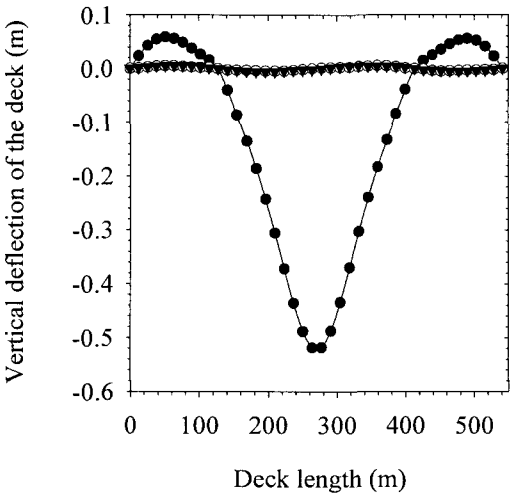

(a) Vertical deflection of the deck.

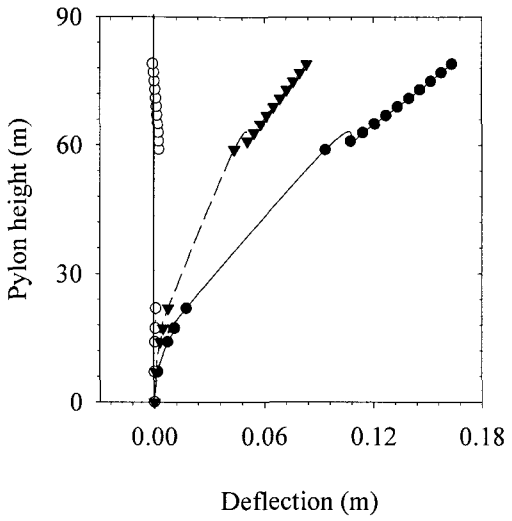

(b) Horizontal deflection of the pylon.

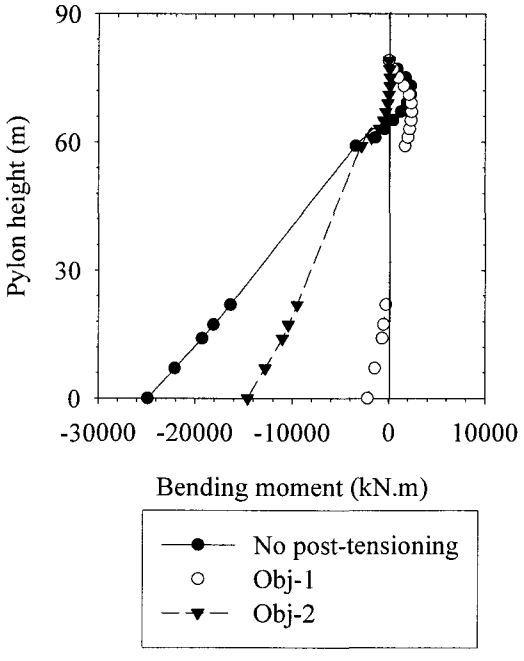

(c) Bending moment of the pylon.

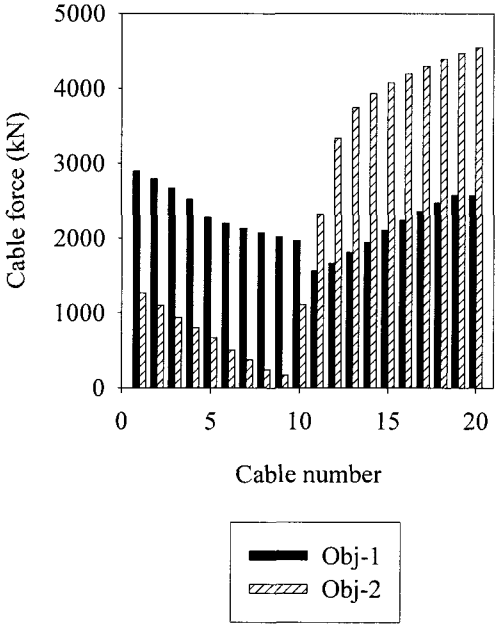

(d) Post-tensioning cable forces.

Fig. 2.6 Effect of minimizing lateral displacements of the pylons' tops.

2.5.4. Assessment for the Effect of the Three Sources of Geometrical Nonlinearities

It is well known that geometric nonlinearities play an important role in the analysis of cable-stayed bridges under design loads. However, the effect of the geometric nonlinearities on the determination of the post-tensioning cable forces is uncertain. Some of the previous studies have considered the effect of the geometric nonlinearities in the determination of the post-tensioning cable forces, however, none of these studies have quantified this effect. The target of this section is to present a comparison between the post-tensioning cable forces with and without the inclusion of the geometric nonlinearities. The effects of large displacement, (P-Δ), and cable sag, which are the three sources of geometric nonlinearities, on the determination of the post-tensioning cable forces are examined. The post-tensioning cable forces for the current bridge are determined on the basis of (1) linear analysis, i.e. first order analysis (LA); (2) nonlinear analysis, i.e. second order analysis, without considering the sagging effect of the cables (NLNS); and (3) full nonlinear analysis, considering the three sources of nonlinearities (NLS).

The results of the analyses, given in Fig. 2.7, show that there is almost no difference between the (LA) and (NLNS) analyses. The bending moment of the deck obtained from the three analyses, provided in Fig. 2.7(a), are the same and equivalent to that of continuous beam resting on rigid supports. The lateral displacements of the pylon's tops, given in Fig. 2.7(b), along the longitudinal direction of the bridge obtained from (LA) and (NLNS) are equal to *0.0082 m.* The corresponding value obtained from (NLS) solution is *0.0087 m*. The values of the bending moment at the pylon base obtained from the three solutions can be detected from Fig. 2.7(c). Both the (LA) and (NLNS) cases

lead to a same value of *2174 kN.m* for the pylon base moment. The corresponding value obtained from (NLS) is *871 kN.m.* The distribution of the cable forces obtained from the three analyses is provided in Fig. 2.7(d). It shows that the differences in the cable forces obtained from the (LA) and (NLS) analyses vary between *4* and *14%.*

The following conclusions can be drawn from these results:

1- The three sources of geometrical nonlinearities have a very slight effect on the determination of the post-tensioning cable forces.

2- The large displacements and (P-Δ) effect do not seem to influence the determination of the post-tensioning cable forces.

3- The sag effect can be considered as the only source of geometric nonlinearities that slightly affects the evaluation of the post-tensioning cable forces.

4- From a practical point of view, the linear analysis is adequate enough to determine the post-tensioning cable forces.

2.6 Conclusions

This study presents a new method that can be used to obtain the optimum post-tensioning cable forces for cable-stayed bridges under the effect of dead load. In this method, the finite element method, B-spline curves, and real coded genetic algorithm (RCGA) are utilized. The B-spline curves are used to model the post-tensioning functions along the bridge deck. The real coded genetic algorithms (RCGA) are employed to optimize shapes of the post-tensioning functions to achieve minimum deflections along the bridge deck. Positions of the control points are treated as the design variables rather than the cable forces.

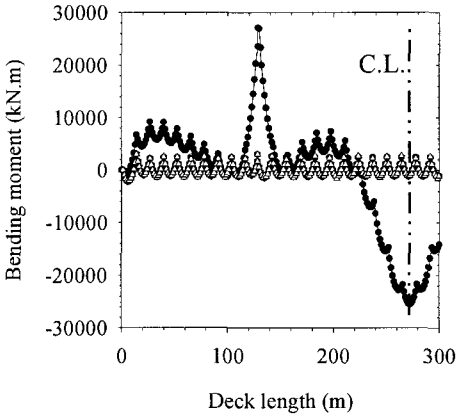

(a) Bending moment of the deck.

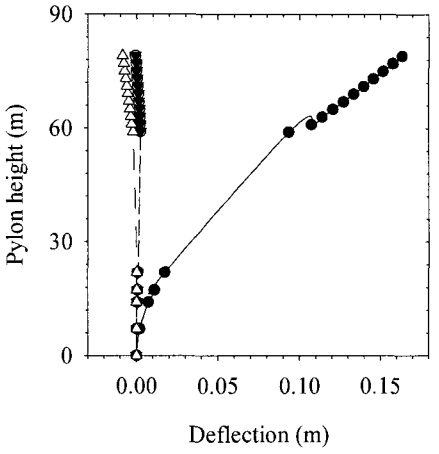

(b) Horizontal deflection of the pylon.

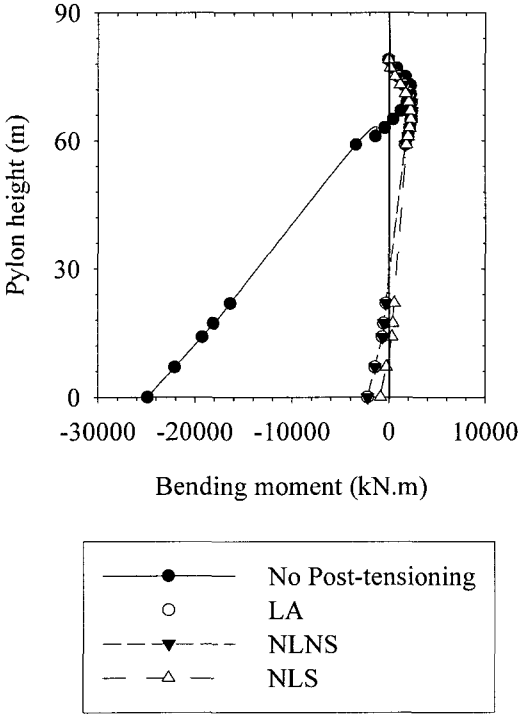

(c) Bending moment of the pylon.

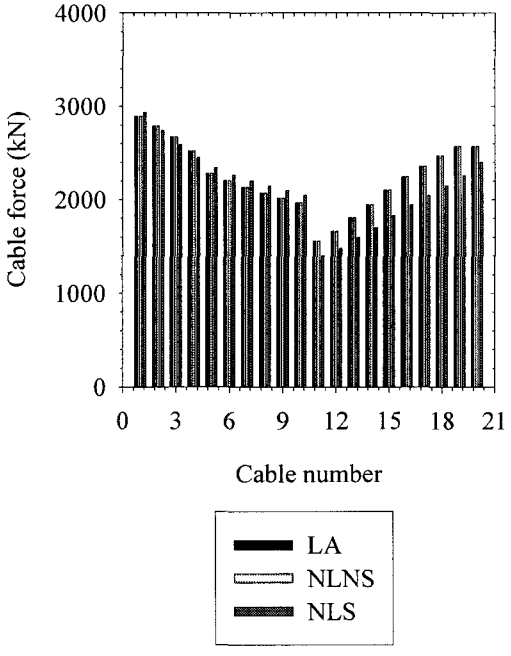

(d) Post-tensioning cable forces.

Fig. 2.7 Effect of geometric nonlinearities on post-tensioning cable forces.

This significantly reduces the number of design variables, leading to a decrease in the computational time, and an improvement in the accuracy of the final solution. In addition, such a reduction increases the probability of finding the global optimum post-tensioning cable force. The proposed method is efficient for bridges having large number of stay cables.

One of the advantages of the proposed method compared to previous techniques is that it minimizes transverse deflections for both the deck and the pylon, simultaneously. It also provides the optimal post-tensioning cable forces distribution that minimizes moment distributions along the deck and the pylon. The results shows that the proposed objective function achieves 95 % reduction in the displacement of the pylon's top and 91 % reduction in the moment at the pylon base, with a uniform distribution of the post-tensioning forces among various cables. Therefore, it leads to the optimal structural design of the whole cable-stayed bridge.

The study shows that the sag effect is the only source of geometric nonlinearity that slightly affects the determination of the post-tensioning cable forces. Accordingly, from an engineering point of view, a linear analysis is sufficient for the determination of the post-tensioning cable forces.

2.7 References

1. Gimsing NJ. Cable supported bridges: Concepts and design. John Wiley& Sons Ltd; 1997.
2. Wang PH, Tseng TC, Yang CG. Initial shape of cable-stayed bridges. J Comput Struct 1993; 46:1095-1106.

3. Negrão JHO, Simões LMC. Optimization of cable-stayed bridges with three-dimensional modelling. J Comput Struct 1997;64:741-758.
4. Simões LMC, Negrão JHJO. Optimization of cable-stayed bridges with box-girder decks. J Adv. Eng. Software 2000; 31:417-423.
5. Chen DW, Au FTK, Tham LG, Lee PKK. Determination of initial cable forces in prestressed concrete cable-stayed bridges for given design deck profiles using the force equilibrium method. J Comput Struct 2000;74:1–9.
6. Janjic D, Pircher M, Pircher H. Optimization of cable tensioning in cable-stayed bridges. J Bridge Eng ASCE 2003;8:131–137.
7. Lee TY, Kim YH, Kang SW. Optimization of tensioning strategy for asymmetric cable-stayed bridge and its effect on construction process. J Struct Multidisc Optim 2008;35:623–629.
8. Wilson JC, Gravelle W. Modelling of a Cable-stayed Bridge for Dynamic Analysis. J Earthquake Eng & Struct Dyn 1991;20: 707-721.
9. Ernst JH. Der E-Modul von Seilen unter berucksichtigung des Durchhanges. Der Bauingenieur 1965; 40(2):52–5 (in German).
10. Weaver W Jr, Gere JM. Matrix Analysis of Framed Structures. 3rd Edn, New York: Van Nostrand Reinhold; 1980.
11. Nazmy AS, Abdel-Ghaffar AM. Three-dimensional nonlinear static analysis of cable-stayed bridges. J. Comput Struct 1990a; 34(2):257–271.
12. Piegl L, Tiller W. The NURBS book. 2nd Edn, Springer, New York;1997.
13. Piegl L. On NURBS: a survey. Computer Graphics and Applications, IEEE 1991;11(1):55 – 71.

14. Pourazady M, Xu X. Direct manipulations of B-spline and NURBS curves. Advances in Engineering Software 2000;31(2):107-118.

15. Rao S S. Engineering optimization: theory and practice. 4th Edn, N.J.: John Wiley & Sons;2009.

16. Gen M, Cheng R. Genetic algorithms and engineering optimization. Wiley, New York; c2000.

17. Gen M, Cheng R. Genetic algorithms and engineering design. Wiley, New York; c1997.

18. Goldberg DE. Genetic Algorithms in search, Optimization and Machine Learning. Addison-Wesley Publishing Company, Inc., New York; 1989.

19. Davis L. Handbook of Genetic Algorithms, Van Nostrand Reinhold, New York; 1991.

20. Michalewicz Z, Fogel DB. How to solve it: modern heuristics. 2nd Edn New York: Springer, c2004.

CHAPTER 3

SURROGATE FUNCTION OF POST-TENSIONING CABLE FORCES FOR SEMI-FAN CABLE-STAYED BRIDGES

3.1 Introduction

Cable-stayed bridges have been known since the beginning of the 18th century, but a great interest has been shown for long-span cable-stayed bridges only in the last thirty years. Cable-stayed bridges provide an economical solution for the range of medium to long-span bridges, and offer varieties to designers regarding not only the materials, but also the geometric arrangements. Compared with suspension bridges, cable-stayed bridges are stiffer and require less material, especially for cables and abutments. Moreover, they are elegant, and much easier in erection (Troitsky, 1988).

Typically, stay cables of a cable stayed bridge are post-tensioned to off-set the effect of the bridge dead load. The post-tensioning cable forces directly influence the performance and the economical efficiency of the bridge, as they control the distribution and magnitude of the internal forces, adjust the bridge deck profile, and affect the overall design of the bridge. The post-tensioning cable forces minimize the vertical deflection of the deck, and the lateral deflection of the pylon along the longitudinal direction of the bridge. Accordingly, the bending moment distribution along the deck becomes equivalent to that of a continuous beam resting on a series of rigid supports located at the cable-deck connections, and the pylon tends to behave as a pure axial member.

The determination of an optimum distribution of post-tensioning cable forces is considered one of the most important and difficult tasks in the design of cable-stayed bridges. The new trend towards very long-span cable-stayed bridges (main span more

than *1000 m*) requires using a large number of stay cables. This trend significantly increases the bridge redundancy, and sophisticates the determination of the optimum post-tensioning cable forces. This topic has been studied by a number of researchers including Wang *et al.* [1993], Simões and Negrão [2000], Negrão and Simões [1997], Chen *et al.* [2000], and Janjic *et al.* [2003]. A critical review for available methods to evaluate post-tensioning cable forces leads to the following observations:

1. Existing commercial software packages can not be used directly to evaluate the post-tensioning forces. Accordingly, specific computer code needs to be developed by the designer to achieve this task, which requires strong programming skills.
2. The evaluation of the post-tensioning forces requires the development of a complete numerical model for the bridge.
3. The input and output data associated with all these methods are large and tedious to prepare and interpret.
4. All the methods are complex (Sung *et al.,* 2006) and (Lee *et al.,* 2008) as they are iterative, and require a wide knowledge of many mathematical and numerical techniques.
5. An increase in the number of stay cables complicates the calculations, and makes it harder to find a suitable solution.
6. Some methods have numerical problems, therefore, the solution is not guaranteed.

The design process of a cable-stayed bridge involves a preliminary study aimed to check the feasibility of the project, as well as to estimate the quantities required for its completion. Usually, this study is very crucial to obtain the optimum design (Hong *et al*, 2002), and it is conducted by considering a large number of design trials. These trials

involve several modifications in the bridge layout including the geometrical configurations, cross sections dimensions, number of cables, arrangement of cables, and type of pylons. A new set of the post-tensioning cables distribution is required for each trial, since each modification affects such a distribution. Unfortunately, the available methods for determining the post-tensioning cable forces are not efficient in this stage, as they require significant computational efforts and excessive time.

On the other side, the existing algorithms for optimizing cable-stayed bridges generate a tremendous number of candidates (cable-stayed bridges) in order to achieve the optimum design solution. Each single candidate has different design variables that lie between the upper and lower bounds of the design variables. Accordingly, the candidate requires a different post-tensioning cables forces distribution. As such, the algorithm for solving such optimization problem is computationally prohibitive, since it leads to a very expensive final solution as experienced by the authors.

In the light of the above, there is an obvious need for a simplified fast method, with sufficient accuracy, that can be used during the preliminary design stages to evaluate the post-tensioning cable forces. Shortening the time spent in the evaluation of the post-tensioning cable forces during the preliminary design stage of the bridge leads to a reduction in the design cost, improvement of the quality of the results, and remarkable benefits for the remaining design stages. In addition, such a fast method will make the optimization studies of this kind of bridges applicable.

In the current study, surrogate polynomial functions that can be used to evaluate post-tensioning cable forces in a semi-fan cable stayed bridge under the action of dead load are developed. Based on the literature review, the current investigation represents the first

attempt to introduce such surrogate functions. The ordinary least squares method (*OLS*), as a technique of fitting data, is utilized to estimate the regression coefficients in post-tensioning polynomial functions. The post-tensioning optimization method developed in Chapter (2) is used to determine the optimum distribution of the cables post-tensioning forces. This adopted method combines the finite element method, the B-spline function, and the real coded genetic algorithm. The current study focuses on bridges with a semi-fan cable arrangement because of its efficiency and the geometrical freedom that it provides to the cable anchor positions on the pylon.

3.2 Analysis Procedure

3.2.1 Semi-Fan Cable-stayed Bridges

In general, harp, fan, and semi-fan arrangements are the most common forms of stay cables arrangements, as shown in Fig. 3.1(a) (Gimsing, 1997). The harp layout appears to be less suitable for large-span bridges, as it needs taller pylon, and produces high forces in the stay cables (Walther *et al.,* 1988). In the fan pattern, increasing the number of the stay cables increases the anchorages weights, and makes them difficult to accommodate. Therefore, the fan patterns are suitable only for moderate spans with a limited number of stay cables (Walther *et al.,* 1988). A semi-fan pattern is preferable for a cable-stayed bridge, as it is provides an intermediate solution between the harp and fan patterns. The semi-fan pattern combines the advantages and avoids the disadvantages of the fan and harp patterns. The semi-fan pattern has been chosen for a large number of modern cable-stayed bridges, e.g. the world's longest cable stayed bridge main span, the Sutong Bridge in China (main span *1088 m*). Therefore, the semi-fan configuration is adopted in this

study. The proposed study can be extended in future to cover the other two cables configurations.

A schematic of a typical semi-fan cable stayed bridge is provided in Fig. 3.1(b), showing the variables defining the geometry of the bridge. The lengths of the main span and the two side spans are (M) *m* and (S) *m*, respectively. The total length of the bridge is denoted as (*L*) *m*. The total height of the pylons' tops above the bridge deck is (H) m. The deck superstructure is supported by four groups of double plane stay cables in semi-fan type arrangement. The single plane in each group has (*N*) stay cables. As such, there are (*8N*) stay cables supporting the whole bridge. The two pylons of the cable-stayed bridge are H-shaped structures with a width of (*B*) m. An upper strut cross beam connects the two upper legs at height (h_B) measured from the deck, and a lower strut cross beam supports the deck, as shown in Figs. 3.1(b) and 3.1(c). The stay cables are distributed within a height of (h_T) from the upper strut. The distance between the cables anchorages is chosen to be *2.0 m*, which is considered to be sufficient for practical installation. As such, the distance (h_T) is considered constant for each specific number of stay cables and is equal to (*N x 2.0 m*).

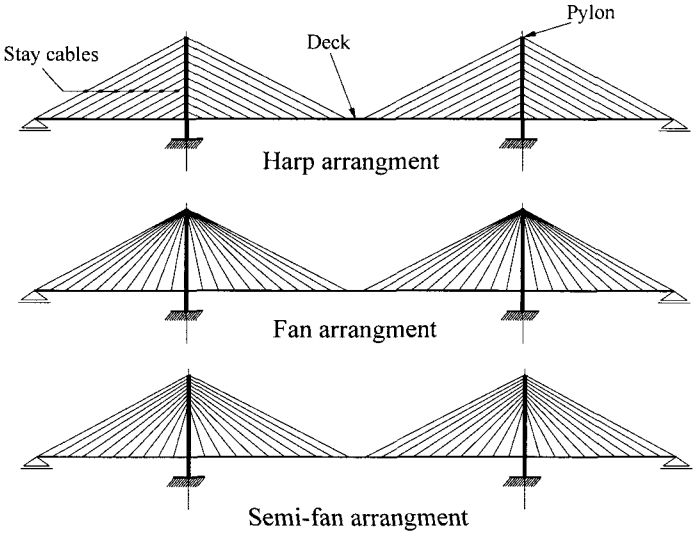

(a) Cable arrangements in cable-stayed bridges

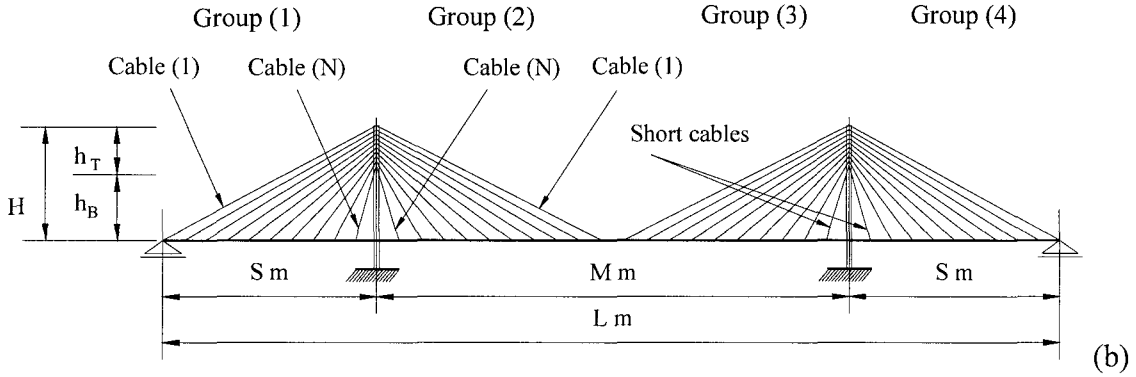

(b)

Geometry of bridge.

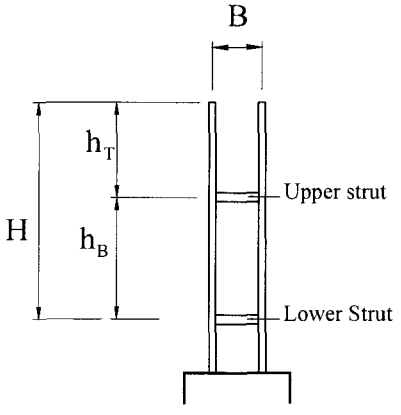

(c) Pylon elevation

Fig. 3.1 Bridge layouts and geometry

3.2.2 Parameters Influencing Post-tensioning Cables Forces

Several parameters can affect the behaviour of cable stayed bridges, such as the number of cables, main span length, height of the pylon above the deck, cross-sectional dimensions of the bridge members, and stay cables arrangement. Moreover, the high redundancy of such structures magnifies the interaction between these design parameters. The order of the sought post-tensioning polynomial function is expected to increase when all the above design parameters are considered. This can lead to a serious abuse of the regression analysis, in the form of formation ill-conditioned matrices and non-accurate estimation of the regression parameters (Montgomery *et al.,* 2006). Therefore, it is advisable to keep the order of the surrogate post-tensioning functions as low as possible. A careful investigation of the behaviour of cable-stayed bridges under the application of the post-tensioning cable forces guides and justifies to the following assumptions:

1. Geometric nonlinearities have very small effect on the evaluation of the post-tensioning cable forces as illustrated in Chapter (2). Consequently, the geometric nonlinear effects are not considered in this study.
2. Since the behaviour of the bridge is linearly elastic, the post-tensioning cable forces changes linearly with the magnitude of the distributed load acting on the deck. The surrogate functions describing the post-tensioning cable forces are developed using a unit value for a uniformly distributed vertical load acting along the bridge deck.
3. The bridge deck is usually composed of a large concrete deck slab having a very large axial stiffness. Consequently, the axial deformation of the deck is very small, and can be neglected.

4. The vertical moment of inertia of the deck has a very slight effect on the cable forces (Walther *et al.*, 1988). Accordingly, the moment of inertia of the deck is not varied in the conducted parametric study.
5. In three spans cable-stayed bridges, the choice of a very stiff pylon is not recommended since the overall stability of the bridge is provided by the stay cables (Walther *et al.*, 1988). Accordingly, the lateral stiffness of the pylon in the longitudinal direction of the bridges is not varied in the parametric study.

In view of the previous assumptions, the parameters that notably govern the magnitude and distribution of the post-tensioning cable-forces are:

1. Number of stay cables in each group (N).
2. Main span length (M).
3. Height of the pylon, which is varied by changing the upper strut height (h_B).

3.2.3 Determination of Post-Tensioning Cable Forces

The optimization method developed in Chapter (2) is adopted in this study to determine the post-tensioning cable forces in semi-fan cable-stayed bridges. The method has several advantages over other post-tensioning methods in the literature. This optimization method is capable of determining the global optimum post-tensioning distribution, while achieving minimum deflections for both the deck and the pylon, simultaneously. The optimization method combines three numerical schemes; finite element modeling (FEM), B-spline function, and real coded genetic algorithm (RCGA). The B-spline curves are used to model the distribution of post-tensioning functions along the bridge. The Genetic Algorithm (GA), as a global search technique, is utilized to optimize the shapes of the

post-tensioning functions, instead of the cable forces. A brief description of the optimization method is given in the next section. More details about this method can be found in Chapter (2).

3.2.3.1 Finite Element Formulation

Three-dimensional frame elements are used to model the deck and the pylons, while three-dimensional cable elements are used to simulate the cables. The deck is modeled using a single spine passing through its shear center (Wilson and Gravelle, 1991). A typical finite element model is shown in Fig. 3.2(a).

3.2.3.2 Representation of the Cable Forces by B-Spline Function

The distributions of post-tensioning cable forces along the span of a cable-stayed bridge show that they follow an arbitrary polynomial function, which can be represented by an p^{th} order polynomial

$$f = a_1 x^n + a_2 x^{n-1} + a_3 x^{n-2} + a_4 x^{n-3} + ... + a_p \tag{3.1}$$

where f is the post-tensioning cable function, and x is the length coordinate along the bridge span. It is difficult to predict the proper range of values of the coefficients a_i for a specific optimization problem. The optimum function f has often a complicated shape that should be described by high order polynomials with a large number of coefficients. Furthermore, the coefficients a_i impart very little geometric insight about the shape of the post-tensioning function.

Due to the limitations and disadvantages of the power polynomial functions, B-spline curves are selected to represent the post-tensioning functions. B-spline curves are

piecewise polynomials that remedy all the shortcomings associated with the power polynomial curves. They are piecewise polynomials that permit the accurate design of complex curves using lower-degree polynomials. They have local control property that allows the user to modify a specific part of a curve and leaves the rest of the curve unchanged. The properties and the advantages of the B-spline curves and B-spline basis function are given in Piegl [1991] and Pourazady and Xu [2000].

A p^{th} degree B-spline curve is defined by

$$C(u)=\sum_{i=0}^{n} N_{i,p}(u)P_i \qquad 0\le u\le 1 \tag{3.2}$$

where u is an independent variable, P_i are the control points. The polygon formed by the P_i is called the control polygon. The $N_{i,p}(u)$ are the p^{th} degree B-spline basis function equation given as:

$$N_{i,0}(u)=\begin{cases}1 & if\ \ u_i\le u\le u_{i+1}\\ 0 & otherwise\end{cases} \tag{3.3-a}$$

$$N_{i,p}(u)=\frac{u-u_i}{u_{i+p}-u_i}N_{i,p-1}(u)+\frac{u_{i+p+1}-u}{u_{i+p+1}-u_{i+1}}N_{i+1,p-1}(u) \tag{3.3-b}$$

and they are defined on nonperiodic and nonunifrom knot vector

$$U=\left\{\underbrace{0,.....,0}_{p+1},u_{p+1},.....,u_{m-p-1},\underbrace{1,.....,1}_{p+1}\right\} \tag{3.4}$$

The degree of the basic function p, number of knots = $(m+1)$, and the number of control points = $(n+1)$ are related by the formula $m = n + p + 1$. In general, slight variations in the location of the control points change the shape of the B-spline function significantly. Therefore, the control points are adopted in this work as design variables. Shape optimizations of post-tensioning cable functions are carried out by the simultaneous

modification of the control points' positions. The process of modification goes on until the shape of the curve satisfies the required criteria of the deck.

Determining the location of a point on a B-spline curve at a certain value u is briefly summarized by the following steps:

1- Assign the number of the control points ($n+1$), the degree of the function (p), and then calculate the number of knots ($m+1$).

2- Define coordinates of the B-spline control points.

3- Calculate the nonzero basis functions.

4- Multiply the values of the nonzero basis function with the corresponding control points.

3.2.3.3 Real Coded Genetic Algorithms

In spite of the apparent simplicity of the post-tensioning shape function, the search space of this function is complex and contains several local minima due to the high redundancy of cable-stayed bridges, and the intersection of the constraints with the objective function (Chapter (2)). The real coded genetic algorithms (RCGA) are employed to optimize the shape of the B-spline curves along the bridge deck. (RCGA) is well suited to structural optimization problems since they have more potential to determine the global optimization solutions (Gen and Cheng, 2000) and (Gen and Cheng, 1997). A complete description of GAs techniques and their variants can be found in Davis [1991].

The x and y-coordinates of the B-spline control points are the design variables (P_i in Fig. 3.2(b)). The design variables define the shape of the B-spline curve that represents the distribution of the post-tensioning cable forces. In Fig. 3.2(b), cables number i,j,k and l

are mapped to their respective post-tensioning force values on the B-spline curves for exemplary purpose. The upper and lower bounds for the x-coordinates are the span length and zero, respectively, i.e. (span length $\geq x \geq 0$). The upper and lower bounds for the y-coordinates are a preset value for the maximum cables tensile force (T_{max}) and zero, respectively, i.e. ($T_{max} \geq y \geq 0$).

The following steps describe how the real coded genetic algorithm is adapted to the problem at hand to find the optimum post-tensioning cable forces.

1. Develop a three dimensional finite element model of the cable-stayed bridge according to the geometry and physical properties of the bridge, as described in Section (3.2.3.1).
2. Create an initial population of the design variables, which are the x and y-coordinates of the B-spline control points, randomly between the lower and upper bounds of each design variable, using the (RCGA) algorithm. Each search point in the population is used to draw a candidate function for the post-tensioning cable forces, as described in Section (3.2.3.2). The initial population contains *100* candidate post-tensioning functions.
3. Use the post-tensioning function to evaluate the forces at all cables. Apply these forces to the *3-D FEM* together with the own weight of the bridge and analyze the structure to obtain the nodal deflections. The corresponding objective function (F) to be minimized is then calculated according to the following equation:

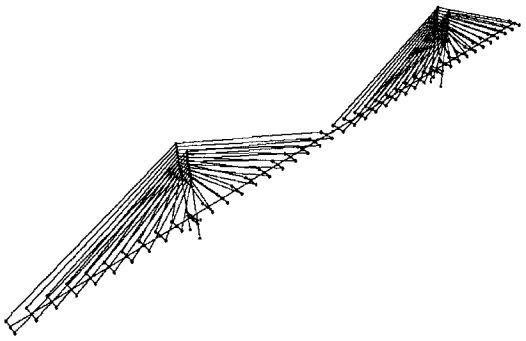

(a) Finite element model.

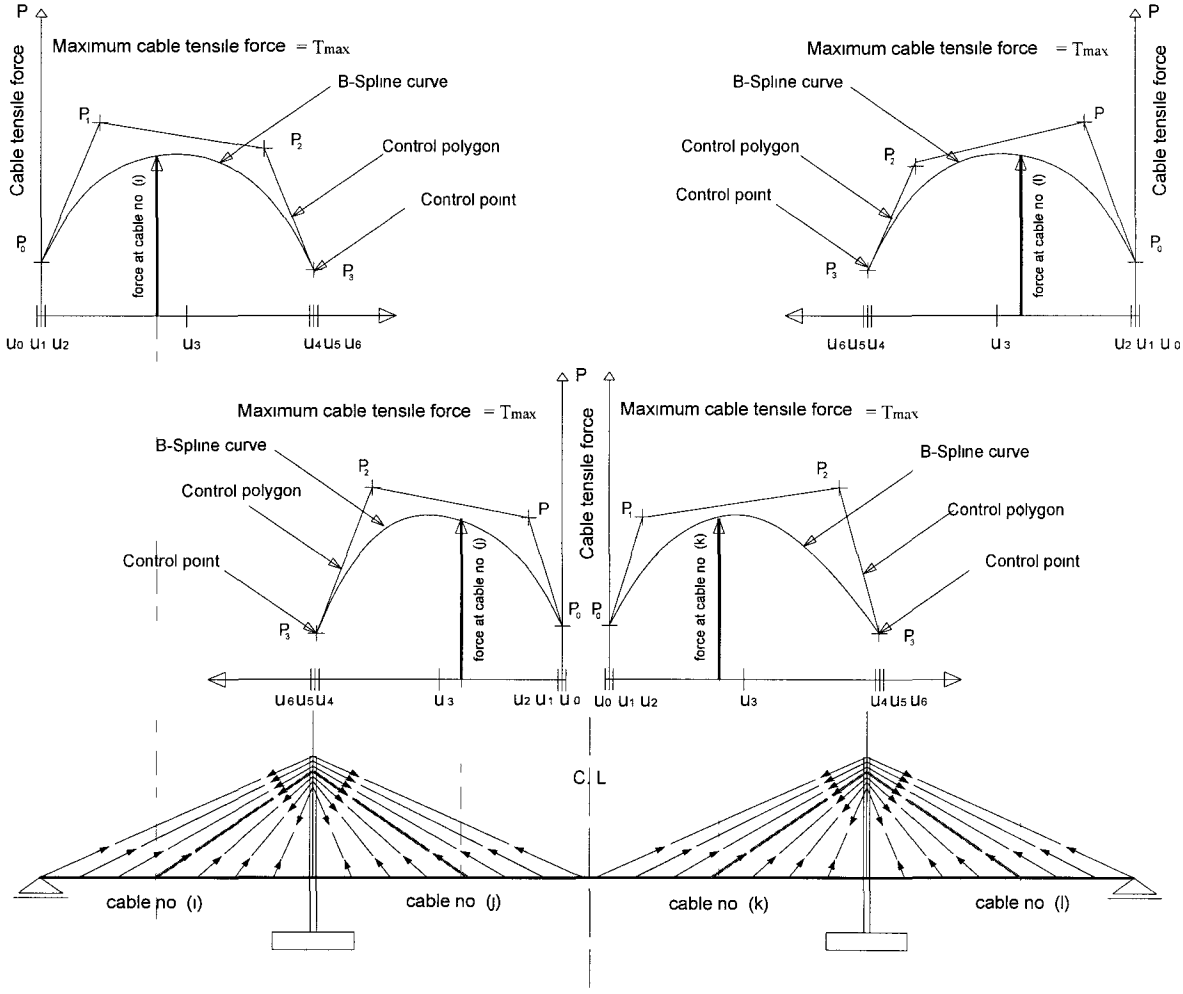

(b) Representation of the cable forces by B-spline curve.

Fig. 3.2 Finite element model and post-tensioning curves.

$$F = \sqrt{(\delta_1^{\,2} + \delta_2^{\,2} + ...)_{deck} + (\delta_{1p}^{\,2} + \delta_{2p}^{\,2} + ...)_{Pylon}} \tag{3.5}$$

where:

$\delta_1, \delta_2, ...$ = vertical deflection of the nodes of the deck spine

$\delta_{1p}, \delta_{2p}, ...$ = lateral deflections of the pylons' tops

Subject to the following constraint:

$$\left| \frac{maximum\ vertical\ deflection\ of\ the\ deck\ (\delta_{max})}{lenght\ of\ main\ span\ (M)} \right| \leq \varepsilon \tag{3.6}$$

where ε is a convergence tolerance, which is set equal to 10^{-4}.

4. Sort the initial population in ascending order according to the value of the objective function (F) such that the first ranked candidate "post-tensioning function" has the minimum value for (F).
5. Generate, using the RCGA, a new population by applying the crossover and mutation operators on the high ranked post-tensioning functions evaluated at step 4. These operators direct the search towards the global optimum solution. A description of these RCGA operators is provided in the next section.
6. Replace the previous population with the newer one containing the new candidate functions, in addition to the best candidate function found so far (elitist selection).
7. Repeat steps from *3* to *6* until the convergence tolerance, described by Eq. (3.6), is achieved.
8. Deliver the candidate post-tensioning function obtained at step *7* as the final solution.

The procedure described above is summarized in the flow chart shown in Fig. 3.3.

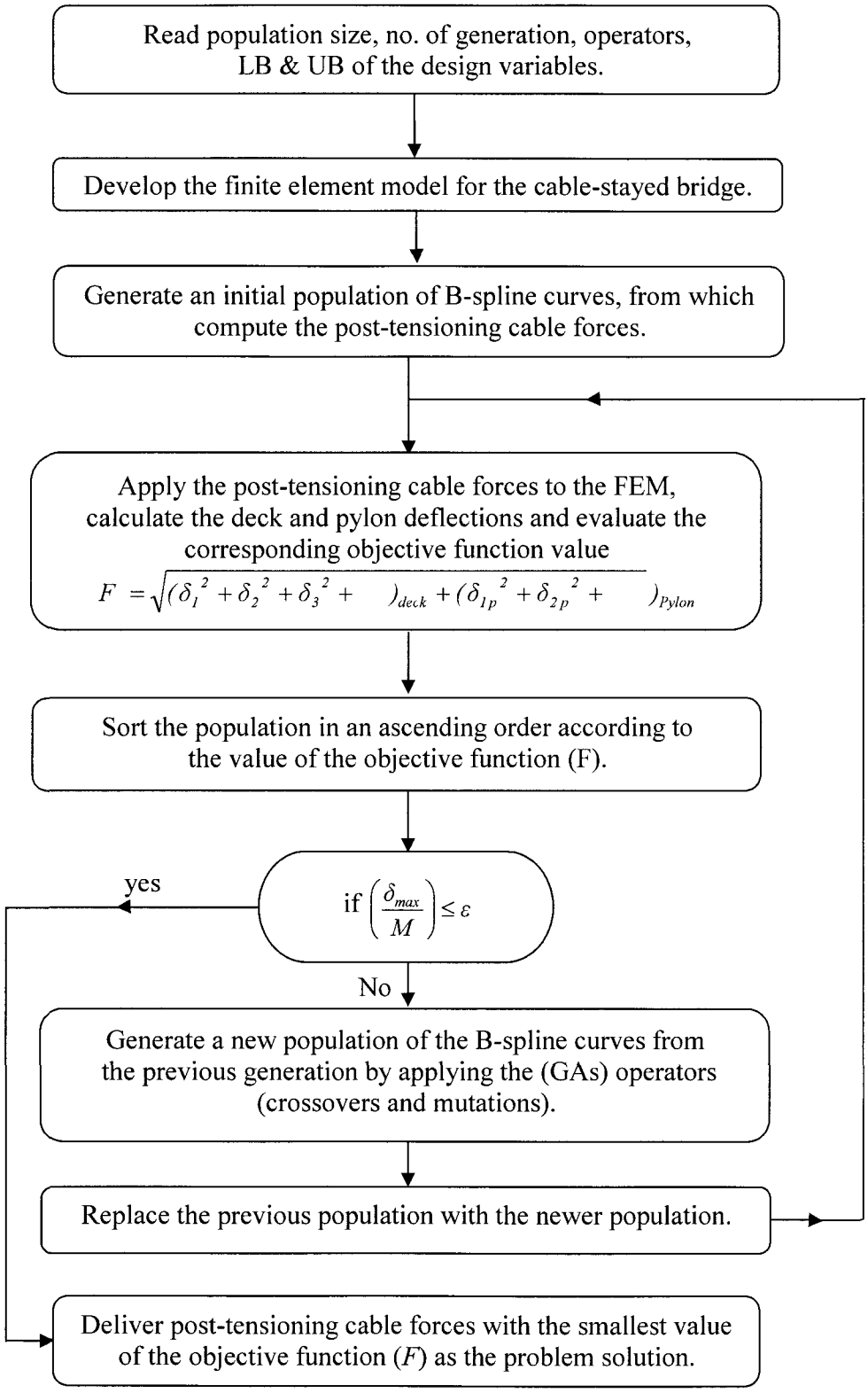

Fig. 3.3 Flow chart for evaluation of the optimum post-tensioning cable forces.

3.2.4 Ordinary Least Squares

The ordinary least squares method (*OLS*), as a technique of fitting data, is utilized in the current study for obtaining estimates of regression coefficients in post-tensioning surrogate polynomial functions. (*OLS*) is selected because it provides simple expressions for the estimated coefficients, in addition to the statistical parameters associated with the developed relations such as the estimation of standard errors (*SE*), and the computation of F-tests (Kutner *et al.*, 2004). (*OLS*) is commonly used to analyze both experimental and observational data due to its good statistical properties.

3.2.4.1 Estimation of Regression Coefficients in Post-Tensioning Functions

In order to present in a dimensionless form, the design parameters are modified as follows:

1. γ_1 = main span length / total length of the bridge = (M/L) (3.7-a)
2. γ_2 = upper strut height / total length of the bridge = (h_B/L) (3.7-b)
3. The total length of the bridge is divided by an arbitrary distance of *1000 m*, leading to the following dimensionless parameter:

   γ_5 = total length of the bridge */1000 m* = $(L/1000)$ (3.7-c)

Several regression models are attempted to determine the one that best fits the post-tensioning cable forces. The following second-order regression model, with three predictor variables, is found to provide accurate means for calculating the post-tensioning cable forces.

$$F_i = \beta_o + \beta_1 X_{i1} + \beta_2 X_{i2} + \beta_3 X_{i3} + \beta_{11} X_{i4} + \beta_{22} X_{i5} + \beta_{33} X_{i6} + \beta_{12} X_{i7} + \beta_{13} X_{i8} + \beta_{23} X_{i9} + \varepsilon_i \quad (3.8)$$

where:

F_i = force in cable number (i)

$\beta_o, \beta_1, \beta_2, \beta_3, \beta_{11}, \beta_{22}, \beta_{33}, \beta_{12}, \beta_{13}, \beta_{23}$ are unknown parameters to be determined from *the regression analysis*

$X_{i1} = \gamma_{i1}^2, \quad X_{i2} = \gamma_{i2}^2, \quad X_{i3} = \gamma_{i5}^2,$

$X_{i4} = \gamma_{i1} \cdot \gamma_{i2}, \quad X_{i5} = \gamma_{i1} \cdot \gamma_{i5}, \quad X_{i6} = \gamma_{i2} \cdot \gamma_{i5},$

$X_{i7} = \gamma_{i1}, \quad X_{i8} = \gamma_{i5}, \quad X_{i9} = \gamma_{i2}$

ε_i are normal errors

The coefficient β_{11} is the interaction effect parameter between the main span length (M) and the upper strut height (h_B). The coefficient β_{22} is the interaction effect parameter between the main span length (M) and the bridge length (L). The coefficient β_{33} is the interaction effect parameter between the upper strut height (h_B) and the bridge length (L). Since the bridge has several cables (N), the previous linear regression model Eq. (3.8) is expressed in matrix terms as follow:

$$F_{Nx1} = \begin{bmatrix} F_1 \\ F_2 \\ \vdots \\ F_N \end{bmatrix}, \qquad X_{NxP} = \begin{bmatrix} 1 & X_{11} & X_{12} & \cdots & X_{1,P-1} \\ 1 & X_{21} & X_{22} & \cdots & X_{2,P-1} \\ \vdots & \vdots & \vdots & & \vdots \\ 1 & X_{N1} & X_{N2} & \cdots & X_{N\,P-1} \end{bmatrix} \tag{3.9-a}$$

$$\beta_{px1} = \begin{bmatrix} \beta_1 \\ \beta_2 \\ \vdots \\ \beta_{P-1} \end{bmatrix}, \qquad \varepsilon_{Nx1} = \begin{bmatrix} \varepsilon_1 \\ \varepsilon_2 \\ \vdots \\ \varepsilon_n \end{bmatrix} \tag{3.9-b}$$

In matrix terms, the general linear regression model, Eq. (3.8) is:

$$F_{Nx1} = X_{Nxp}\,\beta_{Px1} + \varepsilon_{Nx1} \tag{3.10}$$

where:

F is a vector of cable forces

β is a vector of parameters

X is a matrix of constants

ε is a vector of independent normal random variables with expectation

In particular, the (*OLS*) method considers the sum of the (N) squares deviations. This criterion is denoted by Q:

$$Q = \sum_{i=1}^{N} (F_i - \beta_o - \beta_1 X_{i1} - \beta_2 X_{i2} - \beta_3 X_{i3} - \cdots\cdots - \beta_{P-1} X_{i,P-1})^2 \tag{3.11}$$

The least squares coefficients are those values of β_o, β_1, ..., β_{P-1} that minimize Q.

Assume the vector of the least squares estimated regression coefficients b_o, b_1,... b_{p-1} as b:

$$b_{px1} = \begin{bmatrix} b_o \\ b_1 \\ \vdots \\ b_{P-1} \end{bmatrix} \tag{3.12}$$

The least squares normal equations for the general regression model, Eq. (3.10) are:

$$X'\ X\ b = X'\ F \tag{3.13}$$

and the least squares estimators are:

$$b = (X'X)^{-1} X'F \tag{3.14}$$

3.2.5 Development of the Post-Tensioning Functions

A large parametric study is conducted by repeating the finite element/optimization technique, while varying the three parameters (γ_1, γ_2, and γ_5) and the number of cables

(N). The values of the above parameters are chosen to cover a wide range of practical dimensions of cable-stayed bridges. The range and the incremental variation of γ_1, γ_2, γ_5, and (N) are given in Table 3.1. The upper limit of the bridge length (L) is selected to cover a wide range of bridge lengths. The upper and lower bounds of (γ_1) are the most common ratios used today in cable-stayed bridges design, as they do not require stiff pylons. In fact, the increase in inertia of pylons results in an increase in maximum moments in the pylon. Therefore, form an economical point of view, it is better to depend on the stay cables system to support the deck instead of using stiffer pylons. The parametric study is carried out by considering all possible combinations of (γ_1, γ_2, γ_5) and (N). A total number of *1800* analyses are conducted in the study. Each analysis involves the steps described in the flow chart provided in Fig. 3.3. Unfortunately, the estimated computational time for this study is about *300* days on a normal every day personal computer, making it inapplicable. However, the current study has been conducted using a supercomputer, the Shared Hierarchical Academic Research Computing Network, SHARCNET, by allocating *256* CPU days for this research.

Table 3.1 Range of variation and Increment of the geometrical layout

Parameter	Smallest value	Largest value	Increment
$\gamma_1 = (M/L)$	0.48	0.54	0.02
$\gamma_2 = (h_B/L)$	0.03	0.11	0.02
$\gamma_5 = (L/1000m)$	0.20	1.10	0.1
N	5	13	1

A regression analysis is then conducted to analyze the post-tensioning cable forces data and estimates the regression coefficient in the post-tensioning polynomial functions described in Section (3.2.4). The values of these coefficients are given in Appendix (I). Each table in the Appendix (I) presents the coefficients of the post-tensioning functions for a specific number of cables (N). Due to symmetry, the coefficients of the cables forces in Group (1) and (2) are only given. The post-tensioning cable force (F_i) in cable number (i) is given by:

$$F_i = w \left(b_o + b_1\gamma_1^2 + b_2\gamma_2^2 + b_3\gamma_5^2 + b_{11}\gamma_1\gamma_2 + b_{22}\gamma_1\gamma_5 + b_{33}\gamma_2\gamma_5 + b_{12}\gamma_1 + b_{13}\gamma_5 + b_{23}\gamma_2 \right) \tag{3.15}$$

where;

w is the uniform dead load acting on the deck (kN/m).

b_o, b_1,.. are the constant values, given in Appendix (I).

γ_1, γ_2, and γ_5 are the dimensionless parameters, given by Eqs. (3.7-a), (3.7-b), and (3.7-c).

3.2.6 Accuracy Assessment for the Regression Models

In order to verify the accuracy of the developed regression relations, the Econometric View Software (2008) is used to examine the statistical parameters associated with these relations. These statistical parameters are described by Devore [1995] and Anderson and Sclove [1986]. Checking these parameters for the present regression analysis shows that:

1) In all cases, the value of the standard error of the regression model ($\hat{\sigma}^2$) does not exceed 0.0039. This parameter is calculated using the following relation:

$$\hat{\sigma}^2 = MSE = \frac{SSE}{n-(k+1)} \tag{3.16}$$

where *SEE* is the sum of squared residual (or error sum of square), n is the number of data points, and *(k+1)* is the number of repressors including the constant term used in the relation. This implies that almost all points are well described.

2) The coefficient of multiple determination (R^2) is always larger than *0.9802*. This result is corroborated by checking the adjust coefficient of multiple determination ($\overline{R}^2$) which is shown larger than *0.9800* for all cases. These parameters are defined by the following relations:

$$R^2 = 1 - \frac{SSE}{SST} \tag{3.17}$$

where SST is the sum of the squared residuals from a horizontal line passing through the mean value of the data.

$$\overline{R}^2 = 1 - (1 - R^2)\frac{n-1}{n-k} \tag{3.18}$$

3) The probability of the F-statistics is zero for all cases, which allows rejecting the null hypothesis that all constants are zero. It can be calculated using the following relation:

$$F = \frac{R^2/(k-1)}{(1-R^2)^2/(n-k)} \tag{3.19}$$

4) For the case of more than eight stay cables (*N>8*), small percentage (*0.05%*) of the standard residuals for the bottom stay cables (short stay cables shown in Fig. 3.1(b)) is exceeding *2*. Fortunately, increasing the number of stay cables reduces the effect of the lowest stay cable on the deck deflection, since most of the load at this zone is carried by the rigid pylon.

3.3 Numerical Examples

In order to check the adequacy of the developed post-tensioning functions, the post-tensioning cable forces are calculated for a large number of bridges having geometric configurations that do not match any of the parameters used in developing the regression functions. However, for presentation purpose, two bridges are only included. The parameters γ_1, γ_2, γ_5, and N of the two considered bridges are substituted into the developed regression functions and the cables post-tensioning forces are estimated. In addition, finite element/optimization analyses are conducted using the specific dimensions of the two bridges to determine the optimum cable post-tensioning forces. The last set of analyses is considered here as the "exact solution". In assessing the results, the values of the post-tensioning forces are deemed to be acceptable if the maximum deflection along the deck satisfies a minimum tolerance value given by the following relation:

$$\left| \frac{maximum\ vertical\ deflection\ of\ the\ deck\ (\delta_{max})}{length\ of\ main\ span\ (M)} \right| \leq \varepsilon \tag{3.20}$$

where ε is set equal to 1.5^{-4}.

The dimensions and the cross-sections properties of the two bridges are given in Tables 3.2 and 3.3, respectively. The cross-sections properties of the two bridges, which do not affect the values of the post-tensioning cable forces, are assumed to be the same. Fig. 3.4(a) shows that, without applying post-tensioning cable forces, the maximum vertical deflection of the bridge deck (I) is *0.930 m*. After applying the post-tensioning cable forces resulting from both the optimization method (exact method) and the proposed post-tensioning functions, the maximum vertical deflection is reduced to *0.013 m* and *0.046 m*, respectively. Fig. 3.4(b) shows that applying the post-tensioning cable forces

evaluated from the proposed post-tensioning functions reduces the maximum deflection of the bridge deck (II) from *0.519 m* to *0.025 m*, compared with a value of *0.0051 m* evaluated from the exact solution.

It is obvious that the post-tensioning cable forces predicted by the functions are adequate, as the corresponding values for the maximum deck deflection satisfies the tolerance limit. Figs. 3.4(c) and 3.4 (d) show the post-tensioning cable forces along one half of the length of the bridges evaluated from both the optimization method and the developed functions. Because of symmetry, the other half of the bridge will have the same post-tensioning cable forces.

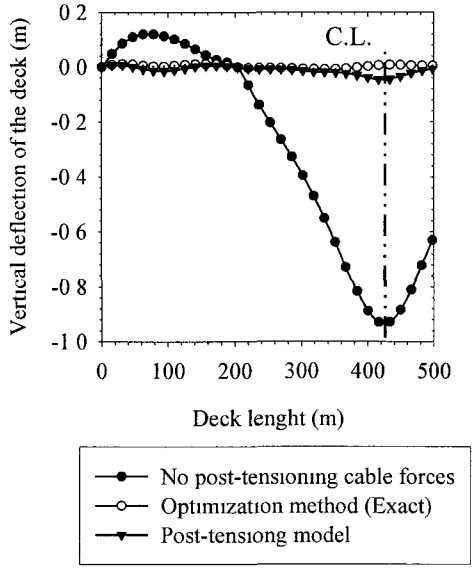

(a) Vertical deflection of the bridge deck (I).

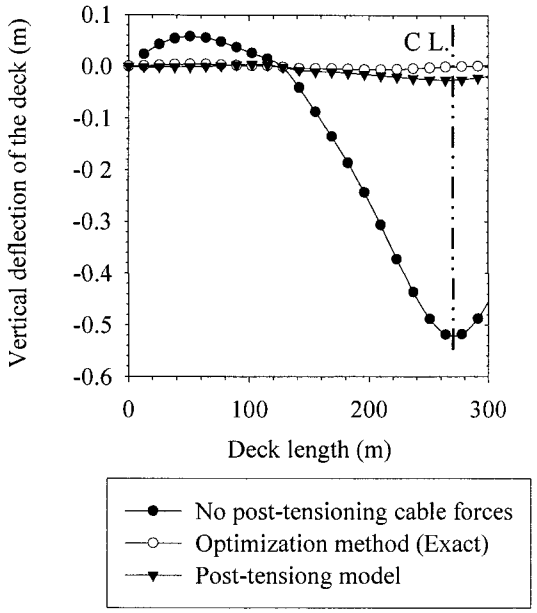

(b) Vertical deflection of the bridge deck (II)

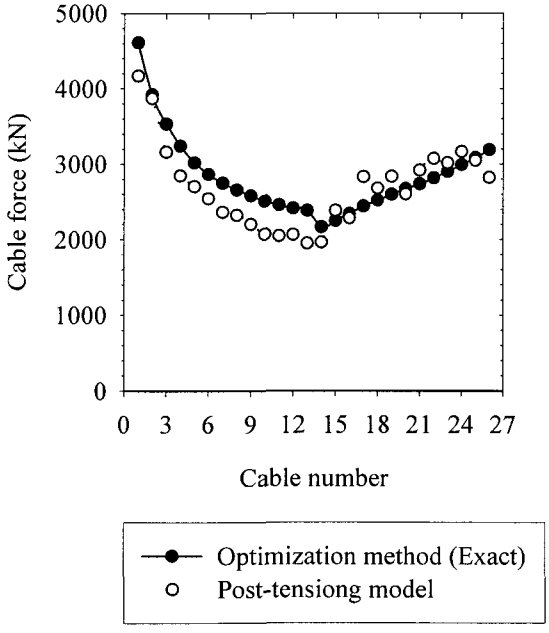

(c) Post-tensioning cable forces of bridge (I)

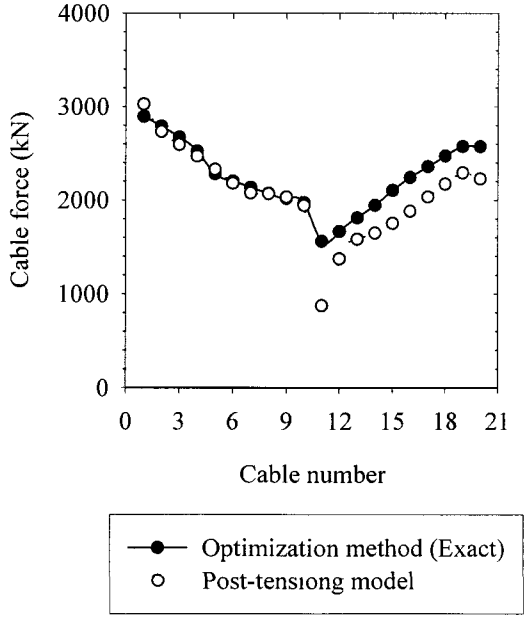

(d) Post-tensioning cable forces of bridge (II)

Fig. 3.4 Deck deflection and post-tensioning cable forces.

3.4 Optimum Geometrical Configurations of Cable-Stayed Bridges (γ_1 And γ_2)

In this section, the developed post-tensioning functions are utilized to assess the variation of the magnitude and distribution of the post-tensioning cable forces with the main span length (*M*) and the upper strut height (h_B). Bridge (*II*) is chosen for this part of the study. The dimensions and the cross-sections properties of the bridge (*II*) are given in Tables 3.2 and 3.3.

Table 3.2 Dimensions of cable-stayed bridges (I) and (II)

Bridge number	Number of stay cables (N)	Length (L) m	Main span length (M) M	Upper strut height (h_B) m	Deck load (w) kN/m
Bridge (I)	13	850	442	85	165.2
Bridge (II) (Chapter (2))	10	542	280	45	165.2

Table 3.3 Cross-section properties of bridges (I) and (II)

	Area (A) m^2	Moment of inertia (I) m^4	Modulus of elasticity (E) kN/m^2	Cable diameter (D_c) m
Deck	0.602	0.704	2×10^8	0.150
Pylon	7.02	13.6	2.5×10^7	0.150

3.4.1 Variations of Main Span Length (M)

The effect of the main span length (M), which is varied by changing the dimensionless parameter (γ_1), on the post-tensioning cable forces, is studied in the section. The post-tensioning cable forces for bridge (II) are evaluated by varying all the parameters given in Table 3.4. Thus, seventy different cases are included in this study.

In general, the maximum deflections associated with the post-tensioning cables forces corresponding to all cases in this study satisfy the tolerance (ε) set by Eq. (3.20). The variation of the bending moment along the pylon with the parameter (γ_1) is shown in Figs. 3.5(a) and 3.5(c), and Figs. 3.6(a) and 3.6(c). The variation of the post-tensioning cable forces with the parameter (γ_1) is shown in Figs. 3.5(b) and 3.5(d), and Figs. 3.6(b) and 3.6(d). The following observations can be drawn from these figures:

Table 3.4 Parameters used to study effect of main span length (M) on the post-tensioning cable forces.

Parameter	Values
γ_1	0.48, 0.50, 0.51, 0.52, 0.54
γ_2	0.07, 0.10
N	5, 7, 8, 9, 10, 11, 13

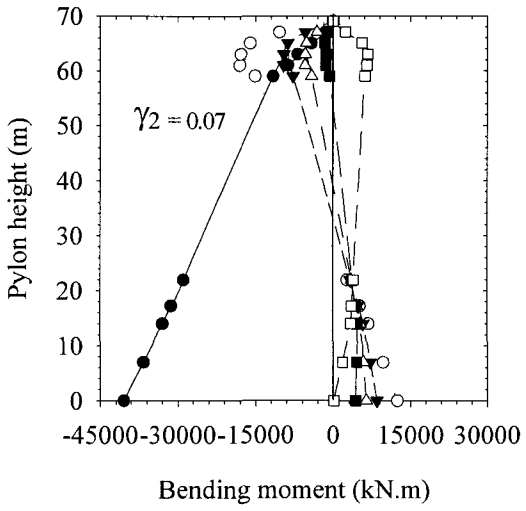

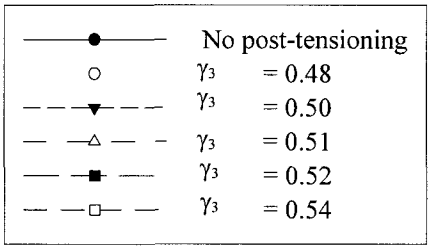

(a) Bending moment of the pylon, case 5 cables.

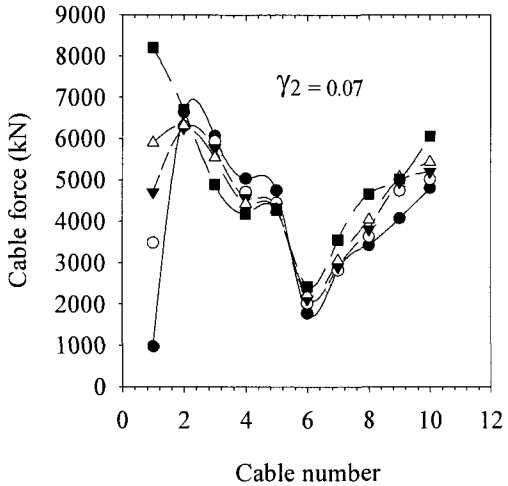

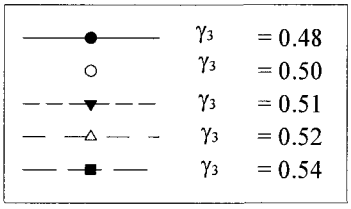

(b) Post-tensioning cable forces, case 5 cables.

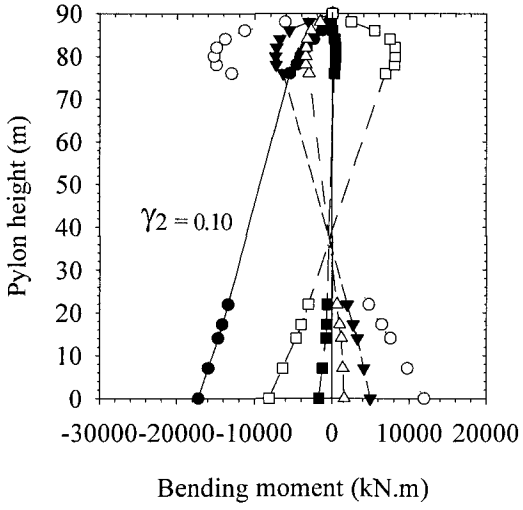

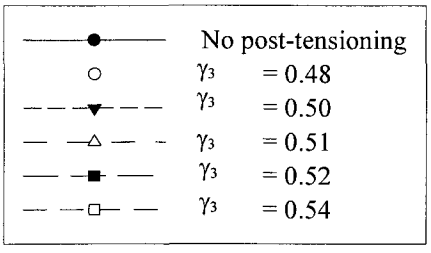

(c) Bending moment of the pylon, case 7 cables.

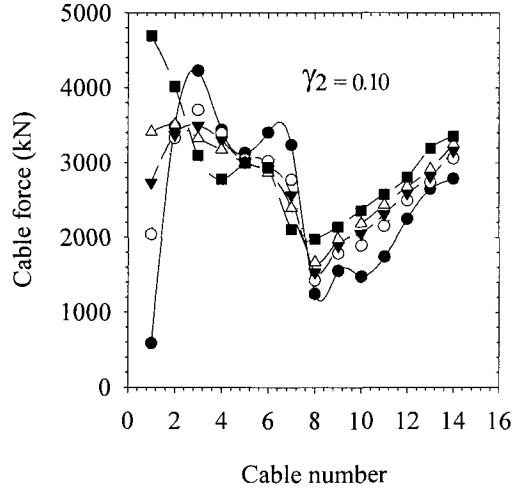

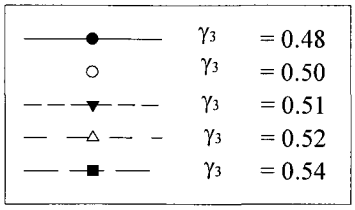

(d) Post-tensioning cable forces, case 7 cables.

Fig. 3.5 Variation of the main span length (M).

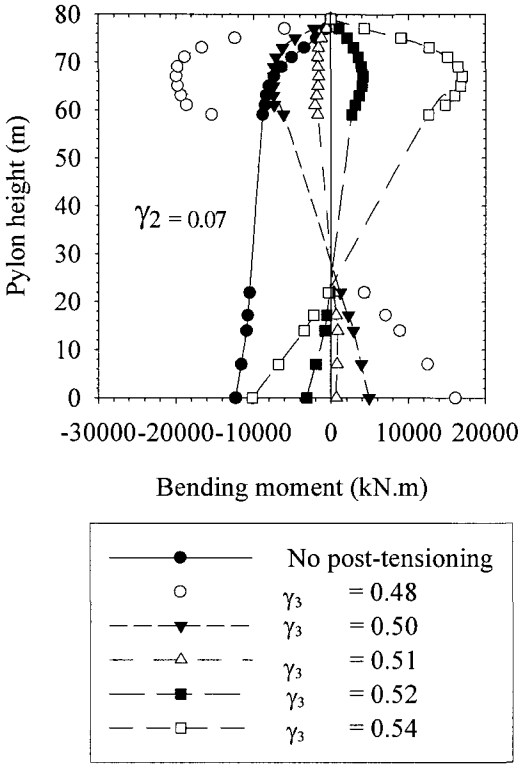

(a) Bending moment of the pylon, case 10 cables.

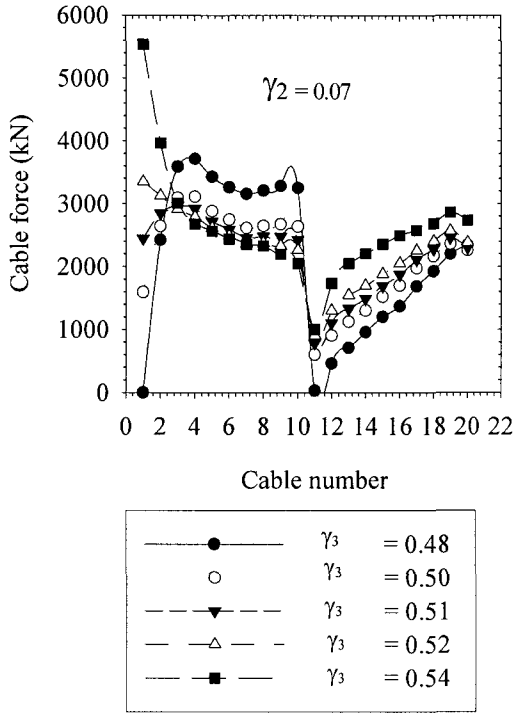

(b) Post-tensioning cable forces, case 10 cables.

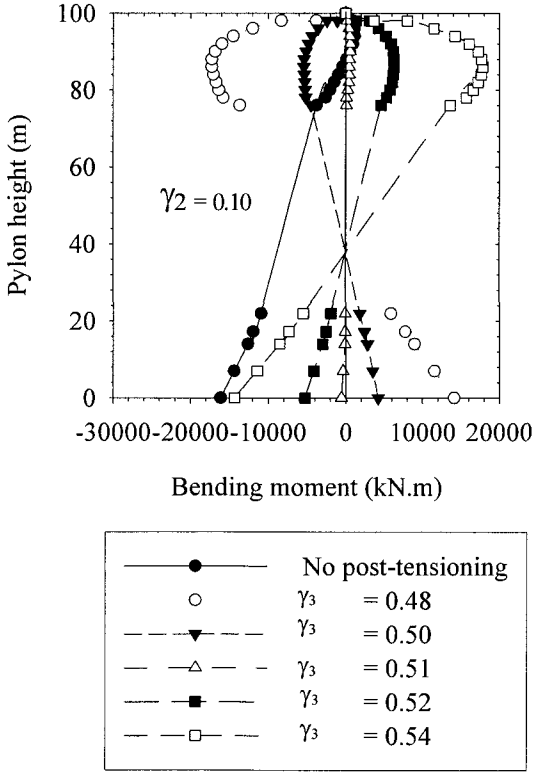

(c) Bending moment of the pylon, case 13 cables.

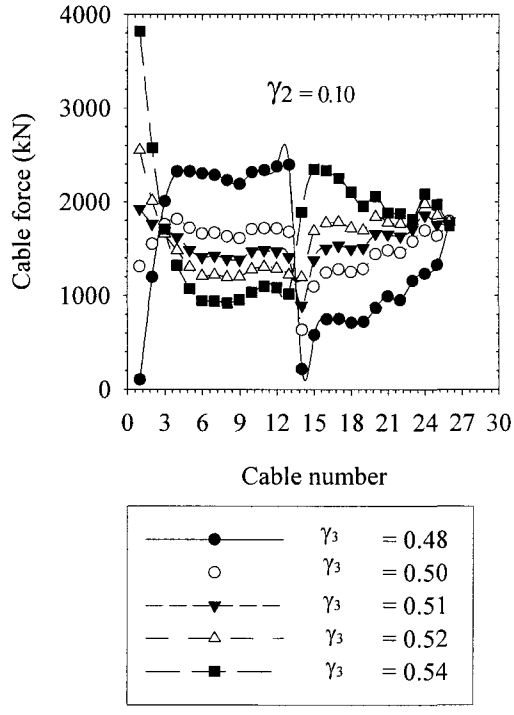

(d) Post-tensioning cable forces, case 13 cables.

Fig. 3.6 Variation of the main span length (M).

1. The value of $\gamma_1 = 0.52$ for cases of five, six, and seven stay cables significantly reduces the bending moment along the pylon when compared with the other ratios, as shown in Figs. 3.5(a) and 3.5(c).
2. The value of $\gamma_1 = 0.51$ for cases of eight to thirteen stay cables significantly reduces the bending moment along the pylon when compared with the other ratios, as shown in Figs. 3.6(a) and 3.6(c).
3. Two values for of γ_1 (*0.48* and 0.54) give higher bending moments along the pylon compared to the other ratios.
4. The range of γ_1 between *0.50* and *0.52* provides the most uniform distribution for the post-tensioning cable forces for all the number of stay cables (N) values, as illustrated in Figs. 3.5(b) and 3.5(d), and Figs. 3.6(b) and 3.6(d).
5. The post-tensioning cable force of the outer cables (longest cables) increases rapidly with the increase of the main span length.
6. An increase in the number of stay cable decreases the post-tensioning cable forces.

In view of the above observations, it is recommended to select the values of the dimensionless parameter (γ_1) between *0.50* and *0.52* for semi-fan cable-stayed bridges. Such a value for (γ_1) reduces the bending moments of the pylon, and provides a uniform distribution of the post-tensioning forces in the stay cables. A reduction in the pylon bending moment makes it behaving as a pure axial column. This reduces the construction cost and facilitates the design process. Meanwhile, a uniform distribution of post-tensioning cable forces reduces the stress concentration at the anchorage points in the pylon and deck, facilitates the post-tensioning process, facilitates the construction and

maintenance processes of the stay cables, reduces the tensile force in the cable back-stays transmitted to the piers, and yields to the best performance of the whole bridge.

3.4.2 Variations of Upper Strut Height (H_b)

In order to investigate the effect of the pylon height, the post-tensioning cable forces for bridge (II) are calculated for three different values of (γ_1) equal to *0.48, 0.51*, and *0.54*, respectively. Each value of (γ_1) corresponds to a specific value for the main span (M). For each value of (γ_1), three different values of (γ_2) equal to *0.03, 0.07*, and *0.11* are considered. They correspond to three different values for the pylon height. Therefore, nine different cases are considered in this part of the study.

The results of the nine analyses are provided in Fig. 3.7. The distributions of the cable forces along the length of the deck are provided in Figs. 3.7(a), 3.7(b), and 3.7(c). The values of the bending moment at the base of the pylon are given in Fig. 3.7(d) for the nine considered cases. The following observations can be drawn from these figures:

1. As a general rule, the increase of the pylon height reduces the post-tensioning cable forces for all values of (γ_1), as shown in Figs. 3.7(a), 3.7(b), and 3.7(c). However, the rate of post-tensioning reduction becomes smaller when the value of (γ_2) is larger than (*0.07*)
2. The effect of increasing the pylon height on the post-tensioning cable forces is more pronounced in the outer stay cables, i.e. the stay cables that are supporting the side spans, than the inner stay cables.

3. Fig. 3.7(d) shows that the increase of the pylon height slightly reduces the bending moment at the pylon base. This effect becomes negligible when the value of (γ_2) exceeds *0.07*.
4. For $\gamma_1 = 0.51$, the change in the pylon height has no effect on the bending moment at the pylon base. As discussed above, at this value of (γ_1), the pylon behaves as a pure axial column with very small bending moment values.

In light of the above, it is clear that the geometric configuration of cable-stayed bridges directly influences the post-tensioning cable forces distributions, which notably affect the internal forces distributions, and the cost of the bridge.

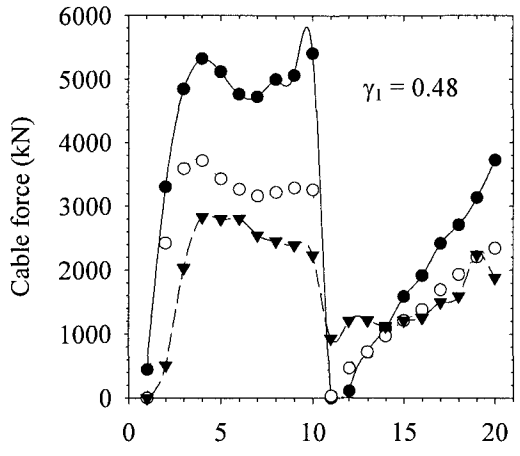

(a) Post-tensioning cable forces.

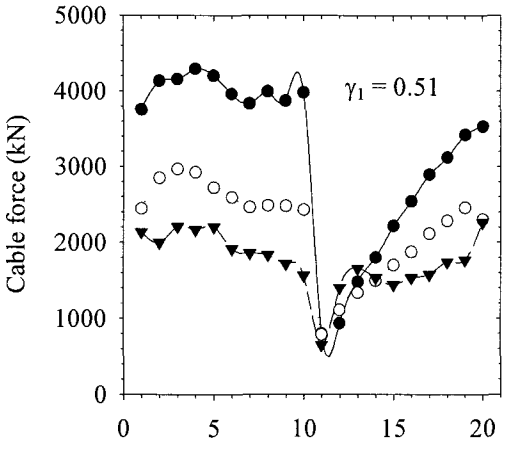

(b) Post-tensioning cable forces.

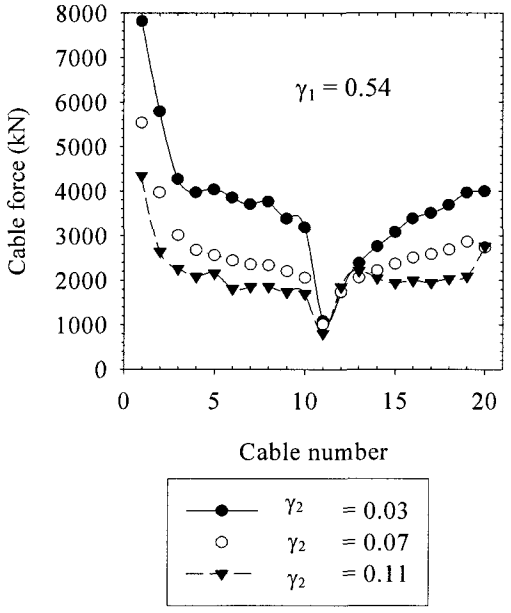

(c) Post-tensioning cable forces.

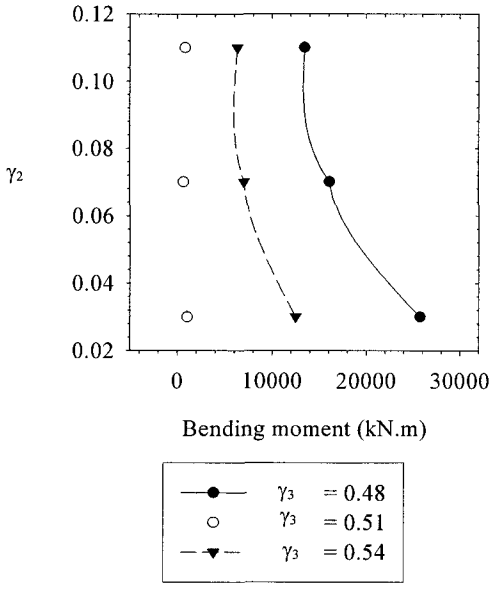

(d) Pylon base bending moment.

Fig. 3.7 Variation of the upper strut height (h_B).

3.5 Conclusions

Surrogate polynomial functions that can be used to evaluate post-tensioning cable forces in semi-cable stayed bridges under the action of dead load are developed. The proposed functions depend on the parameters defining the geometric configuration of the bridges as well as the number of stay cables. The proposed sets of post-tensioning forces minimize the deflections of the deck and the pylons of the bridges. The availability of these post-tensioning force functions is very useful since it saves the significant effort required by the bridge designers to estimate such forces. The post-tensioning functions can be stored as a built-in library in the design software of cable-stayed bridges. The accuracy of the post-tensioning functions is assessed by applying the calculated post-tensioning cable forces on several bridges and comparing the results with those obtained from numerical optimization analyses. The optimum geometric configuration that leads to the most uniform post-tensioning cable forces in semi-fan cable-stayed bridges is investigated. The following conclusions can be drawn from this investigation:

1. The values of the ratio γ_1 (the main span length and the total length) ranging between *0.50* and *0.52* are considered the optimum ratios for all cases as they lead to:
   - Minimum lateral deflection and bending moment in the pylon.
   - Uniform distribution for the post-tensioning cable forces.
2. The increase of the pylon height significantly reduces the required post-tensioning cable-forces.
3. Under the combined effect of dead load and post-tensioning forces, the variation of the pylon height has a slight effect on the bending moment at the pylon's base.

4. The geometrical configuration of a cable-stayed bridge plays a very fundamental role in the design and cost of the bridge.

3.6 References

1. Troitsky M.S., Cable-stayed bridges: theory and design. 2nd Ed. Oxford: BSP; 1988.
2. Wang PH, Tseng TC, Yang CG. Initial shape of cable-stayed bridges. J Comput Struct 1993; 46:1095-1106.
3. Simões LMC, Negrão JHJO. Optimization of cable-stayed bridges with box-girder decks. J Adv. Eng. Software 2000; 31:417-423.
4. Negrão JHO, Simões LMC. Optimization of cable-stayed bridges with three-dimensional modelling. J Comput Struct 1997;64:741-758.
5. Chen DW, Au FTK, Tham LG, Lee PKK. Determination of initial cable forces in prestressed concrete cable-stayed bridges for given design deck profiles using the force equilibrium method. J Comput Struct 2000;74:1–9.
6. Janjic D, Pircher M, Pircher H. Optimization of cable tensioning in cable-stayed bridges. J Bridge Eng ASCE 2003;8:131–137.
7. Sung YC, Chang DW, Teo EH. Optimum post-tensioning cable forces of Mau-Lo His cable-stayed bridge. J Engineering Structures 2006;28:1407-1417.
8. Lee TY, Kim YH, Kang SW. Optimization of tensioning strategy for asymmetric cable-stayed bridge and its effect on construction process. J Struct Multidisc Optim 2008;35:623–629.
9. Hong NK, Chang SP, Lee SC. Development of ANN-based preliminary structural design systems for cable-stayed bridges. Advanced in Engineering Software 2002;33:85-96.

10. Gimsing NJ. Cable Supported Bridges Concept and Design. 2nd edition. New York: John Wiley & Sons Inc.; 1997.

11. Walther, R., Houriet, B., Isler, W., Moia, P., Klein JF. Cable-stayed bridges. Thomas Telford Ltd., Thomas Telford House, London; 1988.

12. Montgomery DC, Peck EA, Vining GG. Introduction to linear regression analysis, 4th edition, Wiley, New York; 2006.

13. Wilson JC, Gravelle W. Modelling of a Cable-stayed Bridge for Dynamic Analysis. J Earthquake Eng & Struct Dyn 1991;20: 707-721.

14. Piegl L. On NURBS: a survey. Computer Graphics and Applications, IEEE 1991;11(1):55 - 71

15. Pourazady M, Xu X. Direct manipulations of B-spline and NURBS curves. Advances in Engineering Software 2000;31(2):107-118.

16. Gen M, Cheng R. Genetic algorithms and engineering optimization, Wiley, New York; c2000.

17. Gen M, Cheng R. Genetic algorithms and engineering design, Wiley, New York; c1997.

18. Davis L. Handbook of Genetic Algorithms, Van Nostrand Reinhold, New York; 1991.

19. Kutner M H, NachBsheim CJ, Neter J. Applied linear regression models, 4th edition, McGraw-Hill/Irwin, Boston, c2004.

20. Econometric Views. Quantitative Micro Software, Version 6.0, CA, USA :Irvine; 2007.

21. Devore, J. L. (2000). Probability and statistics for Engineering and Sciences, 5th Ed., Duxbury Press, An Imprint of Wadsworth Publishing Company, California, USA.

22. Anderson, T. W. and Sclove, S. L. (1986). The Statistical Analysis of Data, 2nd Ed., The Scientific Press, California, USA.

CHAPTER 4

OPTIMAL DESIGN OF SEMI-FAN CABLE-STAYED BRIDGES

4.1 Introduction

Over the last three decades, modern cable-stayed bridges have become one of the most attractive bridge systems. The excellent structural characteristics of cable-stayed bridges, together with the aesthetic appearance, low maintenance cost, and efficient use of structural materials have been highlighted by a number of researchers, e.g. Troitsky [1988], Walther *et al.* [1988], and Gimsing [1997]. The completion of the Sutong Bridge in China, opened a new era for cable-stayed bridges by exceeding a value of *1000 m* for the main span. The typical high cost of cable-stayed bridges, together with the continuous increase in construction material prices, challenge engineers to optimize and improve the design of cable-stayed bridges. Cable-stayed bridges are highly statically indeterminate structures consisting of three major components; the stiffening girder, the stay cables, and the pylons. Achieving the optimum design solution for such structures is a difficult task, since the design is influenced by a large number of variables, such as geometrical configurations, number of stay cables, pylon type, cables arrangement, and the stiffness distribution in the stay cables, the main girder and the pylon. Moreover, cable-stayed bridges should be designed to meet the strength and serviceability requirements imposed by design codes to ensure that the overall bridge components satisfy the safety and functionality criteria. Typically, stay cables of a cable stayed bridge are post-tensioned to off-set the effect of the bridge dead load. The post-tensioning cable forces directly influence the performance and the economical efficiency of the bridge, since they control

the internal force distribution, adjust the bridge deck profile, and affect the overall design of the bridge. The proper set of post-tensioning cable forces adds extra design variables that influence the design of the bridge. As a result, the increase in the number of stay cables complicates the search for an optimum design. In the current practice, a trial-and-error preliminary design study is typically conducted in order to reach the final design of a cable-stayed bridge (Nieto *et al.*, 2009). Such an approach has many drawbacks that can be summarized as follows:

1- Each design trial is affected by the selection of the geometrical configuration, number of cables, and pylon type. Each one of these parameters has a relatively wide range of variation. Accordingly, a large number of trials is needed till the optimum design is reached. This makes the design process expensive, tedious, complex, and time consuming (Hong *et al.,* 2002).

2- Each design trial involves an evaluation for a proper set of post-tensioning cable forces, leading to minimum deflection of the deck and pylon under the action of dead load. The evaluation of such forces requires significant computational efforts. In addition, the problem of evaluation of post-tensioning cable forces might not have a unique solution (Sung *et al.*, 2006).

3- The structural high redundancy, diversity and wide range of design variables, strong effect of the post-tensioning cable forces, and rigorous design constraints produce a complicated cost optimization problem for cable-stayed bridges. Consequently, the available optimization packages are not yet capable of obtaining the optimum design of this kind of bridges.

In the view of the above, it is obvious that the traditional sequential design methods are not the most suitable approaches for designing cable-stayed bridges, and there is a need for the development of a numerical design tool, tailored to optimize the design of long span cable-stayed bridges.

4.2 Background

Since the introduction of the structural optimization techniques, considerable studies have been conducted in order to reach optimum design of cable-stayed bridges. Simões and Negrão [1994] proposed the entropy-based optimization algorithm to optimize the cost of cable-stayed bridges. The locations of stay cable along the main girder and pylon, and the cross-sectional sizes of the deck, pylons, and stay cables were considered as design variables. In this study, an initial starting point was always required to initiate the optimization process, and the post-tensioning cable forces were assumed equal to zero. Moreover, the number of stay cables and the main span length were assumed as preassigned constant parameters.

Long *et al.* [1999] used the internal penalty function algorithm to optimize the cost of cable-stayed bridges with composite superstructure. In this study, the cable-stayed bridge was modelled as 2-D structure, including the geometric nonlinear effect. The cross-sectional dimensions of the bridge members were only considered as the design variables; however, the pylon height, the main span length, and the number of stay cables were assumed as preassigned constant parameters. The effect of the post-tensioning cable forces was not taken into account. In addition, an initial feasible design was needed in order to start the optimization algorithm.

In the research done by Simões and Negrão [2000], a convex scalar function was employed to minimize the cost of a box-girder deck cable-stayed bridge. This function combines dimensions of the cross-sections of the bridge and post-tensioning cable forces. Maximum allowable stresses, minimum stresses in stay cables and deflections of the deck were the three constraints considered in the method. The gradient based non-linear programming techniques used in this study may linger in local optima. This method is very sensitive to the constraints, which should be imposed very cautiously to obtain a practical output Chen *et al.* [2000]. The pylon height and the main span length were not considered within the design variables. Additionally, an initial starting point was required to start the optimization technique.

Lute *et al.* [2009] have demonstrated the capability of support vector machine (SVM) to reduce the computational time of genetic algorithm (GA) for optimizing cable-stayed. The results show that the genetic algorithm (GA) is a good candidate tool for solving cable-stayed bridge optimization problems. The constraints imposed were few, simple, and not based on a standard design code, making them insufficient to assess the strength of the bridge components. In this study, the number of stay cables was treated as a pre-set constant design variable, and the effect of post-tensioning cable forces were neglected.

4.3 Scope and Research Significance

The objective of this study is to develop a numerical design tool capable of reaching the optimum cost design of cable-stayed bridges. The numerical design tool combines a finite element model, real coded genetic algorithm (RCGA), surrogate polynomial functions for

evaluating post-tensioning cable forces, and design methodologies. The advantages of the proposed study over the previous studies can summarized as follows:

1- Most of the previous studies were based on simplified assumptions for design loads, allowable stresses, and constraints making the interpretations of the results questionable. In the current study, the design, loads, and constraints specified by the Canadian Highway Bridge Design Code CAN/CSA-S6-06 [2006] are incorporated into the proposed numerical design tool in order to achieve the minimum cost of the bridge, while satisfying serviceability and strength requirements imposed by the design code.

2- It is well known that the number of stay cables supporting the bridge deck has a great effect on the design of cable-stayed bridges (George, 1999). Indeed, none of the previous studies have examined the effect of the number of the stay cables on the optimum cost design of the bridge. In the current study, the number of stay cables is considered within the set of design variables. As such, the numerical model is capable of predicting the optimum number of stay cables, associated with a minimum cost for the bridge.

3- Two approaches can be used to include the post-tensioning cable forces in cable-stayed bridge optimization techniques. The first approach deals with these forces as discrete design variables, which tremendously increases the number of design variables. Increasing the number of design variables increases the complexity of the optimization search space, as well as the computational time required to get the optimum solution. Moreover, it deteriorates the performance of the optimization technique by decreasing the probability of finding the global optimum solution. The

second approach involves evaluation for the optimum post-tensioning distribution for each single new candidate "cable-stayed bridge" in the optimization problem. As mentioned earlier, the distribution of post-tensioning cable forces is not unique. Therefore, a special post-tensioning optimization problem should be conducted for each single new candidate. On the other hand, a large number of new candidates is always required in the optimization techniques in order to achieve the optimum solution. Therefore, the algorithms solving such optimization problems become computationally prohibitive, since they lead to very expensive final solutions as experienced previously by the author. As a result, most of the previous cable-stayed bridges optimization studies have not considered the post-tensioning cable forces in the optimization process. In the current study, the surrogate post-tensioning polynomial functions developed in the second chapter are adopted to evaluate the post-tensioning cable forces. These functions are stored as a built-in library in the current numerical design model. Utilizing the post-tensioning polynomial functions significantly reduces the number of design variables, as well as the computational time required to reach the optimum solution.

4- The main span length (distance between two pylons) is one of the major design parameter in the design of cable-stayed bridges. Agrawal [1997] studied the effect of the main span length on both positive and negative deck moments. None of the previous studies investigated the influence of this ratio on the optimum cost design of the bridge. In the current study, the main span length is considered as a design variable. As such, the proposed numerical model is able to determine the optimum length that leads to an optimum design of the whole bridge.

5- The search space of the cable-stayed bridges cost functions is expected to be complex and to contain several local minima. This is due to the high nonlinearity of the constraint functions, and the intersection of the constraints with the objective function. Most of the previous studies have employed direct search algorithms, which always require one feasible point in order to start the optimization process. For complicated structures such as cable-stayed bridges, a feasible point may be difficult to estimate at the initial stage of the design. Furthermore, direct search algorithms are typically incomplete algorithms, as the search may stop even if the best solution found by the algorithm is not optimal, i.e. they get trapped in the closest local minimum. Therefore, Genetic Algorithm (GA), as a global optimization method, is utilized in this study to obtain the global optimum design of cable-stayed bridges.

The current study focuses on the optimization of three-span composite cable-stayed bridges with semi-fan cable arrangement. The composite concrete-steel deck consists of a grid of welded steel plate girders with two main steel girders located at the deck edges and topped by a precast concrete slab. The advantages of composite decks are explained by some authors, e.g. Svensson *et al.* [1986] and Troitsky [1988]. The semi-fan is considered to be the ideal solution for a cable-stayed bridge, as it is an intermediate solution between the harp and fan patterns. The semi-fan pattern combines the advantages and avoids the disadvantages of both patterns. The considered bridges have two H-shaped pylons, which are made of reinforced concrete with hollow rectangular cross-section. Although, the numerical tool developed in the current study is limited to the above described configuration, the same approach can be easily extended to include

other configurations in terms of number of spans, stay cables pattern, pylon shape, and deck cross-section type.

The study starts by describing various components of the numerical design tool including the design variables, the design constraints, the objective function, the finite element model, the post-tensioning polynomial functions, load considerations, the optimization technique, and the bridge optimum design algorithm. The Quincy Bayview Bridge, located in Illinois, USA, as a three-span composite cable-stayed bridge, is selected to conduct a case study based on the developed numerical design tool. The effects of the design variables such as the post-tensioning cable forces, pylon height, main span length, and number of stay cables, on the cost design of the cable-stayed bridge are explored. Finally, the optimal design of the bridge is obtained, while varying all of these design variables.

4.4 Optimum Design Formulation

4.4.1. Design Variables

The design parameters that affect the optimum cost design of cable-stayed bridges are considered as design variables in the proposed numerical design model. The vector of design variables $\boldsymbol{x}$ include the number of stay cables, geometric configuration, and cross-sectional dimensions of bridge elements. Those are:

1. Number of stay cables in each single plane (N), shown in Fig. 4.1(a).
2. Diameter of each stay cable (D_i), where (i) is the stay cable number.
3. Main span length (M), shown in Fig. 4.1(a), which is varied by changing a dimensionless parameters ($\gamma_1 = M/L$), where (L) is the total length of the bridge.

4. Height of the upper strut cross beam (h_B), shown in Figs. 4.1(a) and 4.1(d), which is varied by changing a dimensionless parameters ($\gamma_2 = h_B/L$). This ratio defines the height of the lowest cable anchor positions from the deck level (the short cables), as shown in Fig. 4.1(a).
5. Thickness of the concrete deck slab (t_s), shown in Fig. 4.1(b).
6. Height of the two steel main girders (H_G), shown in Fig. 4.1(c).
7. Width of the top flange (B_{FT}), which is varied using the dimensionless ratio ($\gamma_3 = B_{FT}/H_G$), as shown in Fig. 4.1(c).
8. Width of the bottom flange (B_{FB}), which is varied using the dimensionless ratio ($\gamma_4 = B_{FB}/H_G$), as shown in Fig. 4.1(c).
9. Thickness of the top flange (t_{FT}), shown in Fig. 4.1(c), which is calculated based on CAN/CSA-S6-06 [2006] by:

$$t_{FT} = \frac{B_{FT}\sqrt{F_y}}{2\ F_{FT}} \tag{4.1}$$

where

B_{FT} = width of the top flange.

F_y = steel yield strength.

F_{FT} = Factor defining the thickness of the upper flange. The values of F_{FT} given in the CAN/CSA-S6-06 [2006] are proposed in order to prevent premature local buckling of the flange. The range of values depends on the classification of the steel section and is provided in Table 4.1.

10. Thickness of the bottom flange (t_{FB}), shown in Fig. 4.1(c), which is calculated based on CAN/CSA-S6-06 [2006] by:

$$t_{FB} = \frac{B_{FB}\sqrt{F_y}}{2\ F_{FB}} \tag{4.2}$$

where

B_{FB} = width of the bottom flange.

F_{FB} = Factor defining the thickness of the bottom flange. Similar to the top flange, the range of values for the factor F_{FB} preventing local buckling of the bottom flange is provided in Table 4.1, for different class sections.

11. The main girders web thickness (t_w), shown in Fig. 4.1(d), which is calculated based on CAN/CSA-S6-06 [2006] by:

$$t_w = \frac{H_G}{\left(\frac{F_{W1}}{\sqrt{F_y}}\left[1 - F_{W2}\frac{F_{fw}}{F_{yw}}\right]\right)} \tag{4.3}$$

where,

F_{w2} = *0.39, 0.61*, and *0.65* for Class *1, 2* and *3,* respectively, as provided in Table 10.9.2.1, CAN/CSA-S6-06 [2006].

F_{fw} = factored compressive force in the web component at ultimate limit state.

F_{yw} = axial compressive force at yield stress.

F_{W1}= Factor defining the thickness of the web, in order to prevent premature local buckling of the web. The range of values of F_{W1} is defined by the CAN/CSA-S6-06 [2006], and is provided in Table 4.1 for various class sections.

12. The depth, width, and thickness of the pylon cross-section, (H_P), (B_P), and (t_P), respectively, which are shown in Fig. 4.1(e).

It should be mentioned that the vector of design variables

$$\boldsymbol{x} = \{x_i\} = \{N, \gamma_1, \gamma_2, D, t_s, H_G, \gamma_3, \gamma_4, F_{FT}, F_{FB}, F_{w1}, H_P, B_P, t_P\} \tag{4.4}$$

does not include the height of the pylon from the foundation to the deck level since this value is usually governed by the clearance requirement. Moreover, the width of the bridge roadway (B), shown in Fig. 4.1(b), is always determined based on the traffic flow requirement, therefore, it is not considered among the design variables. It should be noted that the floor system can be dealt with separately in the design of the bridge (Long *et al.* 1999).

Table 4.1 Factors decide thickness of steel main girders [Clause 10.9.2 ,CAN/CSA-S6-2006]

	Class 1	Class 2	Class 2
Upper flange	$F_{FT} \leq 145$	$145 \leq F_{FT} \leq 170$	$170 \leq F_{FT} \leq 200$
Lower flange	$F_{FB} \leq 145$	$145 \leq F_{FB} \leq 170$	$170 \leq F_{FB} \leq 200$
Web	$F_{W1} \leq 1100$	$1100 \leq F_{W1} \leq 1700$	$1700 \leq F_{W1} \leq 1900$

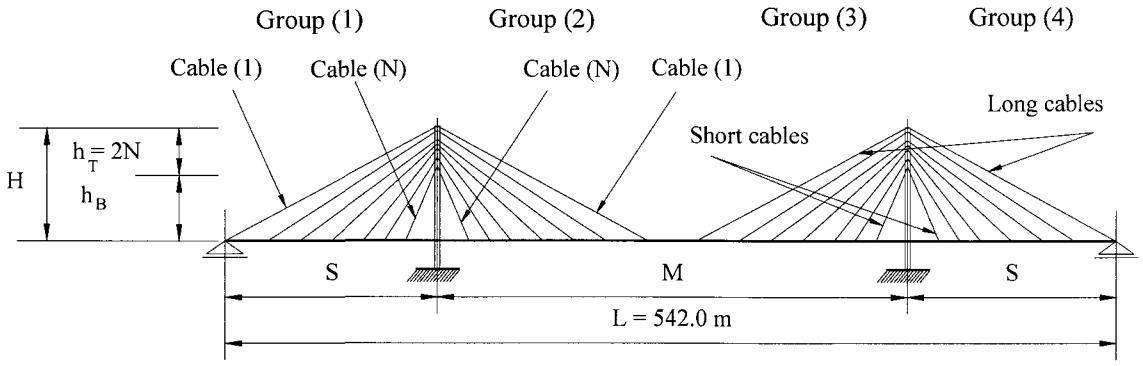

(a) Geometry of bridge.

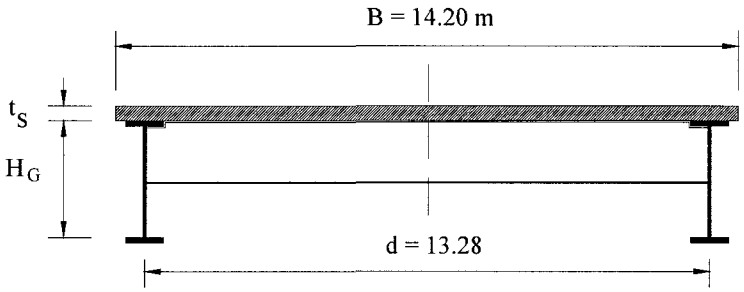

(b) Cross-section of the bridge deck.

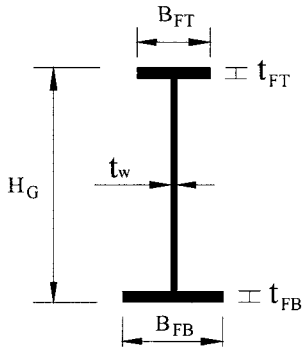

(c) Steel main girder.

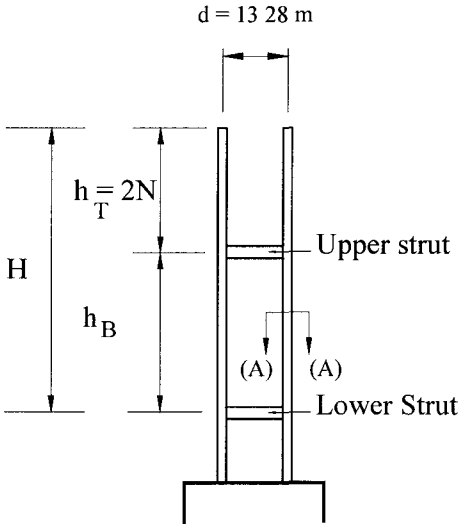

(d) Pylon elevation.

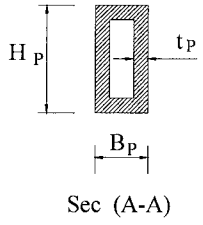

(e) Pylon cross-section.

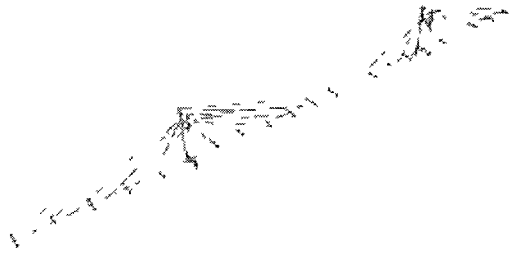

(g) Finite element model.

Fig. 4.1 Bridge layouts, cross-sections, and finite element model.

4.4.2 Design Constraints

The design of cable-stayed bridges involves checking stresses in stay cables, deck girders, and pylons due to dead, live, and wind loads acting on the bridge. The design criteria imposed by the Canadian Highway Bridge Design Code CAN/CSA-S6-06 [2006] and pertaining to the considered type of bridges are included in the numerical code as design constraints functions. The upper limit of these constraints functions is zero. The constraint functions g_i for each component of the bridge are described below:

4.4.2.1 Stay cables

The stay cables resist only tensile forces.

$$g_1 = T_{fCable} - 0.55\ T_{uCable} \leq 0 \tag{4.5}$$

where,

T_{fCable} = the factored tensile force in the stay cable.

T_{uCable} = the specified minimum tensile resistance = $\frac{(\pi D^2)}{4} T_{cCable}$

D = Diameter of the stay cable.

T_{cCable} = Ultimate tensile strength of the stay cable.

4.4.2.2 Composite Concrete-Steel Deck

The bridge deck is subjected to bending moment, axial force, and shear force.

- **Bending Moment**

$$g_2 = M_{fDeck} - M_{rDeck} \leq 0 \tag{4.6}$$

where,

M_{fDeck} = factored bending moment in the deck.

M_{rDeck} = factored moment resistance of the composite section. The procedure to evaluate this resistance is provided in Appendix (II).

- **Axial Tensile Force**

$$g_3 = T_{fDeck} - T_{rDeck} \leq 0 \tag{4.7}$$

where,

T_{fDeck} = the factored tensile force in the deck.

T_{rDeck} = factored tensile resistance of the deck, as described in Appendix (II).

- **Axial Compression Force**

$$g_4 = C_{fDeck} - C_{rDeck} \leq 0 \tag{4.8}$$

where

C_{fDeck} = factored compressive force in the deck.

C_{rDeck} = factored compressive resistance of the deck, as described in Appendix (II).

- **Combined Axial and Bending Moment (Interaction Diagram)**

In order to check the combined effect of the axial load and bending moment on the main deck girders, the interaction diagram of the composite cross-section is constructed by assuming a series of strain distributions, each corresponding to a particular point on the interaction diagram, and computing the corresponding force and moment resistance values. The factored moment and axial forces should be contained within the design interaction diagram using the following:

$$g_5 = F_{(M_f, N_f)Deck} - F_{(M_r, N_r)Deck} \leq 0 \tag{4.9}$$

where,

$F_{(M_f N_f)Deck} = \sqrt{M_{fDeck}^2 + C_{fDeck}^2}$, as shown in Fig. II(f) of Appendix (II).

$F_{(M_r N_r)Deck} = \sqrt{M_{rDeck}^2 + C_{rDeck}^2}$, as shown in Fig. II(f) of Appendix (II).

where,

M_{fDeck} = factored bending moment in the deck.

C_{fDeck} = factored compressive force in the deck.

M_{rDeck} = factored moment resistance of the composite section, as described in Appendix (II).

C_{rDeck} = factored compressive resistance of the deck, as described in Appendix (II).

- **Shear Force**

$$g_6 = V_{fDeck} - V_{rDeck} \leq 0 \tag{4.10}$$

where,

V_{fDeck} = factored shear force.

V_{rDeck} = factored shear resistance of the web steel main girder, as described in Appendix (II).

- **Combined Shear and Moment**

The combined effect of the shear and moment are checked by:

$$g_7 = 0.727\frac{M_{fDeck}}{M_{rDeck}} + 0.455\frac{V_{fDeck}}{V_{rDeck}} - 1 \leq 0 \tag{4.11}$$

where,

M_{fDeck} = factored bending moment in the deck.

M_{rDeck} = factored moment resistance of the composite section, as described in Appendix (II).

V_{fDeck} = factored shear force.

V_{rDeck} = factored shear resistance of the web steel main girder, as described in Appendix (II).

- **Deflection**

In a cable-stayed bridge, the post-tension forces in the stay cables control the deck behaviour in such a way that the vertical deflections under dead load are almost zero. The CAN/CSA-S6-06 [2006] does not specify a deflection criterion for long span bridges. According to AASHTO LRFD [2007], the maximum deflection of the bridge deck under live load should satisfy the following constraint, Long *et al.* [1999]:

$$g_8 = \frac{800\delta_{max}}{L} - 1.0 \leq 0 \tag{4.12}$$

δ_{max} = the maximum deflection limit of the bridge deck due to live load.

$\frac{L}{800}$ = the allowable deflection limit prescribed by AASHTO LRFD [2007].

L = the total length of the bridge.

4.4.2.3 Pylon

- **Buckling**

The buckling capacities of the pylons are calculated in both the longitudinal and transverse directions of the bridge. The axial force in the pylon is calculated and compared to the critical buckling load as follows:

$$g_9 = F_{fPylon} - F_{rPylon} \leq 0 \tag{4.13}$$

where,

F_{fPylon} = factored axial force in the pylon.

F_{rPylon} = critical buckling load of the pylon.

- **Axial Compression and Bending**

The interaction diagram for the pylons cross-sections is constructed and used to check the combined effect of the axial force and bending moment on the pylon as follows:

$$g_{10} = F_{(M_f, N_f)Pylon} - F_{(M_r, N_r)Pylon} \leq 0 \tag{4.14}$$

where,

$F_{(M_f, N_f)Pylon} = \sqrt{M_{fPylon}^2 + P_{fPylon}^2}$, as shown in Fig. II(f) of Appendix (II).

$F_{(M_r, N_r)Pylon} = \sqrt{M_{rPylon}^2 + P_{rPylon}^2}$, as shown in Fig. II(f) of Appendix (II).

P_{fPylon} = factored compressive force in the pylon.

M_{fPylon} = factored bending moment in the pylon.

P_{rPylon} = factored compressive resistance of the pylon.

M_{rPylon} = factored moment resistance of the pylon.

4.4.3 Objective Function

The objective function (F) to be minimized is the total cost of the cable-stayed bridge, including the cost of the stay cables, the structural concrete, and the structural steel, and it can be defined as:

$$F(\mathbf{x}) = \gamma_{cables} V_{cables}(\mathbf{x}) C_{cables} + V_c(\mathbf{x}) C_{concrete} + \gamma_s V_{steel}(\mathbf{x}) C_{steel} \tag{4.15}$$

where,

$\mathbf{x}_t$ is the vector of design variables, defined in Section (4.4.1).

γ_{cable} and γ_s are the unit weights of stay cables and structural steel, respectively.

V_{cable}, V_c, and V_{steel} are the volumes of cables, concrete, and structural steel, respectively. C_{cable}, $C_{concrete}$, and C_{steel} are the unit prices of stay cables, concrete, and steel, respectively.

The unit prices of the bridge components used in the current study are obtained from one of the major consulting firms specialized in designing such structures. These prices include both the material cost and the construction cost. However, these prices are expected to change with time and to vary from location to another. It should be noted that the unit prices of stay cables and structural steel depend on the weight, while that of concrete depends on the volume.

4.4.4 Finite Element Model

The three components of the bridge are modeled using three-dimensional line elements. A three-dimensional frame element is used to model the deck and the pylon, while a three-dimensional cable element is used to simulate the cables. The deck is modeled using a single spine passing through its shear center. The translational and rotational stiffness of the deck are calculated and are assigned to the frame elements of the spine. The cable anchorages and the deck spine are connected by massless, horizontal rigid links to achieve the proper offset of the cables from the centerline of the deck (Wilson and Gravelle, 1991). The finite element model (FEM) of the bridge is shown in Fig. 4.1(f).

4.4.5 Post-Tensioning Polynomial Functions

The post-tensioning polynomial functions developed in Chapter (2) are employed in the numerical design model to evaluate the post-tensioning forces in the stay cables under the

action dead load. Such functions are capable of determining the global optimum post-tensioning distribution, achieving minimum deflections for both the deck and the pylon, simultaneously. They are functions of the number of stay cables (N), main span length (M), and height of the upper strut cross beam above the deck (h_B). In view of the results presented in chapter 2, the post-tensioning cable force (F_i) in a cable (i) is given by:

$$F_i = b_o + b_1\gamma_5^2 + b_2\gamma_2^2 + b_3\gamma_1^2 + b_{11}\gamma_5\gamma_2 + b_{22}\gamma_5\gamma_1 + b_{33}\gamma_2\gamma_1 + b_{12}\gamma_5 + b_{13}\gamma_1 + b_{23}\gamma_2 \quad (4.16)$$

where;

b_o, b_1,.... are the constant values, provided in Appendix (I).

γ_1, γ_2, and γ_5 are equal to (M/L), (h_B/L), and ($L/1000$), respectively.

M, h_B, and L are the main span length, height of the upper strut cross beam, and total length of the bridge, respectively.

4.4.6 Load Considerations

The design load specifications and combinations used in this study are based on the Canadian Highway Bridge Design Code CAN/CSA-S6-06 [2006]. The straining actions at all bridge components are calculated due to the following loads:

- **Dead Load**

According to clause 3.6 of the CAN/CSA-S6-06 [2006], the dead loads shall include the weight of the structure components and appendages fixed to the structure, such as wearing surface, and traffic barriers.

- **Live Load**

According to clause 3.8.3.2 of the CAN/CSA-S6-06 [2006], the following two cases can be considered for live load calculation:

a) CL-W truck.

b) CL-W truck with each axle reduced to *80%* and superimposed with a uniformly distributed load (q_L) of *9 kN/m/lane*.

For short and medium span bridges, the critical effect always occurs due to a single axle, group of axels, or single truck. For long span bridges, the distributed lane loads usually provide the critical force effect and largest deflection. Therefore, the live load applied in this study is taken as follows:

Live load = $m_F\, n_{Lane}\, q_L$ (4.17)

where m_F = modification factor used when more than one design lane is loaded, as stated in clause 3.8.4.2, Table 3.8.4.2, CAN/CSA-S6-06 [2006], n_{Lane} = the number of lanes. The nine live load patterns used to obtain the optimum cost design of the cable-stayed bridge are illustrated in Fig. 4.2, (Walther *et al.*, 1988).

- **Wind Load**

According to clause 3.10.5, CAN/CSA-S6-06 [2006], cable-stayed bridges are considered sensitive to wind load, and wind tunnel tests may be required to determine the lift (C_N), torsional (C_M), and drag (C_D) shape coefficients of the deck. The hourly mean reference wind pressure, q, shall be taken for return period of *100* years, clause 3.10.1.1, CAN/CSA-S6-06 [2006]. Therefore, the wind load is calculated as follows:

$$q_{wT} = C_T\, q\, h \quad (4.18\text{-a})$$

$$q_{wM} = C_M\, q\, h\, B \quad (4.18\text{-b})$$

$$q_{wD} = C_D\, q\, h \quad (4.18\text{-c})$$

where, h = the wind exposure depth

B = the width of the deck

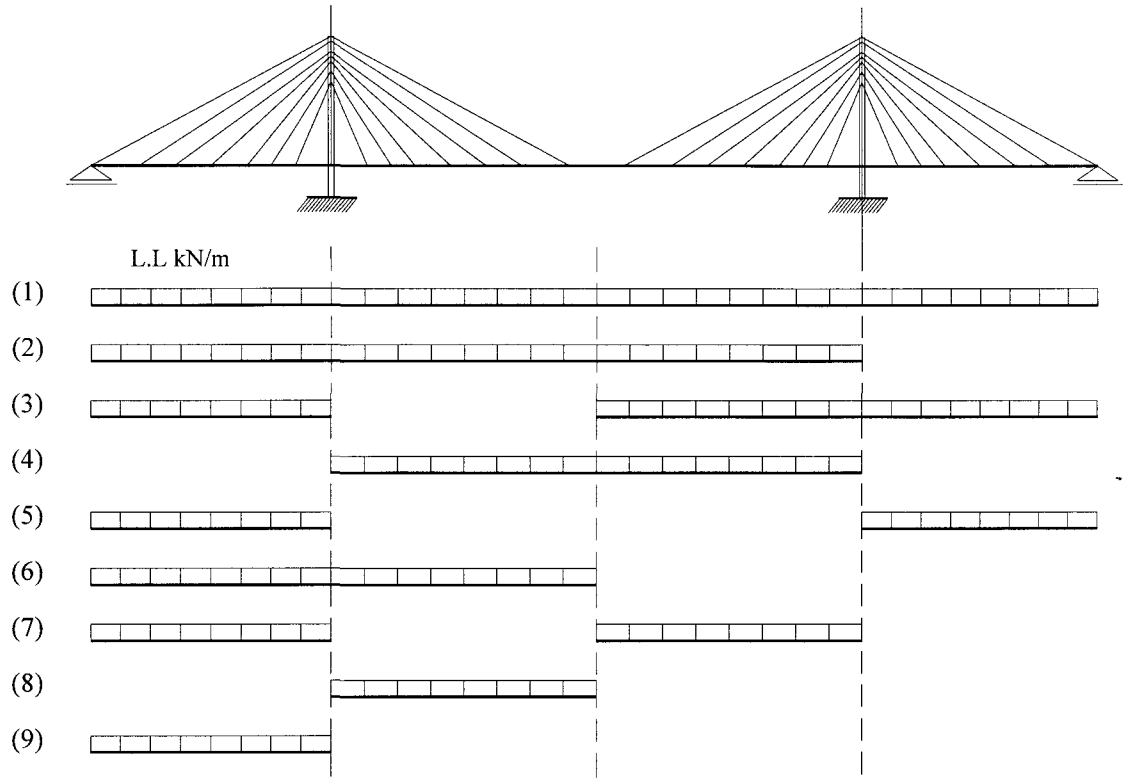

Fig. 4.2 Live load cases used in the numerical model.

- **Load Factors and Combinations**

The load factors and combinations provided in Tables 3.5.1 (a) of the CAN/CSA-S6-06 [2006] are:

$$1.1\,D + 1.7\,L \tag{4.19}$$

$$1.1\,D + 1.4\,L + 0.5\,W \tag{4.20}$$

$$1.1\,D + 1.65\,W \tag{4.21}$$

where, D = Dead load, L = Live load, and W = Wind load.

4.4.7 The Optimization Technique

As mentioned before, the cost optimization problem for cable-stayed bridges is complex and contains several local minima. As such, Genetic Algorithms (GAs) are adopted in the current study to find the global optimum solution of the bridges. During the last decade, genetic algorithms (GAs), which are global optimization algorithms based on the theory of biological evolution and adaptation, have proved to be powerful, efficient, capable of handling large number of variables, and robust in finding global optimal solutions (Gen and Cheng, 2000).

4.4.7.1 Real Coded Genetic Algorithms

The real coded genetic algorithm (RCGA) is a variant of genetic algorithms that are suited for the optimization of multiple-optima objective functions defined over continuous variables (Davis, 1991). The algorithm operates directly on the design variables, instead of encoding them into binary strings, as in the traditional genetic algorithms. Section (4.5) describes how the real coded genetic algorithm (RCGA) is adapted to the problem at hand to find the optimum cost design of the cable-stayed bridge.

4.4.7.2 Genetic Operators

The mutation operators allow the (RCGA) to avoid local minima by searching for solutions in remote areas of the objective function landscape. In the current study, the operators used are boundary mutation, non-uniform mutation, and uniform mutation. The first operator searches the boundaries of the independent variables for optima lying there,

the second is random search that decreases its random movements with the progress of the search, and the third is a totally random search element. The crossover operators produce new solutions from parent solutions having good objective function values. In the current study, this translates into producing new bridges from pairs of low cost bridge. The crossover operators used are the arithmetic, uniform and heuristic crossovers. The first produces new solutions in the functional landscape of the parent solutions. The second one is used to create a new solution randomly from two parents, while the last one extrapolates the parent solutions into a promising direction. Details of such operators are given by Michalewicz and Fogel [2004].

The above operators are applied on each population with the following values:

1) Population size = *100* solution instances (candidate cable-stayed bridges).

2) 4 instances undergo boundary mutation.

3) 4 instances undergo non-uniform mutation.

4) 4 instances undergo uniform mutation.

5) 2 instances undergo arithmetic crossover.

6) 2 instances undergo uniform crossover.

7) 2 instances undergo heuristic crossover.

4.4.7.3 Penalized Objective Function

A simple method to penalize infeasible solutions is to apply a penalty function to those solutions, which violate the constraints defined in Section (4.4.2). The penalized objective function for a problem with n constraints is generally defined as follows:

$$F_p(\boldsymbol{x}) = F(\boldsymbol{x}) + \sum_{i=1}^{n} \alpha_i \delta_i \qquad (4.22)$$

where $\begin{cases} \delta_i = g_i, & for \ \ g_i > 0 \\ \delta_i = 0, & for \ \ g_i \le 0. \end{cases}$

$F_p(\boldsymbol{x})$ is the penalized objective function, $F(\boldsymbol{x})$ is the unpenalized objective function, Eq. (4.15), x_i is the vector of design variables, δ_i is a violation factor for the ith constraint, and α_i is a penalty parameter "certain suitable coefficient" imposed for violation of constraint i, which depends on the type of the optimization problem. This constant ensures that the summation terms in the above equation have the same order of magnitude; therefore, the search does not become dominated by one of the constraint functions. Prior to the optimization process, the values of these constants are determined by conducting a Monte Carlo simulation of the independent values, and obtaining the value of the objective and constraint functions corresponding to each simulation. This is followed by an order of magnitude analysis of the obtained results.

4.5 Bridge Optimum Design Algorithm

The analysis sequence combining the finite element model, post-tensioning polynomial functions, design methodologies, and real coded genetic algorithm (RCGA) for finding the optimum cost design of cable-stayed bridges is given as follows:

1. Create an initial population of the design variables, which are defined in Section (4.4.1), randomly selected by the (RCGA) algorithm between the lower and upper bounds of each design variable. The design variables define the geometric configuration, the number of stay cables, and cross-sectional dimensions of the bridge. The choice of the lower and upper bound for each design variable depends on the designer experience.

2. Develop a three dimensional finite element model (FEM) for each search point in the population, i.e. each cable-stayed bridge, according to the geometry and physical properties of the bridge, as described in Section (4.4.4).
3. Calculate the post-tensioning cable force in each stay cable using the post-tensioning built-in library functions, as illustrated in Section (4.4.5). Apply these forces to the 3-D FEM together with other types of loads, i.e. dead, live, and wind loads, and analyze the structure to determine the internal forces and displacements of the bridge components.
4. Check that these internal forces and displacements satisfy the design constraints defined in Section (4.4.2). If any of these constraints are not satisfied, the result of this specific bridge is excluded by applying a suitable penalty function given by Eq. (4.22). The chosen penalty function is added to the value of the objective function, which is calculated by the numerical code for each set of selected design variables.
5. Sort the initial population in ascending order according to the value of the objective function such that the first ranked candidate "cable-stayed bridge" has the minimum value of the feasible cost design.
6. Generate, using the GA, a new population (*100* cable-stayed bridges) by applying the crossover and mutation operators on the high ranked cost functions evaluated at step 5 to produce a new generation with better fitness. These operators direct the search towards the global optimum solution.
7. Replace the previous population with the newer one containing the new candidate cable-stayed bridges, in addition to the best candidate cable-stayed bridge found so far (elitist selection).

8. Repeat steps *2* to *7* for a certain number of generations, taken as *100* iterations in the current study, till a global optimum solution is reached.
9. Deliver the candidate cable-stayed bridge with the highest fitness "smallest values of the objective function" obtained at step *8* as the final solution.

The procedure described above is summarized in the flow chart shown in Fig. 4.3.

4.6 Example and Results

In order to demonstrate the efficiency and the practical usefulness of the proposed numerical design model, five numerical design cases are performed. The geometric configuration of the Quincy Bayview Bridge is used as a basis in these analyses. In the first case, the design cost of the cable-stayed bridge is obtained, while the geometric configurations and the number of stay cables are kept constant and equal to the original values of the Quincy Bayview Bridge. The bridge cost obtained from this case, is considered as the "reference design" in order to compare the optimum solutions obtained for the other five cases. The effect of the post-tensioning cable forces on the bridge cost is then assessed in the second example.

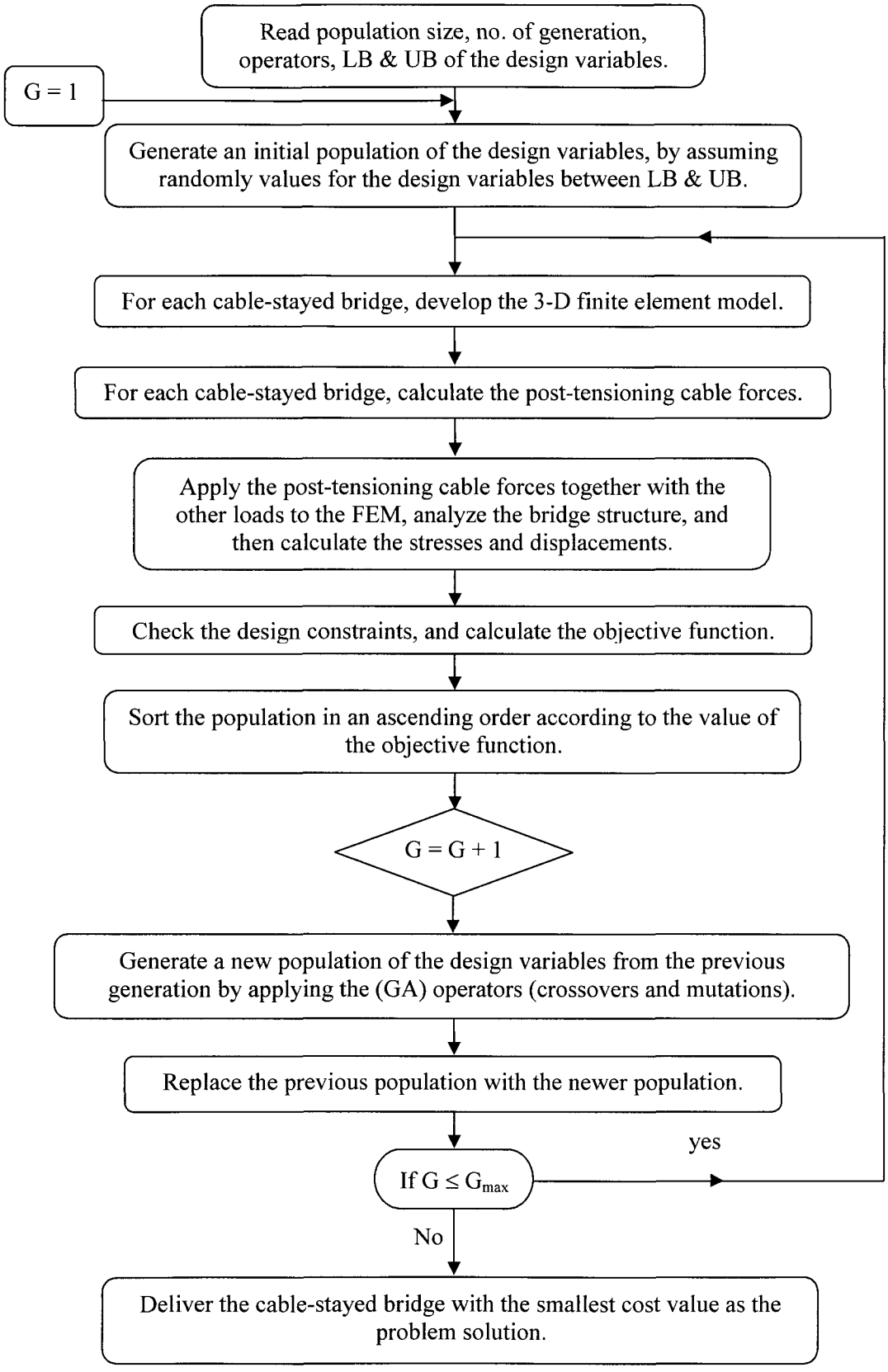

Fig. 4.3 Flow chart for evaluation of the minimum cost of the cable-stayed bridge.

In the third case, the effect of the geometric configuration on the design cost of the bridge is investigated by allowing the main span length and the height of the pylon to vary, while keeping the number of stay cables constant and equal to that used in the original bridge. In the fourth case, the effect of the number of stay cables on the design cost of the bridge is investigate by allowing the number of stay cables to vary, while maintaining the geometric configuration similar to that used in the original bridge. In the final case, the optimal design of the present bridge is obtained by varying all design variables.

4.6.1 Description of the Bridge

A layout of the geometry of the Quincy Bayview Bridge is shown in Fig. 4.1(a) (Wilson and Gravelle, 1991). In all the considered analysis cases, the following parameters are maintained constant:

1. A semi-fan type arrangement is used for the stay cables.
2. The deck has two lanes of traffic (n_{Lanes}= *2.0*).
3. The deck consists of precast slab with a total width (B) of *14.20 m*, and two steel main girders located at the outer edges of the deck, as shown in Figs. 4.1(b) and 4.1(c).
4. The distance between the stay cables anchorages along the pylon is taken as *2.0 m,* as a reasonable distance for practical installation. Therefore, the distance (h_T), shown in Figs. 4.1(a) and 4.1(d), is equal to (N *x 2.0 m*), where (N), is the number of stay cables.
5. The total length of the bridge (L) = *542.0 m,* as shown in Fig. 4.1(a).
6. The two pylons are H-shaped structures with a width (d) of *13.28 m*.

All other geometric parameters shown in Figs. 4.1(a) and 4.1(d) represent the design variables.

The real bridge has four groups of double plan stay cables with seven cables ($N=7$) in each group. The main span length (M) is *274.0 m* and the two equal sides (S) have spans of *134 m* each. The total height of the pylons' tops above the bridge deck (H) is *49.0 m*. An upper strut cross beam connects the two upper legs at height (h_B) of *35.0 m* from the deck, and a lower strut cross beam supports the deck, as shown in Fig. 4.1(d). The properties and unit prices of the materials used in the numerical example are tabulated in Table 4.2.

Besides the structural self-weight of the bridge, a layer of asphalt having a thickness of *0.09 m*, two concrete traffic barriers having an average thickness and height of *0.325 m* and *0.85 m*, respectively, and floor cross beams with an estimated load per unit area of *0.75 kN/m*^{2} are added as dead loads (Long *et al*, 1999). It should be noted that the self-weight of the bridge varies for different optimization cases, since it depends on the cross sectional design variables of the deck and the pylon. The magnitude of the live load is calculated using Eq. (4.17), and is equal to *16.2* kN/m for the assumed number of lanes. The cable-stayed bridge is assumed to be located in Victoria , British Colombia. Accordingly, the hourly mean reference wind pressure q is taken equal to *690 N/m*^{2}, as specified in Table A3.1.7 of Appendix A3.1, CAN/CSA-S6-06 [2006]. The angle of attack of the wind on the deck is assumed to be zero. Therefore, only the drag pressure is included in the study. The wind force acting on the concrete barriers is taken into account. The drag shape coefficient (C_D) is assumed to be *0.8* (Walther *et al.*, 1988). The wind exposure depth (h), defined in Eq. (4.18), is equal to the height of the main girder

deck plus the height of traffic barrier. The penalty parameters used to estimate the penalized objective function Eq. (4.22), are tabulated in Table 4.3.

Table 4.2 Material properties of the bridge.

Material	Properties	
Steel	Modulus of elasticity, (E_s)	= 200 GPa
	Unit weight, (γ_s)	= 77 kN/m^3
	Poisson's ratio, (v_s)	= 0.30
	Yield strength, (F_y)	= 350 MPa
	Unit price (C_{steel})	= 12,000 \$/ton
Concrete	Modulus of elasticity, (E_c)	= 24.87 GPa
	Unit weight, (γ_c)	= 24.0 kN/m^3
	Poisson's ratio, (v_c)	= 0.20
	Compressive strength, (f_c')	= 30 MPa
	Unit price ($C_{concrete}$)	= 4,218 \$/m^3
Cables	Modulus of elasticity, (E_{sc})	= 205 GPa
	Unit weight, (γ_{scable})	= 82.40 kN/m^3
	Ultimate tensile strength, (T_{cCable})	= 1.6 GPa
	Unit price (C_{cable})	= 60,000 \$/ton
Reinforcement steel	Yield strength, (f_y)	= 400 MPa
Asphalt	Unit weight, ($\gamma_{Asphalt}$)	= 23.5 kN/m^3

Table 4.3 Penalty parameters

Constraint	Penalty parameter (α_i)
Axial tension (Eq. 4.4)	50×10^3
Bending moment (Eq. 4.5)	50×10^3
Axial tensile (Eq. 4.6)	50×10^3
Axial Compression (Eq. 4.7)	50×10^3
Combined axial and bending (Eq. 4.8)	4×10^3
Shear force (Eq. 4.9)	50×10^3
Combined shear and moment (Eq. 4.10)	50×10^6
Deflection (Eq. 4.11)	100×10^6
Axial compression and bending (Eq. 4.12)	50×10^3
Buckling (Eq. 4.13)	50×10^3

4.6.2 Case (1): Reference Cost of Quincy Bayview Bridge.

For the sake of comparison, the cost design of the considered cable-stayed bridge is obtained, assuming the number of stay cables in each group (N), main span length (M), and the height of the upper strut cross beam above the deck (h_B) are constant and equal to the original values of the Quincy Bayview Bridge. The other eleven design variables defined in Section (4.4.4) are allowed to vary between the upper and lower bounds presented in Table 4.4. The post-tensioning cable forces are evaluated in this analysis using the built-in post-tensioning functions, and are applied at the cable anchor positions on the deck and pylon. The optimum values of the design variables and minimum cost design of the bridge are summarized in Table 4.5. The cost design obtained from this

analysis will be named as Case (1) and will be considered in as the "reference cost" to compare cost solutions obtained for different cases.

Table 4.4 Lower and upper bounds of the design variables

Design variable	Lower bound	Upper bound
N (number of stay cables in each single plane)	5	13
D_i (diameter of each stay cables)	0.01 m	0.25 m
γ_1 = (M/L) = (Main span length / bridge length)	0.48	0.54
γ_2 = (h_B/L) = (height of upper strut cross beam / bridge length)	0.03	0.12
t_s = thickness of the concrete deck slab	0.15 m	0.40 m
H_G = height of the two steel main girders	0.50 m	5.0 m
γ_3 = (B_{FT}/ H_G) = (width of top flange / height of main girder)	0.15	0.20
γ_4 = (B_{FB}/ H_G) = (width of bottom flange / height of main girder)	0.20	0.25
F_{FT} = factor decides the thickness of upper flange	145	200
F_{FB} = factor decides the thickness of lower flange	145	200
T_{W1} = factor decides the thickness of web	1100	1900
H_P = depth of the pylon cross-section	1.0 m	5.0 m
B_P = width of the pylon cross-section	1.0 m	5.0 m
t_P = thickness of the pylon cross-section	0.5 m	1.0 m

Table 4.5 Reference cost of Quincy Bayview Bridge.

Design variable	Case (1)
No. of stay cables in each single plane (N)	7
γ_1 = (M/L) = main span / bridge span	0.506
γ_2 = (h_B/L) = upper strut height / bridge span	0.065
Max. diameter of cables (D_{max})	0.08 m
Min diameter of cables (D_{min})	0.05 m
Thickness concrete slab (t_s)	0.15 m
Main girder height (H_G)	2.90 m
Width of upper flange (B_{FT})	0.551 m
Width of lower flange (B_{FB})	0.638 m
Thickness of upper flange	0.035 m
Thickness of lower flange	0.037 m
Thickness of web	0.018 m
Pylon depth	3.5 m
Pylon width	1.5 m
Pylon thickness	0.50 m
Pylons cost	$ 3,306,912
Deck cost	$ 13,999,430
Cables cost	$ 11,205,851
Total cost	$ 28,512,194 (Reference cost)

4.6.3 Case (2): Effect of the Post-Tensioning Cable Forces on the Bridge Cost

In this section, the cost design of the present cable-stayed bridge is determined, assuming zero values for the post-tension forces. Similar to Case (1), the main span length (M), the height of the upper strut cross beam above the deck (h_B), and number of stay cables in each group (N) are kept constant and equal to the original values of the Quincy Bayview Bridge. Table 4.6 presents the optimum values of the design variables obtained from this analysis. The corresponding minimum cost design "Case (2)" is provides in Table 4.6 and compared to the cost of Case (1). The costs of each individual component of the bridge (the pylon, the deck, and the stay cables) are provided in the table.

The results show that the deck cost for Case (1) is *43.2%* less than that for Case (2). However, the costs of the pylon and stay cables are almost the same in both cases, i.e. most of the bridge cost reduction happens in the deck cost. The post-tensioning cable forces have a significant effect on the behaviour of the deck and, consequently, its cost. They reduce the band enveloped by the maximum positive and maximum negative bending moment of the deck, as shown in Fig. 4.4. Based of the above results, it is obvious that the post-tensioning cable forces have a significant contribution on the cost design of the bridge, and neglecting these forces may lead to unrealistic solutions.

Table 4.6 Bridge design with and without inclusion post-tensioning cable forces.

Design variable	Case (1)	Case (2)
No. of stay cables in each single plane (N)	7	7
γ_1 = (M/L) = main span / bridge span	0.506	0.506
γ_2 = (h_B/L) = upper strut height / bridge span	0.065	0.065
Max. diameter of cables (D_{max})	0.08 m	0.08 m
Min diameter of cables (D_{min})	0.05 m	0.04 m
Thickness concrete slab (t_s)	0.15 m	0.15 m
Main girder height (H_G)	2.90 m	4.28 m
Width of upper flange (B_{FT})	0.551 m	0.813 m
Width of lower flange (B_{FB})	0.638 m	0.856 m
Thickness of upper flange	0.035 m	0.049 m
Thickness of lower flange	0.037 m	0.047 m
Thickness of web	0.018 m	0.028 m
Pylon depth	3.5 m	3.5 m
Pylon width	1.5 m	1.5 m
Pylon thickness	0.50 m	0.50 m
Pylons cost	$ 3,306,912	$ 3,306,912
Deck cost	$ 13,999,430	$ 24,655,409
Cables cost	$ 11,205,851	$ 10,834,776
Total cost	$ 28,512,194 (Reference cost)	$ 38,797,097

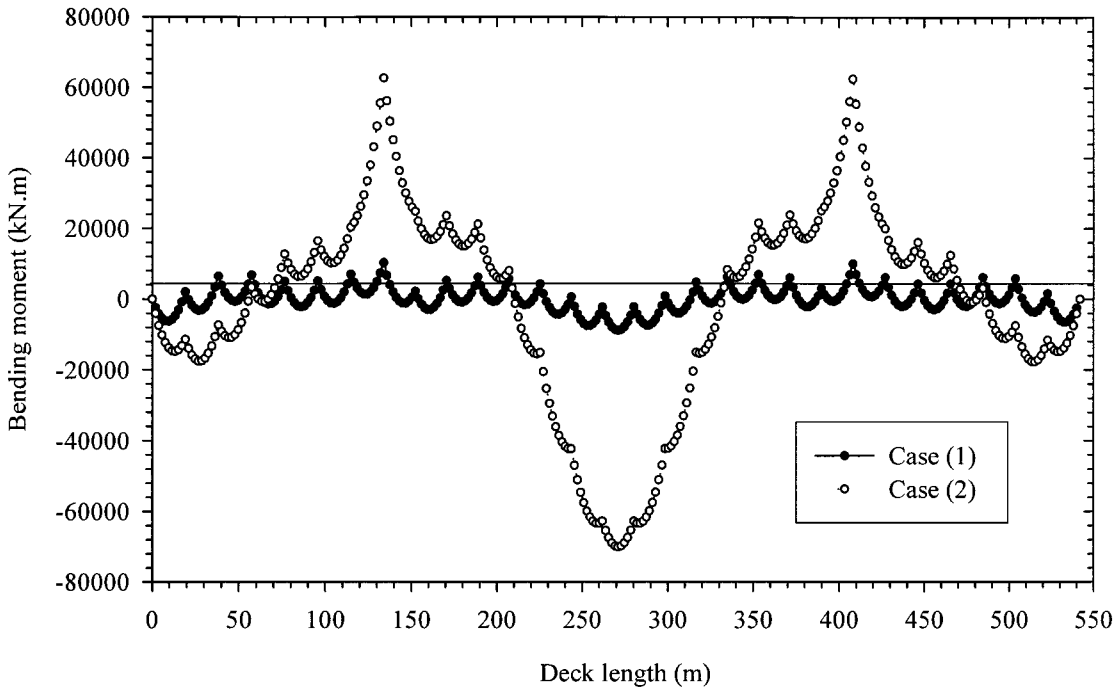

Fig. 4.4 Bending moment of the deck resulting from Case (1) and (2) under the action of DL and LL.

4.6.4 Case (3): Effect of Geometric Configurations on Bridge Cost

The increase in the pylon height above the deck level reduces the post-tensioning cable forces (Troitsky, 1988), which directly reduces the diameters of stay cables and the compressive forces acting on the deck and the pylons. However, this increase enlarges the pylon height, and the stay cables lengths. On the other hand, the main span length has a notable influence on the distribution of post-tensioning cable forces and bending moments along the deck and the pylons (Agrawal, 1997).

Increasing the ratio of main span length to bridge length significantly beyond a value of *0.5* increases the tensile force in the cable back-stays transmitted to the piers. On the other hand, a small value of (γ_1) may lead to a large uplift of the main span. In this case, some stay cables become subjected to net compression and, therefore, will not participate

in the deck supporting system (Troitsky, 1988). The objective of this section is to asses the variation of the cost of the bridge with the pylon height and the main span length. A number of optimization analyses are conducted in this section. All these analyses involve the use of fixed number of stay cables $N = 7$. Each optimization analysis involves specific values for the dimensionless parameters ($\gamma_1 = M/L$) and ($\gamma_2 = h_B/L$). Other design variables, described in Table 4.4, are included in each optimization analysis. The values of (γ_1) and (γ_2) considered in this study are provided in Table 4.7. The costs obtained from these analyses are compared to the reference cost "Case (1)" and the results are provided in Figs. 4.5, 4.6, 4.7, and 4.8.

Table 4.7 Parameters used to study effect of geometric configuration on the bridge cost.

Parameter	Values
No. of stay cables in each single plane (N)	7
$\gamma_1 = (M/L)$ = main span / bridge span	0.48, 0.50, 0.52, 0.54
$\gamma_2 = (h_B/L)$ = upper strut height / bridge span	0.037, 0.065, 0.092, 0.120

The variation of the pylon cost with the height of the pylon above the deck level is shown in Fig. 4.5. In general, the pylon cost increases with the increase in the pylon height. The results show that the pylon cost remains almost constant with the variation of main span length (M). This is interpreted by the application of the post-tensioning cable forces. For each main span value, a set of post-tensioning forces is applied leading to minimum deflection and minimum bending moment along the pylon. As such, the structural

behaviour of the pylon, and consequently its cost, remains unchanged with the variation of the main span.

The variation of the deck cost with the height of the pylon above the deck level is shown in Fig. 4.6. It can be seen that the increase in the pylon height is always accompanied with a decrease in the deck cost. Increasing the pylon height, reduces the moments and normal forces acting on the deck, leading to a relatively small deck cross-section.

The variation of the stay cables cost with the height of the pylon above the deck level is shown in Fig. 4.7. It can be seen that in most cases, the stay cables cost is reduced with the increase in the pylon height. This trend changes for the case of $\gamma_1 = 0.54$, when γ_2 exceeds a value of 0.092. Generally, the reduction of the stay cables cost becomes less significant beyond a ratio of $\gamma_2 = 0.092$. It can be also shown from the results that the decrease in the ratio of main span length to bridge length ($\gamma_1 = M/L$) decreases the cost of the stay cables.

The variation of the optimum cost design of the bridge with the height of the pylon above the deck level is shown in Fig. 4.8. It is seen that the bridge cost design remarkably decreases with the increase in the pylon height. However, the rate of reduction becomes less noticeable beyond a ratio of upper strut cross beam height to bridge length of 0.092 ($\gamma_2 = h_B/L = 0.092$). The results also show that the cost design of the bridge decreases almost linearly with the decrease in the ratio of main span length to bridge length ($\gamma_1 = M/L$). Compared to the reference design, Fig. 4.8 shows that by decreasing the ratio of main span length to bridge length ($\gamma_1 = M/L$) from 0.505 to 0.480 and increasing the ratio of upper strut cross beam height to bridge length ($\gamma_2 = h_B/L$) from 0.065 to 0.120, a reduction in the bridge cost of 10% can be achieved.

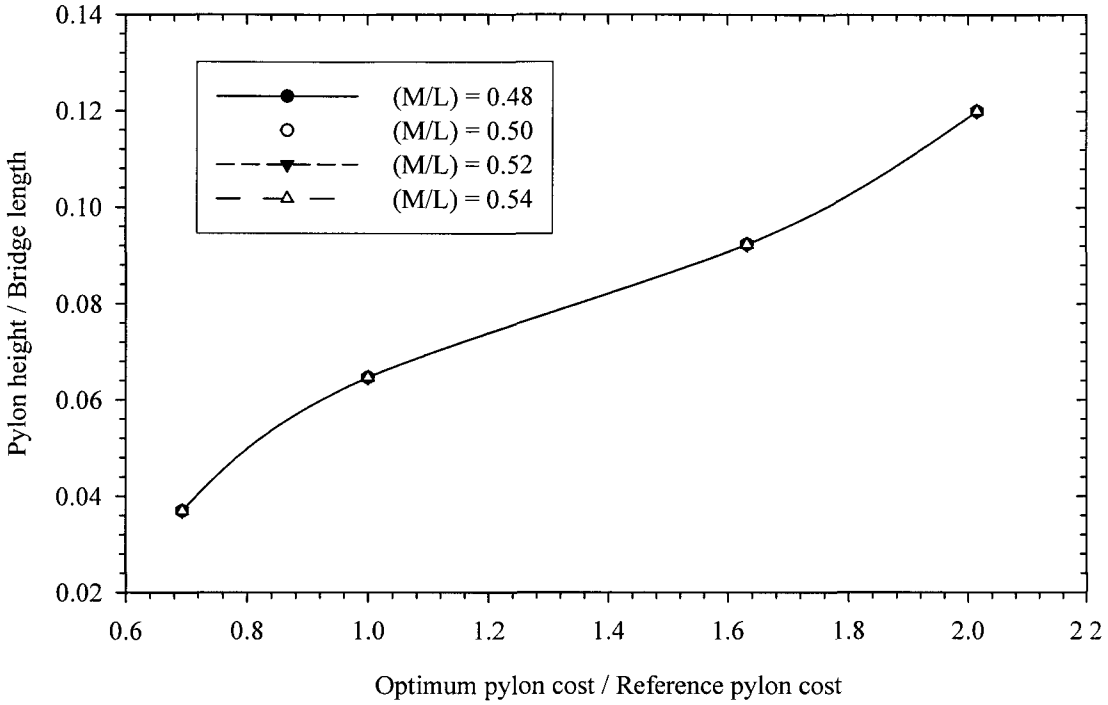

Fig. 4.5 Variation of pylon cost with height of the pylon and main span length.

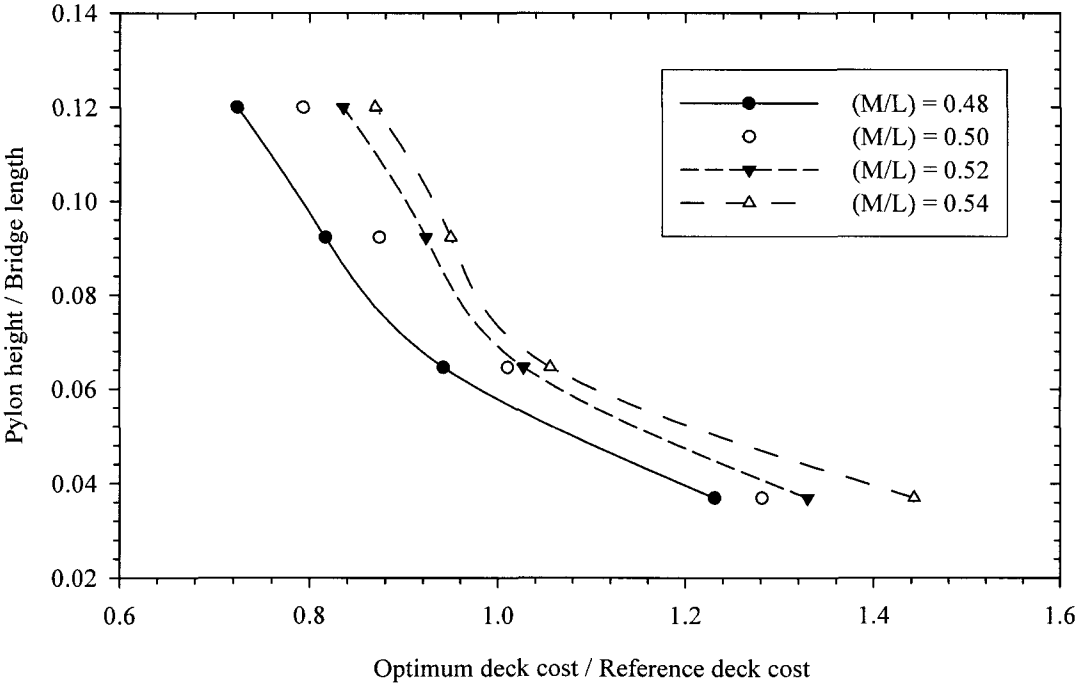

Fig. 4.6 Variation of deck cost with height of the pylon and main span length.

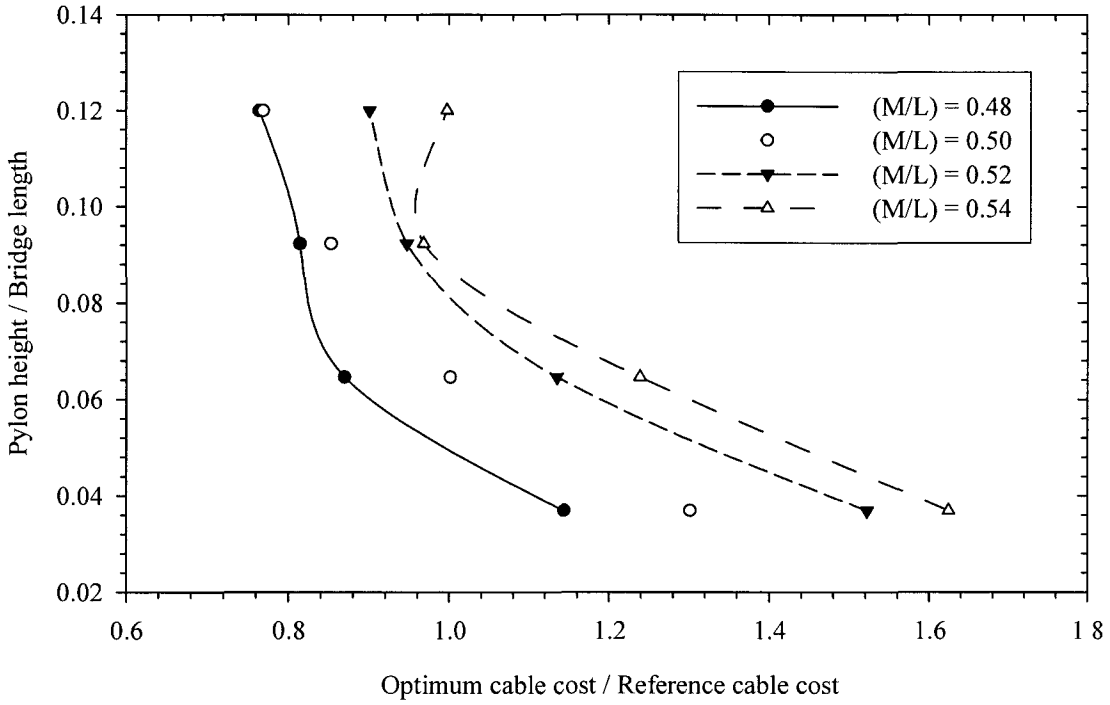

Fig. 4.7 Variation of stay cables cost with height of the pylon and main span length.

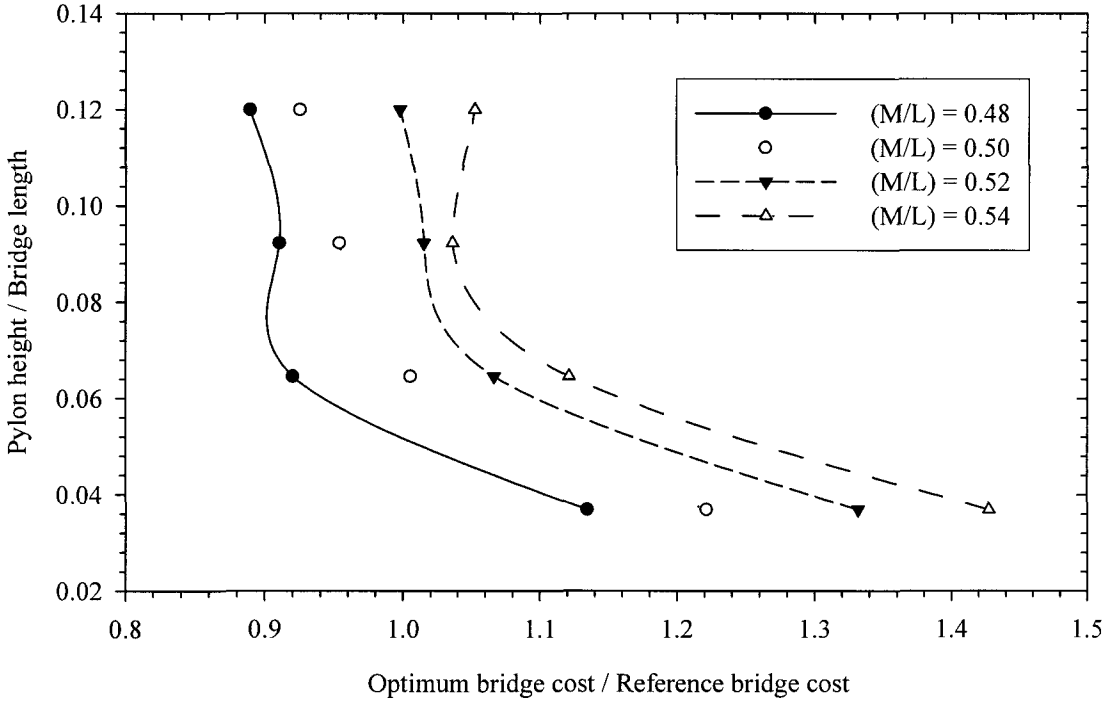

Fig. 4.8 Variation of bridge cost with height of the pylon and main span length.

4.6.5 Case (4): Effect of Number of Cables on the Bridge Cost

For a cable-stayed bridge, the choice of the number of stay cables supporting the deck is considered one of the most decisive factors in the design process. The increase in the number of stay cables decreases the panel length (length between two consecutive stay cables), which reduces the bending moment along the longitudinal direction of the deck and, consequently, the deck cross-section. Moreover, this increase reduces the post-tensioning cable forces, which reduces the stresses concentration at the anchorage points in the pylon and deck, and facilitates the construction and the maintenance of stay cables. However, it is preferable to have minimum number of cable connections to reduce the efforts needed to adjust the forces in the stay cables during the bridge operation (Troitsky, 1988). Furthermore, the unit cost of stay cables is relatively high compared to other construction materials, thus, it is crucial to optimize the cost of these stay cables. The aim of this section is to asses the influence of the number of stay cables on the cost of cable-stayed bridge. The bridge used in this section has the same main span length (M), and height of the upper strut cross beam (h_B) as those of the Quincy Bayview Bridge. Various optimization analyses are repeated by varying the number of stay cables (N) using values of *5, 6, 7, 8, 9, 10, 11, 12, and 13,* respectively.

The variations of the cost of the bridge components with the number of stay cables are shown in Fig. 4.9. It can be seen that the cost of the bridge deck consistently decreases with the increase in the number of stay cables; however, beyond a value of twelve stay cables in each group ($N = 12$), the deck cost slightly increases. Fig. 4.9 shows that an increase in the number of stay cables from seven to ten leads to a reduction of *10%* in the deck cost. It can be also seen from Fig. 4.9 that the cost of the pylon increases gradually

with the increase in the number of stay cables. This is explained by the fact that the increase in the number of stay cables requires a higher pylon to accommodate the cable anchor positions on the pylon.

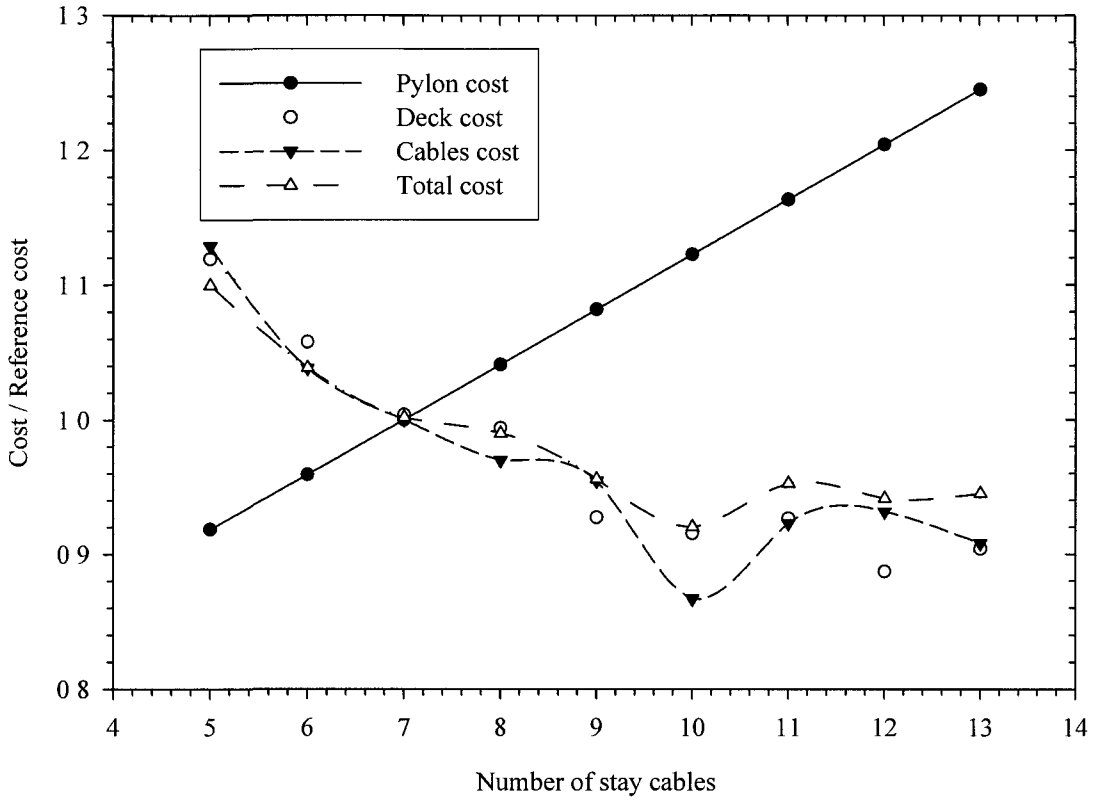

Fig. 4.9 Variation of bridge components cost with number of stay cables.

Moreover, it can be seen from Fig. 4.9 that the cost of stay cables decreases with the increase in the number of stay cables. However, this trend reverses when the number of stay cables is increased from 10 to 12. The results show that an increase in number of stay cables from seven to ten leads to a reduction of *14%* in cost of stay cables. Finally, it can be seen from Fig. 4.9 that the total cost of the cable-stayed bridge gradually decreases with the increase in the number of stay cables up to ten stay cables ($N = 10$). When the number of stay cables reaches eleven ($N = 11$), the total cost of the bridge

slightly increases. Beyond this number of cables, the bridge cost becomes almost constant. Compared to the reference design, by increasing the number of stay cables from seven to ten, a reduction of *8%* in the total cost of the bridge can be achieved. Based on the above results, it is obvious that the increase in the number of stay cables decreases the total cost the cable-stayed bridge. However, beyond a certain value, such an increase in (N) becomes counter-productive.

4.6.6 Case (5): Optimal Design of the Bridge

In this section, the optimal design of the bridge is determined by allowing all the design variables described in Section (4.2) to vary. The upper and lower bounds of each design variable are tabulated in Table 4.4. The reference design "Case (1)" and the optimal design "Case (5)" solutions obtained from this analysis are summarized in Table 4.8.

It can be noticed from the results that, in spite of increasing the number of stay cables from seven "Case (1)" to eight "Case (5)", a reduction in the stay cables cost of *23.8%* is achieved. It can be also noticed that a reduction of *23.2%* in the deck cost, and an increase of *49%* in the pylon cost are obtained compared to the reference design. Finally, comparing the total costs of the bridge for the optimal and reference design shows that up to *15%* saving is achieved when all the design variables are included in the optimization routine. It can be concluded that implementing all the design variables in the optimization techniques is important to achieve the minimum cost design of cable-stayed bridges.

Table 4.8 Comparison of the solutions for Case (1) and Case (5).

Design variable	Case (1)	Case (5)
No. of cables of each group (N)	7	8
γ_1 = Main span (M) / Bridge span (L)	0.506	0.481
γ_2 = upper strut height (h_B) / Bridge span (L)	0.065	0.109
Max. diameter of cables (D_{max})	0.08 m	0.07 m
Min diameter of cables (D_{min})	0.05 m	0.03 m
Thickness concrete slab (t_s)	0.15 m	0.15 m
Main girder height (H_G)	2.900 m	2.507 m
Width of upper flange (B_{FT})	0.551 m	0.417 m
Width of lower flange (B_{FB})	0.638 m	0.510 m
Thickness of upper flange	0.035 m	0.021 m
Thickness of lower flange	0.037 m	0.029 m
Thickness of web	0.018 m	0.016 m
Pylon depth	3.5 m	4.0 m
Pylon width	1.5 m	2.0 m
Pylon thickness	0.50 m	0.50 m
Pylons cost	$ 3,306,912	$ 4,946,085
Deck cost	$ 13,999,430	$ 10,740,590
Cables cost	$ 11,205,851	$ 8,528,538
Total cost	$ 28,512,194	$ 24,215,214
	(Reference cost)	(Minimum cost)

4.7 Conclusions

In this study, an implementation of a powerful optimization technique in the design of semi-fan cable-stayed bridge has been introduced. The proposed numerical code integrates a finite element model, real coded genetic algorithm (RCGA), surrogate polynomial functions for evaluating post-tensioning cable forces, and design methodologies based on the Canadian Highway Bridge Design Code CAN/CSA-S6-06. Initially, the problems are solved as unconstrained minimization problems then the constraints are implemented in the form of penalty functions. The effects of the post-tensioning cable forces, the geometrical configuration, and the number of stay cables on the cost design of the bridge have been investigated. Finally, the optimum values of the design variables for a real cable-stayed bridge are provided under different design conditions. The conclusions that can be drawn from this study are:

1. By applying the appropriate post-tensioning forces to the stay cables, a reduction of 43.2% is achieved in the cost of the considered cable-stayed bridge. Most of this reduction occurs in the bridge deck. The costs of the pylons and the stay cables remain almost unchanged. This is due to the large reduction of maximum positive and negative bending moments of the deck resulting from the application of the post-tensioning cable forces.
2. The cost design of the cable-stayed bridge is greatly affected by the variations of the height of the pylon above the deck and the main span length. Therefore, these two parameters should be considered within the design variables.

3. Under a fixed value for the number of stay cables, the study conducted to assess the effects of the height of the pylon above the deck and the main span length on the cost design reveals that :
    a. The increase in the pylon height decreases the cost of the entire cable-stayed bridge. However, this reduction becomes less significant beyond a ratio of upper strut height to bridge length of *0.092*.
    b. The increase in the pylon height reduces the cost of the bridge deck and increases the cost of the pylon.
    c. The increase in the pylon height reduces the cost of stay cables; however, this trend becomes negligible beyond a ratio of upper strut height to bridge length of *0.092*. Only for $\gamma_1 = 0.54$ and $\gamma_2 \geq 0.092$, the cost of the stay cables increases with pylon height.
4. The cost design of the stay-cable bridge is notably affected by the selection of the number of stay cables. Accordingly, the number of stay cables should be included within the set of design variables.
5. The study conducted to assess the effect of varying the number of stay cables on the design cost, while maintaining the height of the pylon above the deck and the main span length constant reveals that:
    a. The increase in the number of stay cables gradually decreases the total cost the cable-stayed bridge up to ten stay cables in each single group ($N=10$). Beyond this limit, the cost of bridge slightly increases and then becomes almost constant.
    b. The increase in the number of stay cables increases the cost of the pylon, due to the increase in the pylon height to accommodate the cable anchor positions.

c. The increase in the number of stay cables decreases the cost of the deck; however, this decrease becomes less significant when the number of stay cable in each single group increases beyond a value of twelve (*N=12*).

d. The increase in the number of stay cables decreases the cost of stay cables until the number of stay cables reaches ten (*N=10*). Beyond this number, the stay cables cost increases.

6. The inclusion of all design variables in the optimization routine leads to the best optimum solution.

7. Compared to an optimization solution involving fixed geometric configuration to the values applied in the real bridge, up to *15%* reduction in the total cost of the bridge can be achieved when all design variables are included

4.8 References

1. Troitsky M.S., Cable-stayed bridges: theory and design. 2nd Ed. Oxford: BSP; 1988.

2. Walther R., Houriet B., Isler W., Moia P., Klein JF. Cable-stayed bridges. Thomas Telford Ltd., Thomas Telford House, London; 1988.

3. Gimsing NJ. Cable Supported Bridges Concept and Design. 2nd edition. New York: John Wiley & Sons Inc.; 1997.

4. Nieto F, Hernández S, Jurado J Á. Optimum design of long-span suspension bridges considering aeroelastic and kinematic constraints. J Struct. Multidisc Optim 2009;39:133-151.

5. Hong NK, Chang SP, Lee SC. Development of ANN-based preliminary structural design systems for cable-stayed bridges. Advanced in Engineering Software 2002;33:85-96.
6. Sung YC, Chang DW, Teo EH. Optimum post-tensioning cable forces of Mau-Lo His cable-stayed bridge. J Engineering Structures 2006;28:1407-1417.
7. Simões LMC, Negrão JHJO. Sizing and geometry optimization of cable-stayed bridges. J Computer & structure 1994; 52:309-321.
8. Long W, Troitsky, MS, Zielinski ZA. Optimum design of cable stayed bridges, J Structural Engineering and Mechanics 1999; Vol. 7, No. 3, 241-257.
9. Simões LMC, Negrão JHJO. Optimization of cable-stayed bridges with box-girder decks. J Adv. Eng. Software 2000; 31:417-423.
10. Chen DW, Au FTK, Tham LG, Lee PKK. Determination of initial cable forces in prestressed concrete cable-stayed bridges for given design deck profiles using the force equilibrium method. J Comput Struct 2000;74:1–9.
11. Lute V, Upadhyay A, Singh KK. Computationally efficient analysis of cable-stayed bridge for GA-based optimization. Eng Appl Artif Intell 2009;22(4-5):750-758.
12. Canadian Highway Bridge Design Code, (2006), CAN/CSA-S6-06.
13. George HW. Influence of deck material on response of cable-stayed bridges to live loads. J.Bridge Eng. 1999;4(2):136-42.
14. Agrawal TP. Cable-stayed bridges - parametric study. J.Bridge Eng. 1997;2(2):61-7.
15. Svensson HS, Christopher BG, Saul R. Design of a cable-stayed steel composite bridge. Journal of structural engineering New York, N.Y. 1986;112(3):489-504.

16. AASHTO (2007). *LRFD Bridge Design Specifications*, 4th Edition, Washington, D. C., USA

17. Wilson JC, Gravelle W. Modelling of a Cable-stayed Bridge for Dynamic Analysis. J Earthquake Eng & Struct Dyn 1991;20: 707-721.

18. Gen M, Cheng R. Genetic algorithms and engineering optimization. Wiley, New York; c2000.

19. Davis L. Handbook of Genetic Algorithms, Van Nostrand Reinhold, New York; 1991.

20. Michalewicz Z and Fogel DB. How to solve it: modern heuristics. 2nd Edn New York: Springer, c2004.

CHAPTER 5

DATABASE FOR THE OPTIMUM DESIGN OF SEMI-FAN CABLE-STAYED BRIDGES

5.1 Introduction

Cable-stayed bridges have received much attention and popularity because of their aesthetic appearance, efficient utilization of structural materials, ease of erection, and ability to overcome long spans crossings. The recent advances in the design and construction methods and the availability of high strength steel cables have enabled construction of not only longer but also lighter and slender bridges. Optimizing the design of cable-stayed bridges is becoming necessary with the typical high cost of such bridges, the increase of bridge spans, and the inflation in construction material prices.

In general, reaching an optimum design solution for cable-stayed bridges is a challenge task due to several reasons. Cable-stayed bridges are large, sophisticated, and highly statically indeterminate structures, consisting of three major components; stiffening girders, stay cables, and pylons (Gimsing, 1997). The overall behaviour of such structures is affected by the interaction between a large number of design parameters, such as the main span length, height of the pylon, number of stay cables, pylon configuration, deck material, and the stiffness distribution in the bridge structural components (Walther *et al.*, 1988). Typically, the design of cable-stayed bridges involves conducting a large number of preliminary design trials till reaching the final design solution. (Nieto *et al.*, 2009). Each design trial involves significant amount of calculations. The analyses should include various forms of geometric nonlinearities including the cables sag, large displacements,

and (P-Δ) effects (Nazmy and Abdel-Ghaffar, 1990). Each analysis trial involves the evaluation of a set of cables-pretension forces that counter balance the effect of dead loads. The design should satisfy all the serviceability and strength criteria specified in the design codes. All these make such an iterative design process tedious, time consuming, and expensive (Hong *et al.*, 2002).

The high redundancy of cable-stayed bridges, large number of design variables, strict constraints imposed by the design codes, highly geometrically nonlinear hehaviour, and robust effect of post-tensioning cable forces make it difficult to obtain an optimum design solution using traditional design methods and available optimization packages. A number of algorithms have been proposed in the literature for solving cable-stayed bridges optimization problem.

Simões and Negrão [1994] proposed the entropy-based optimization algorithm in order to optimize the cost of cable-stayed bridges. The locations of the stay cable anchors on both the main girder and pylons, and the cross-sectional properties of the deck, pylons, and stay cables were considered as design variables. In this study, a starting point is required to initiate the optimization process. The post-tensioning cable forces are not taken into account. In addition, the number of stay cables and the main span length are assumed to have pre-assigned constant values.

Long *et al.* [1999] used the internal penalty function algorithm to optimize the cost of cable-stayed bridges with composite steel concrete deck. The effect of the post-tensioning cable forces was not also taken into account in this study. Only the cross-sectional dimensions of the bridge members were considered as the design variables. The pylon height, the main span length, and the number of stay cables were assumed as constant

parameters. In addition, an initial feasible design was required in order to start the optimization algorithm.

Simões and Negrão [2000] employed a convex scalar function to minimize the cost of a box-girder deck cable-stayed bridge. This function combines the cross-section dimensions of various components of the bridge and the post-tensioning cable forces. The gradient based non-linear programming technique used in this study may linger in local optima. As reported by Chen *et al.* [2000], this method is very sensitive to the selection of constraints, which should be imposed very cautiously to obtain a practical output. The pylon height and the main span length were not considered within the design variables. Additionally, a starting point was required to initiate the optimization process.

Lute *et al.* [2009] demonstrated the capability of support vector machine (SVM), which is a learning method used for regression, to reduce the computational time of genetic algorithm (GA) for optimizing cable-stayed bridges. The imposed constraints were few, simple, and not based on a standard design code, making them insufficient to assess the strength of the bridge components. In this study, the number of stay cables was treated as a pre-set constant variable, and the effect of post-tensioning cable forces was also neglected.

An algorithm for optimizing the design of cable-stayed bridges was introduced in Chapter 4. The algorithm utilizes surrogate polynomial functions for evaluating the optimum post-tensioning cable forces. The number of stay cables, main span length, height of the pylon, and cross-sectional dimensions of the deck, pylons, and stay cables are assumed as the design variables. The design criteria specified in the Canadian Highway Bridge Design Code CAN/CSA-S6-06 [2006] are included in the numerical

scheme as design constraints. The real coded genetic algorithm (RCGA), as a global optimization method, is employed to obtain the global optimum design of the bridges.

The objective of this chapter is to develop database, in the form of tables and curves, for the optimum design parameters of cable-stayed bridges. Using the numerical model developed in Chapter 4, the optimum values for the number of stay cables, main span length, height of the pylon above the deck, and cross-sectional dimensions of the bridge components are evaluated for different bridge lengths. Such database will help designers to estimate quantities required for the preliminary design of the bridge. It can be used to obtain the initial configuration and various design parameters that are needed for further structural analyses. The optimum design parameters are developed for composite steel concrete cable-stayed bridges with semi-fan cable arrangements. The advantages of this type of composite deck are explained by Svensson *et al.* [1986]. The composite deck system was used in a large number of cable-stayed bridges, such as the Quincy Bayview Bridge, Annacis Island Bridge, and Qingzhou Bridge, located in USA, Canada, and China, respectively, (Troitsky, 1988) and (Ren and Peng, 2005). The semi-fan is considered to be the ideal solution for a cable-stayed bridge, as it represents an intermediate solution between the harp and fan patterns. It combines the advantages and avoids the disadvantages of the harp and fan patterns.

5.2 Description of Composite Bridges

A schematic diagram of a typical three span cable stayed bridge is provided in Fig. 5.1(a). The main span length is (*M*) *m* and the two equal sides have spans of (*S*) *m* each, as shown in Fig. 5.1(a). The deck superstructure is supported by four groups of double plane

stay cables in a semi-fan type arrangement. The single plane in each group has (N) stay cables. As such, there are ($8N$) stay cables supporting the whole bridge. The distance between the stay cables anchorages along the pylon is taken as *2.0 m,* which is considered as a reasonable distance for practical installation. Therefore, the distance (h_T), shown in Figs. 5.1 (a) and 5.1(d), is equal to (N *x 2.0 m*), where (N) is the number of stay cables. The cross-section of the bridge deck consists of two steel main girders located at the outer edge of the deck, as shown in Figs. 5.1 (b) and 5.1(c), and topped by a precast concrete slab having a thickness (t_s) and a width (B), as shown in Fig. 5.1(b). The two girders are connected by a set of equally spaced floor steel beams. The two pylons of the cable-stayed bridge have an H-shape with a width *(d)*, as shown in Fig. 5.1(d). The total height of the pylons' tops above the bridge deck is (H), as shown in Figs. 5.1 (a) and 5.1(d). An upper strut cross beam connects the two upper legs at a height (h_B) measured from the deck level. The depth, width, and thickness of the pylon cross-section, shown in Fig. 5.1(e), are (H_P), (B_P), and (t_P), respectively. The assumed properties and estimated unit prices of the materials, which are used in the optimization study, are provided in Table 5.1. The optimum design database covers bridge lengths ranging between *250 m* and *700 m* with an increment of *50 m* and is developed for the following two cases:

- Case (1): the deck has two lanes of traffic (n_{Lane}= *2*) with a width *(B)* of *14.20 m.*
- Case (2): the deck has four lanes of traffic (n_{Lane}= *4*) with a width *(B)* of *20.50 m.*

As such, fourty optimization analyses are conducted in this study. The width of the deck for the two-lane and four-lane cases is determined according to Table 3.8.2 of the CAN/CSA-S6-06 [2006].

Table 5.1 Material properties of the bridge.

Material	Properties	
Steel	Modulus of elasticity, (Es)	= 200 GPa
	Unit weight, (γ_s)	= 77 kN/m^3
	Poisson's ratio, (v_s)	= 0.30
	Yield strength, (F_y)	= 350 MPa
	Unit price (C_{steel})	= 12,000 $/ton
Concrete	Modulus of elasticity, (E_c)	= 24.87 GPa
	Unit weight, (γ_c)	= 24.0 kN/m^3
	Poisson's ratio, (v_c)	= 0.20
	Compressive strength, (f_c')	= 30 MPa
	Unit price ($C_{concrete}$)	= 4,218 $/m^3
Cables	Modulus of elasticity, (E_{sc})	= 205 GPa
	Unit weight, (γ_{scable})	= 82.40 kN/m^3
	Ultimate tensile strength, (T_{cCable})	= 1.6 GPa
	Unit price (C_{cable})	= 60,000 $/ton
Reinforcement steel	Yield strength, (f_y)	= 400 MPa
Asphalt	Unit weight, ($\gamma_{Asphalt}$)	= 23.5 kN/m^3

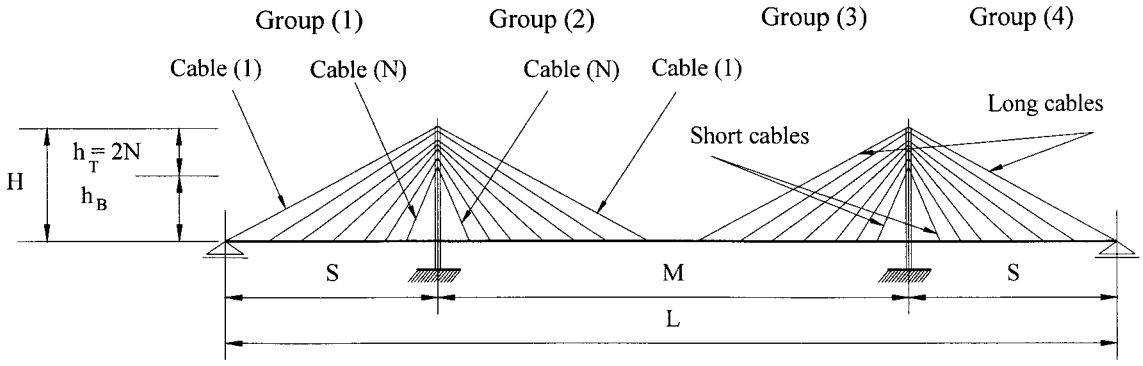

(a) Geometry of bridge.

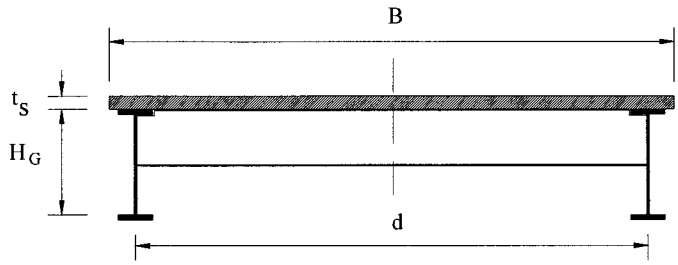

(b) Cross-section of the bridge deck.

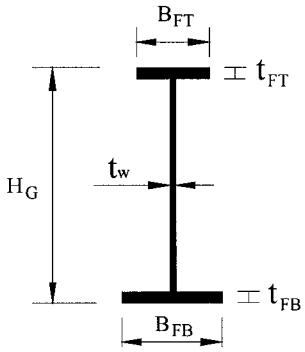

(c) Steel main girder.

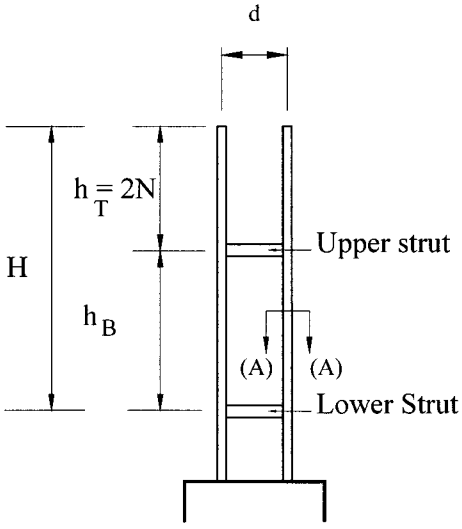

(d) Pylon elevation.

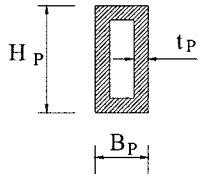

Sec. (A-A)

(e) Pylon cross-section.

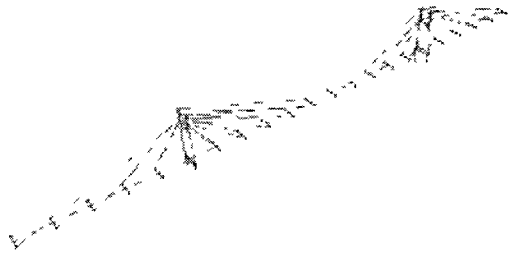

(g) Finite element model.

Fig. 5.1 Bridge layouts, cross-sections, and finite element model.

5.3 Optimum Design Algorithm

The optimization algorithm presented in the previous chapter is used to develop the optimum design database for semi-fan cable-stayed bridges. The optimization algorithm combines a finite element model, real coded genetic algorithm (RCGA), and surrogate polynomial functions for evaluating post-tensioning cable forces. The design loads and constraints used in the optimization algorithm are based on the Canadian Highway Bridge Design Code CAN/CSA-S6-06 [2006]. A brief overview of this model is presented in this Chapter.

5.3.1 Design Variables

The design parameters can be divided into two categories: (a) parameters defining the geometric configuration of the bridge, and (b) parameters describing the cross-sectional dimensions of various components of the bridge.

The geometric configuration parameters are:

1. Number of stay cables in each single plane (N), shown in Fig. 5.1(a).
2. Main span length (M), shown in Fig. 5.1(a), which is varied by changing a dimensionless parameters ($\gamma_1 = M/L$), where (L) is the total length of the bridge.
3. Height of the upper strut cross beam (h_B), shown in Figs. 5.1 (a) and 5.1(d), which is varied by changing a dimensionless parameters ($\gamma_2 = h_B/L$). This parameter defines the height of the lowest cable anchor position relative to the deck level.

The cross-sectional parameters are:

1. Diameter of each stay cable (D_i), where (i) is the stay cable number.
2. Thickness of the concrete deck slab (t_s), shown in Fig. 5.1(b).

3. Height of the two steel main girders (H_G), shown in Fig. 5.1(c).
4. Width of the main girders top flanges (B_{FT}), which is varied using the dimensionless ratio ($\gamma_3 = B_{FT}/ H_G$), as shown in Fig. 5.1(c).
5. Width of the main girders bottom flanges (B_{FB}), which is varied using the dimensionless ratio ($\gamma_4 = B_{FB}/ H_G$), as shown in Fig. 5.1(c).
6. Thickness of the main girders top flanges (t_{FT}), shown in Fig. 5.1(c), which is calculated based on CAN/CSA-S6-06 [2006] using the following relation:

$$t_{FT} = \frac{B_{FT}\sqrt{F_y}}{2\ F_{FT}} \tag{5.1}$$

where

B_{FT} = width of the top flanges.

F_y = steel yield strength.

F_{FT} = Factor defining the thickness of the upper flanges. The values of F_{FT} proposed in the CAN/CSA-S6-06 [2006] are selected in order to prevent premature local buckling of the flanges. The range of values depends on the classification of the steel section and is provided in Table 5.2.

7. Thickness of the main girders bottom flanges (t_{FB}), shown in Fig. 5.1(c), which is calculated based on CAN/CSA-S6-06 [2006] using the following relation:

$$t_{FB} = \frac{B_{FB}\sqrt{F_y}}{2\ F_{FB}} \tag{5.2}$$

where

B_{FB} = width of the bottom flanges.

F_{FB} = Factor defining the thickness of the bottom flanges. Similar to the top flanges, the range of values for the factor F_{FB} preventing local buckling of the bottom flanges is provided in Table 5.2, for different class sections.

8. The main girders web thickness (t_w), shown in Fig. 5.1(d), which is calculated based on CAN/CSA-S6-06 [2006] using the following relation:

$$t_w = \frac{H_G}{\left(\frac{F_{W1}}{\sqrt{F_y}}\left[1 - F_{W2}\frac{F_{fw}}{F_{yw}}\right]\right)} \tag{5.3}$$

where,

F_{w2} = *0.39, 0.61*, and *0.65* for Class *1, 2* and *3,* respectively, as provided in Table 10.9.2.1, CAN/CSA-S6-06 [2006]. .

F_{fw} = factored compressive force in the web component at ultimate limit state.

F_{yw} = axial compressive force at yield stress.

F_{W1}= Factor defining the thickness of the web, in order to prevent premature local buckling. The range of values of F_{W1} is defined by the CAN/CSA-S6-06 [2006], and is provided in Table 5.2 for various class sections.

9. The depth, width, and thickness of the pylons cross-sections, (HP), (BP), and (tP), respectively, which are shown in Fig. 5.1(e).

As such, the vector of design variables can be summarized as:

$$\boldsymbol{x} = \{x_i\} = \{N, \gamma_1, \gamma_2, D, t_s, H_G, \gamma_3, \gamma_4, F_{FT}, F_{FB}, F_{w1}, H_P, B_P, t_P\} \tag{5.4}$$

The height of the pylon from the foundation to the deck levels is not included among the set design variables, since this parameter is governed by the clearance requirement. It should be noted that the design of the floor system, including the cross beams spacing and dimensions, and slab longitudinal reinforcement, can be carried on independently of

the design of the main girders and the towers, which is the focus of this study (Long *et al.,* 1999).

Table 5.2 Factors decide thickness of steel main girders [Clause 10.9.2, CAN/CSA-S6-2006]

	Class 1	Class 2	Class 3
Upper flange	$F_{FT} \leq 145$	$145 \leq F_{FT} \leq 170$	$170 \leq F_{FT} \leq 200$
Lower flange	$F_{FB} \leq 145$	$145 \leq F_{FB} \leq 170$	$170 \leq F_{FB} \leq 200$
Web	$F_{W1} \leq 1100$	$1100 \leq F_{W1} \leq 1700$	$1700 \leq F_{W1} \leq 1900$

5.3.2 Design Constraints

The design constraints can be categorized into: a) strength constraints that follow the limit state design specifications given in CAN/CSA-S6-06 [2006] code for the stay cables, deck main girder and pylons under all load combinations specified in the code, b) serviceability constraint that follows the deflection limit imposed by the AASHTO LRFD [2007] under live load. Details about these design constraints are given in Chapter 4.

5.3.3 Objective Function

The goal of the optimization algorithm is to determine a set of design variables in such a way that the final design provides the minimum cost of the bridge. In order to penalize the infeasible solutions, which violate the design constraints, a penalty function is included in the objective function. The penalized objective function $F_p(\boldsymbol{x})$ takes the following form:

$$F_p(\boldsymbol{x}) = F(\boldsymbol{x}) + \sum_{i=1}^{n} \alpha_i gi \tag{5.5}$$

where $\begin{cases} \delta_i = g_i, \quad for \ \ g_i > 0 \ \ (if \ constraint(g_i) \ \ is \ \ violated). \\ \delta_i = 0, \quad for \ \ g_i \leq 0. (if \ constraint(g_i) \ \ is \ \ satisfied). \end{cases}$

$F(\boldsymbol{x})$ = the total cost of the bridge and can be expressed as:

$$F(\boldsymbol{x}) = \gamma_{cables} V_{cables}(\boldsymbol{x}) C_{\boldsymbol{cables}} + V_c(\boldsymbol{x}) C_{concrete} + \gamma_s V_{\boldsymbol{steel}}(\boldsymbol{x}) C_{\boldsymbol{steel}} \quad (5.6)$$

$\boldsymbol{x}_i$ = the vector of design variables, defined in Section (3.1).

g_i= constraint function.

δ_i = a violation factor for the ith constraint.

α_i = a penalty parameter "certain suitable coefficient" imposed for violation of constraint i, which depends on the type of the optimization problem.

γ_{cable} and γ_s = the unit weights of stay cables and structural steel, respectively.

V_{cable}, V_c, and V_{steel} = the volumes of cables, concrete, and structural steel, respectively.

$C_{cable}, C_{concrete}$, and C_{steel} = the unit prices of stay cables, concrete, and steel, respectively.

The values of the unit prices used in the optimization algorithm are provided in Table 5.1.

5.3.4 Assumed Loads

The values of the loads applied in the analyses as well as the considered load cases and load combinations are taken from the CAN/CSA-S6-06 [2006].

- **Dead load**

The dead loads include the structural self-weight of the bridge, a layer of asphalt having a thickness of *0.09 m*, two concrete traffic barriers having an average thickness and height of *0.325 m* and *0.85 m*, respectively. In addition, a load per unit area of *0.75 kN/m*^{2} as

estimated by Long *et al.* [1999] to simulate the weight of the floor cross beams, is included

- **Live load**

According to the CAN/CSA-S6-06 [2006], the magnitude of the live load is equal to *16.2* kN/m and *25.2* kN/m for the case of two and four lanes, respectively. The nine live load patterns used to obtain the optimum cost design of the cable-stayed bridge are illustrated in Fig. 5.2, (Walther *et al.*, 1988).

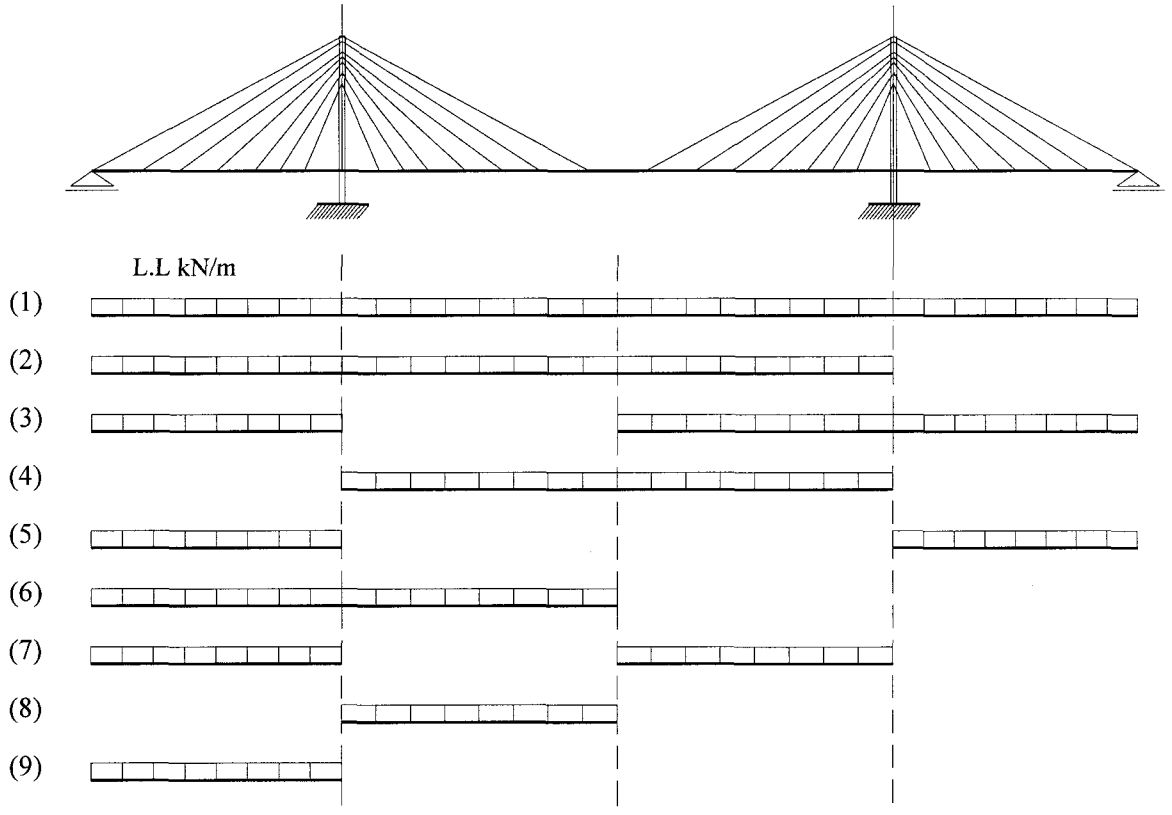

Fig. 5.2 Live load cases used in the optimization algorithm.

- **Wind load**

The bridge is assumed to be located in Victoria , British Colombia. The angle of attack of the wind on the deck is assumed to be zero. Therefore, only the drag pressure is included in the study. The load per unit length q_w is calculated as follows:

$$q_w = q\, C_D\, h \tag{5.7}$$

where,

q *is* the hourly mean reference wind pressure. For the assumed location, it has a value of $690\ N/m^2$, as specified in the CAN/CSA-S6-06 [2006].

h is the wind exposure depth. It is evaluated as the summation of the height of the main girder deck and the height of traffic barrier.

C_D is the drag shape coefficient. In view of the study conducted by Walther *et al.* [1988], a value of 0.8 is assumed for the considered open cross section type.

- **Load factors and load combinations**

In view of the CAN/CSA-S6-06 [2006], the following two loading combinations are considered:

$$1.1\,D + 1.7\,L \tag{5.8}$$

$$1.1\,D + 1.4\,L + 0.5\,W \tag{5.9}$$

$$1.1\,D + 1.65\,W \tag{5.10}$$

where, D = Dead load, L = Live load, and W = Wind load.

5.3.5 Optimization Process

The optimization algorithm for finding the optimum cost design of cable-stayed bridges is explained in the flow chart shown in Fig. 5.3. It involves the following steps:

1. The real coded genetic algorithm (RCGA) creates an initial population of the design variables which are defined in Section (5.3.1). The population has *100* candidates (*100* bridges) selected randomly between the lower and upper bounds of each design variable, presented in Table 5.3. The design variables define the geometric configuration and cross-sectional dimensions of the bridge.
2. A three dimensional nonlinear finite element model (FEM) is created for each candidate (bridge), as shown in Fig. 5.1(g). Three-dimensional truss elements that account for the effect of sagging using an equivalent elastic modulus (Ernst, 1965) is employed to simulate the cables. Three-dimensional frame elements, which account for the effect of geometric nonlinearity, are used to model the deck and the pylons.
3. The post-tensioning cable forces in the stay cables are calculated using the surrogate post-tensioning functions developed in Chapter 3. The structure is then analyzed under the combined effect of the cables post-tensioning forces and the factored loads described above. The displacements, and internal forces and bending moments are determined for all elements of the bridge.
4. The strength and serviceability design constraints are assessed. If any of these constraints is not satisfied, the result of this specific bridge configuration is excluded from the search space by applying the penalized objective function given by Eq. (5.5).

5. The initial population is sorted in ascending order according to the value of the objective function such that the first ranked candidate (bridge) has the minimum value of the feasible cost design.
6. The (RCGA) generates a new population (*100* bridges) by applying the crossover and mutation operators on the high ranked cost functions evaluated at step *5* to produce a new generation with better fitness (lower cost). These operators direct the search towards the global optimum solution. Details of such operators are given by Michalewicz and Fogel [2004].
7. The previous population is replaced with the newer one containing the new candidate cable-stayed bridges, in addition to the best candidate cable-stayed bridge found so far (elitist selection).
8. Steps *2* to *7* are repeated for a certain number of generations taken as *100* iterations in the current study till a global optimum solution is reached.
9. The candidate cable-stayed bridge with the highest fitness "smallest values of the objective function" obtained at step *8* is delivered as the final solution.

Table 5.3 Lower and upper bounds of the design variables.

Design variable	Lower bound	Upper bound
N (number of stay cables in each single plane)	5	13
D_i (diameter of each stay cables)	0.01 m	0.25 m
γ_1 = (M/L) = (Main span length / bridge length)	0.48	0.54
γ_2 = (h_B/L) = (height of upper strut cross beam / bridge length)	0.03	0.12
t_s = thickness of the concrete deck slab	0.15 m	0.40 m
H_G = height of the two steel main girders	0.50 m	5.0 m
γ_3 = (B_{FT}/ H_G) = (width of top flange / height of main girder)	0.15	0.20
γ_4 = (B_{FB}/ H_G) = (width of bottom flange / height of main girder)	0.20	0.25
F_{FT} = factor decides the thickness of upper flange	145	200
F_{FB} = factor decides the thickness of lower flange	145	200
T_{W1} = factor decides the thickness of web	1100	3000
H_P = depth of the pylon cross-section	1.0 m	6.0 m
B_P = width of the pylon cross-section	1.0 m	5.0 m
t_P = thickness of the pylon cross-section	0.25 m	1.0 m

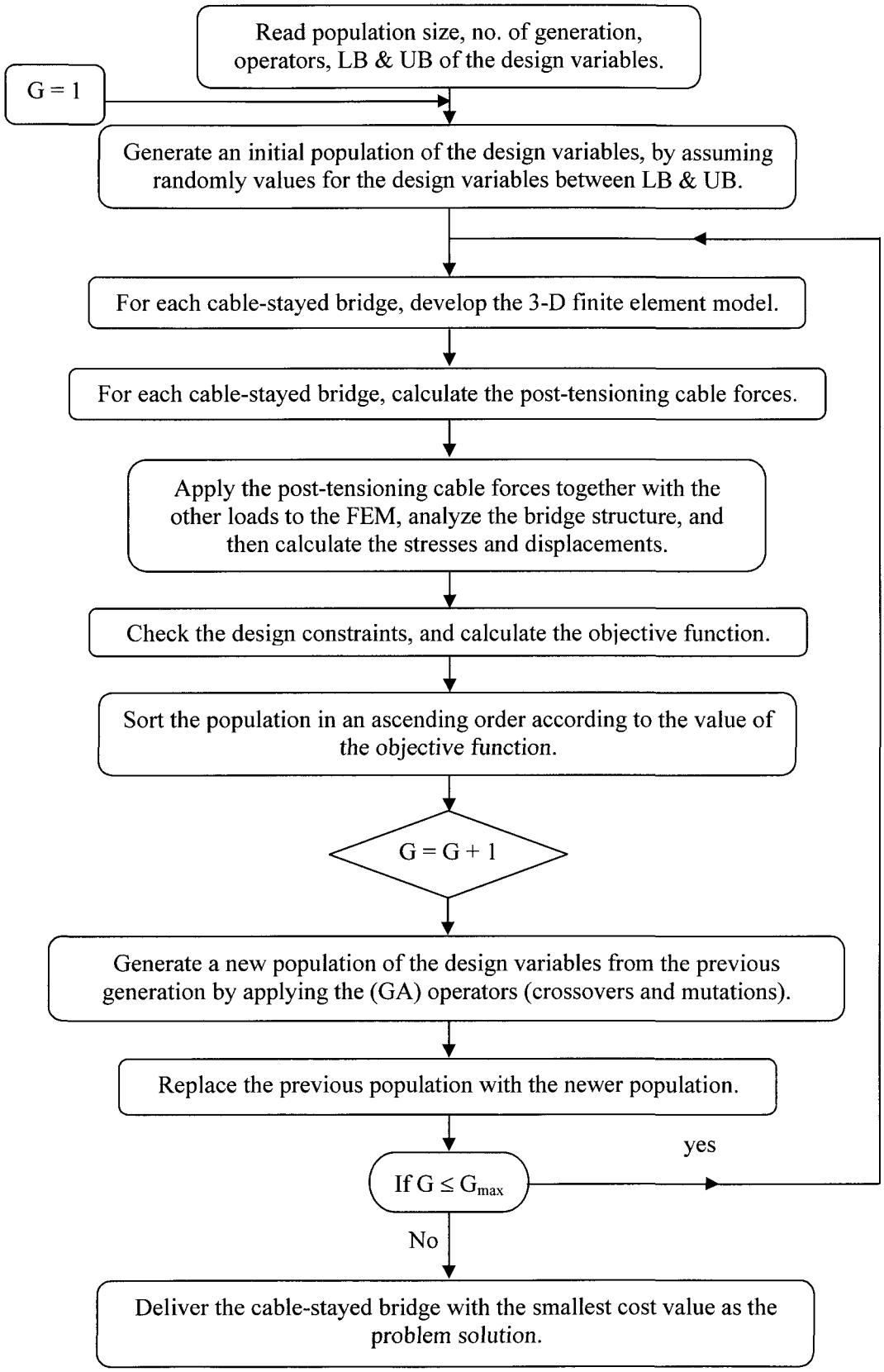

Fig. 5.3 Flow chart for evaluation of the minimum cost of the cable-stayed bridge.

5.4 Results and Discussion

The following subsections show the results of *40* optimization analyses conducted for Case (1) and Case (2), which correspond to bridges with two lanes and four lanes, respectively. The results cover bridge lengths ranging between *250 m* and *700 m,* with an increment of *50 m*. The optimum values of the design variables as well as their variations with the total bridge length (L) are reported.

5.4.1 Optimum Number of Stay Cables (N)

The selection of the number of stay cables is one of the most decisive factors in the design of cable-stayed bridges. Using a small number of stay cables leads to large cable forces, which require strong and complicated post-tensioning machineries. Excessive cable forces also increase the stress concentrations at the anchorage points in both the pylon and the deck. This necessitates stiffening large areas of the deck and pylon to distribute the trust (Troitsky, 1988). Meanwhile, large spacing between the stay cables increases the bending moment along the longitudinal direction of the deck and, consequently, the deck cross-section. On the other hand, the unit cost of the stay cables is relatively high compared to the materials used in other components of the bridge. Thus, an optimum number of stay cables can provide a compromise between the enhancement in the structural performance and the cost premium resulting from the high cost of the stay cables.

Fig. 5.4(a) shows the variation of the optimum number of stay cables with the bridge length for Case (1). The general trend shows an increase in the number of stay cables with the increase in the bridge length. However, the range of lengths between *250 m* and

300 m has a constant number of *5* stay cables, and the range of lengths between *450 m* and *550 m* has a constant number of *8* stay cables. A similar behaviour is shown in Fig. 5.4(b) for Case (2). Generally, the optimum number of stay cables for the four-lane case (Case 2) is larger than that for the two-lane case (Case 1). This is true with the exception for the smallest and largest values of (L) considered in the analyses. Also, it can be noticed that Case (2) exhibits a sharper variation in the optimum number of stay cables with the length (L).

5.4.2 Optimum Cables Diameters

The optimum diameters of stay cables obtained from Case (1) and Case (2) analyses are given in Tables 5.4 and 5.4, respectively. As shown in the tables, the number of reported cables varies for different lengths. This is a reflection for the variation of the number of optimum cables with the length of the bridge. The labels for the cable numbers follows the trend shown in Fig. 5.1(a).

In general, the optimum sizes of stay cables for Case (2) are larger than those for Case (1). It can be seen from Tables 5.4 and 5.5 that the optimum diameter values are bound between $0.02m$ and $0.06m$ ($0.02m \leq D \leq 0.06m$) for Case (1), and are bound between $0.03m$ and $0.08m$ ($0.03m \leq D \leq 0.08m$) for Case (2). Due to symmetry, the cables' diameters of Group (1) and Group (2) are equal to the corresponding ones of Group (4) and Group (3), respectively.

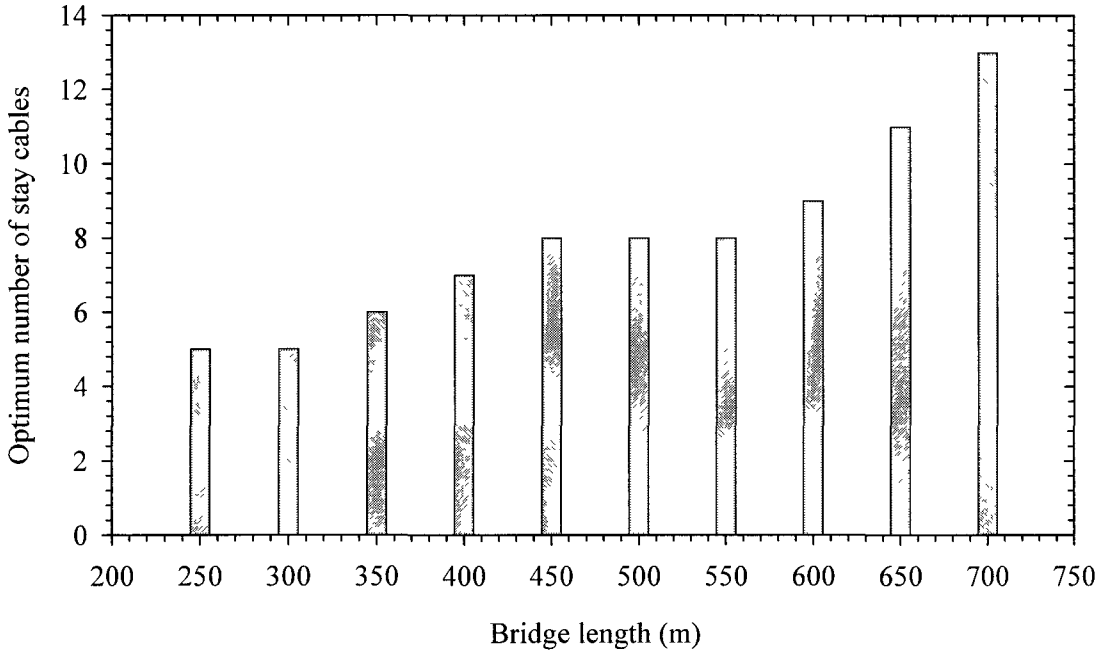

(a) Case (1) "two lanes".

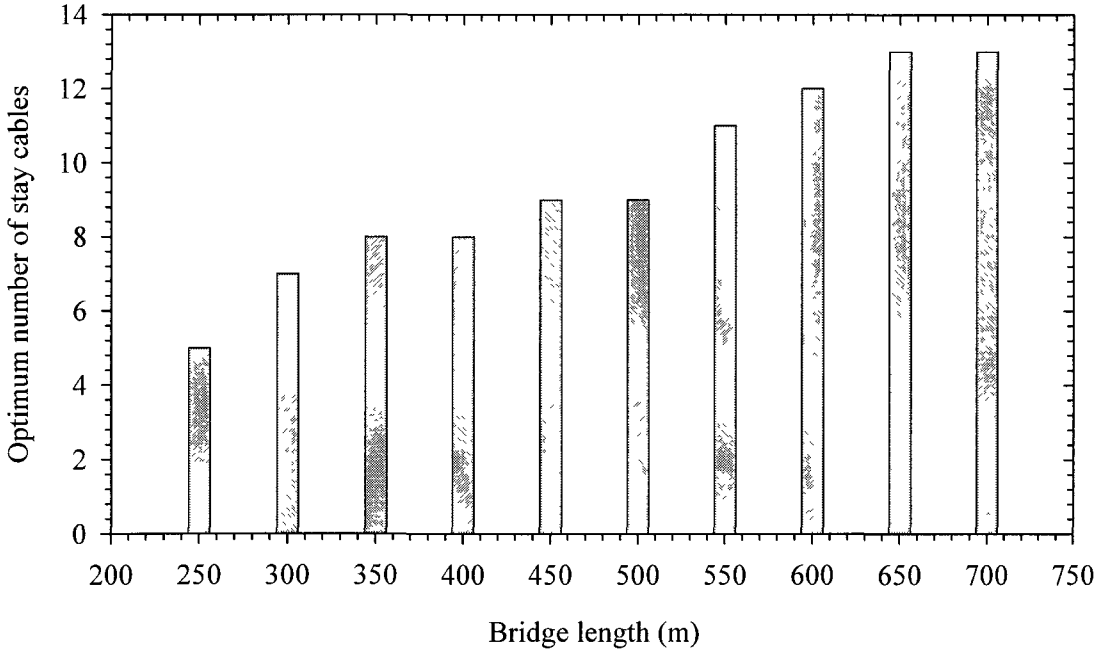

(b) Case (2) "four lanes".

Fig. 5.4 Optimum number of stay cables.

Table 5.4(a) Diameters of stay cables for Case (1).

	Group (1) and (4)		Group (2) and (3)			Group (1) and (4)		Group (2) and (3)	
L (m)	Cable No.	D (m)	Cable No.	D (m)	L (m)	Cable No.	D (m)	Cable No.	D (m)
250	1	0.03	1	0.05	300	1	0.03	1	0.05
	2	0.05	2	0.05		2	0.06	2	0.05
	3	0.05	3	0.05		3	0.06	3	0.05
	4	0.05	4	0.04		4	0.06	4	0.05
	5	0.05	5	0.04		5	0.06	5	0.04
350	1	0.04	1	0.05	400	1	0.04	1	0.05
	2	0.05	2	0.05		2	0.06	2	0.05
	3	0.06	3	0.05		3	0.06	3	0.05
	4	0.06	4	0.05		4	0.06	4	0.05
	5	0.05	5	0.05		5	0.05	5	0.05
	6	0.05	6	0.04		6	0.06	6	0.05
						7	0.06	7	0.04
450	1	0.02	1	0.05	500	1	0.02	1	0.05
	2	0.05	2	0.05		2	0.05	2	0.06
	3	0.06	3	0.05		3	0.06	3	0.05
	4	0.06	4	0.05		4	0.06	4	0.05
	5	0.05	5	0.05		5	0.06	5	0.05
	6	0.05	6	0.05		6	0.06	6	0.05
	7	0.05	7	0.04		7	0.06	7	0.05
	8	0.06	8	0.03		8	0.06	8	0.04
550	1	0.02	1	0.06	600	1	0.03	1	0.06
	2	0.06	2	0.06		2	0.05	2	0.06
	3	0.07	3	0.06		3	0.06	3	0.06
	4	0.07	4	0.06		4	0.06	4	0.05
	5	0.06	5	0.05		5	0.06	5	0.05
	6	0.06	6	0.05		6	0.06	6	0.05
	7	0.06	7	0.05		7	0.06	7	0.05
	8	0.06	8	0.04		8	0.05	8	0.04
						9	0.06	9	0.05

Table 5.4(b) Diameters of stay cables for Case (1).

	Group (1) and (4)		Group (2) and (3)			Group (1) and (4)		Group (2) and (3)	
L (m)	Cable No.	D (m)	Cable No.	D (m)	L (m)	Cable No.	D (m)	Cable No.	D (m)
650	1	0.04	1	0.06	700	1	0.05	1	0.05
	2	0.06	2	0.05		2	0.04	2	0.05
	3	0.06	3	0.06		3	0.06	3	0.05
	4	0.06	4	0.06		4	0.06	4	0.05
	5	0.06	5	0.05		5	0.06	5	0.05
	6	0.06	6	0.05		6	0.06	6	0.05
	7	0.06	7	0.05		7	0.06	7	0.05
	8	0.06	8	0.05		8	0.06	8	0.05
	9	0.06	9	0.05		9	0.06	9	0.05
	10	0.06	10	0.04		10	0.06	10	0.05
	11	0.06	11	0.03		11	0.06	11	0.05
						12	0.06	12	0.04
						13	0.06	13	0.02

Table 5.5(a) Diameters of stay cables for Case (2).

	Group (1) and (4)		Group (2) and (3)			Group (1) and (4)		Group (2) and (3)	
L (m)	Cable No.	D (m)	Cable No.	D (m)	L (m)	Cable No.	D (m)	Cable No.	D (m)
250	1	0.04	1	0.06	300	1	0.05	1	0.06
	2	0.07	2	0.06		2	0.06	2	0.06
	3	0.07	3	0.06		3	0.07	3	0.06
	4	0.07	4	0.06		4	0.07	4	0.06
	5	0.07	5	0.05		5	0.06	5	0.06
						6	0.07	6	0.05
						7	0.07	7	0.04
350	1	0.04	1	0.06	400	1	0.04	1	0.07
	2	0.06	2	0.06		2	0.07	2	0.06
	3	0.06	3	0.06		3	0.07	3	0.07
	4	0.07	4	0.06		4	0.07	4	0.07
	5	0.06	5	0.06		5	0.07	5	0.06
	6	0.06	6	0.05		6	0.06	6	0.06
	7	0.06	7	0.05		7	0.06	7	0.06
	8	0.06	8	0.04		8	0.07	8	0.05
450	1	0.04	1	0.07	500	1	0.05	1	0.07
	2	0.06	2	0.07		2	0.07	2	0.07
	3	0.07	3	0.06		3	0.08	3	0.07
	4	0.07	4	0.06		4	0.08	4	0.07
	5	0.07	5	0.06		5	0.08	5	0.07
	6	0.07	6	0.06		6	0.08	6	0.07
	7	0.07	7	0.06		7	0.08	7	0.06
	8	0.07	8	0.05		8	0.07	8	0.06
	9	0.07	9	0.05		9	0.07	9	0.05

Table 5.5(b) Diameters of stay cables for Case (2).

	Group (1) and (4)		Group (2) and (3)			Group (1) and (4)		Group (2) and (3)	
L (m)	Cable No.	D (m)	Cable No.	D (m)	L (m)	Cable No.	D (m)	Cable No.	D (m)
550	1	0.05	1	0.07	600	1	0.04	1	0.07
	2	0.07	2	0.06		2	0.07	2	0.07
	3	0.07	3	0.07		3	0.08	3	0.07
	4	0.07	4	0.07		4	0.08	4	0.07
	5	0.08	5	0.06		5	0.08	5	0.07
	6	0.07	6	0.06		6	0.08	6	0.07
	7	0.07	7	0.06		7	0.08	7	0.06
	8	0.07	8	0.06		8	0.08	8	0.06
	9	0.07	9	0.06		9	0.08	9	0.06
	10	0.08	10	0.05		10	0.08	10	0.06
	11	0.08	11	0.03		11	0.08	11	0.05
						12	0.08	12	0.03
650	1	0.04	1	0.07	700	1	0.05	1	0.07
	2	0.06	2	0.07		2	0.06	2	0.07
	3	0.07	3	0.07		3	0.07	3	0.07
	4	0.07	4	0.07		4	0.07	4	0.07
	5	0.07	5	0.06		5	0.07	5	0.06
	6	0.07	6	0.07		6	0.07	6	0.07
	7	0.07	7	0.06		7	0.07	7	0.06
	8	0.06	8	0.06		8	0.07	8	0.06
	9	0.06	9	0.06		9	0.07	9	0.06
	10	0.07	10	0.06		10	0.07	10	0.07
	11	0.07	11	0.06		11	0.07	11	0.06
	12	0.07	12	0.06		12	0.08	12	0.06
	13	0.08	13	0.04		13	0.08	13	0.04

5.4.3 Optimum Height of the Pylons

In general, the increase of the pylons' height above the deck level decreases the forces in the stay cables (Troitsky, 1988). This directly reduces the diameters of the stay cables and the compressive forces acting on the deck and the pylons. On the other hand, the increase in the height of the pylon and, in turn the cable lengths, means more material and extra

cost. As such, one would expect that an optimum value exists for the pylon height, which minimizes the cost of the bridge. One of the variables used in the optimization analyses is the height of upper strut beam relative to the deck (h_B). This value reflects the total height of the pylon relative to the deck (H). The distance h_T bound between (H) and (h_B) includes the anchor cables and is equal to ($2N$) m. The variations of the variable ($\gamma_1 = h_B/L$) with the bridge length (L) are shown in Figs. 5.5(a) and 5.5(b) for Case (1) and Case (2), respectively. For Case (1), the ratio (γ_1) increases with (L) gradually till reaching an asymptotic value of 0.1 at $L=400$ m. Beyond this value, the ratio remains almost constant. For case (2), the trend is different as the ratio increases almost linearly with (L) within the entire range.

5.4.4 Optimum Main Span Length (M)

The main span length (M) has a large effect on the distribution of cable forces and bending moments along the deck and the pylons (Agrawal, 1997). Increasing the length of the main span significantly increases the tensile forces in the back-stay cables, which are transmitted to the piers. However, if the length of the main span decreases beyond a certain value, the back-stay cables can be subjected to compression forces, which can exceed the post-tensioning applied to offset effect of dead load. In this case, the back-stay cables will be subjected to net compression and, consequently, will not contribute into the deck supporting system. Such a situation should be avoided and has been eliminated from the feasible solutions in the optimization routine.

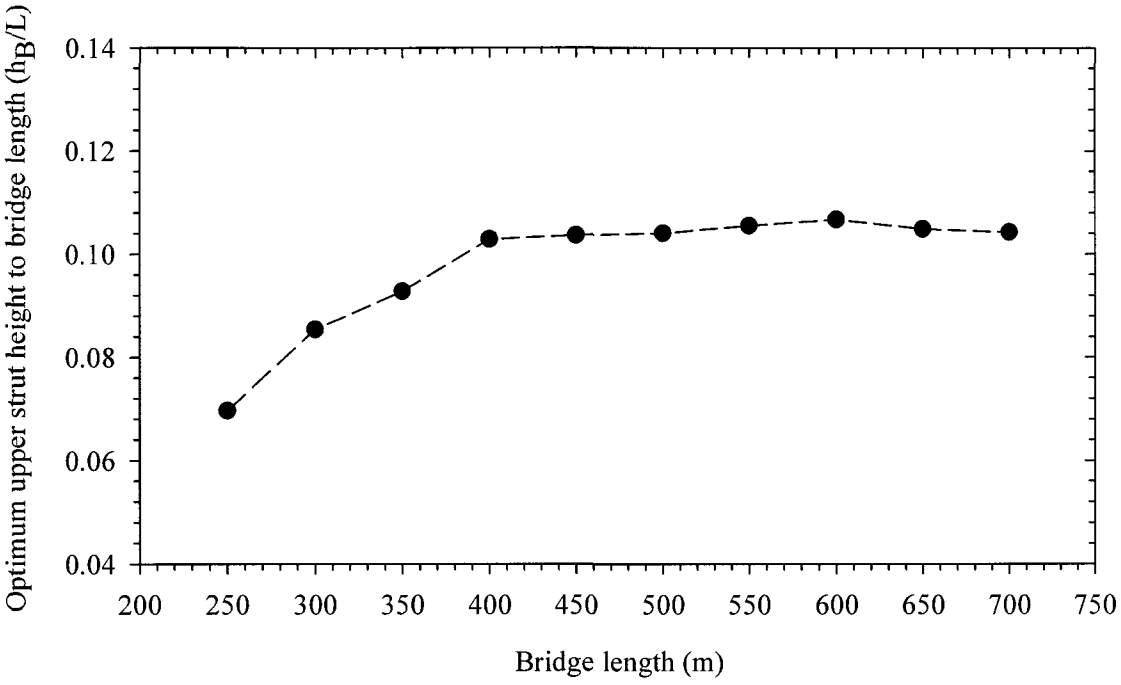

(a) Case (1) "two lanes".

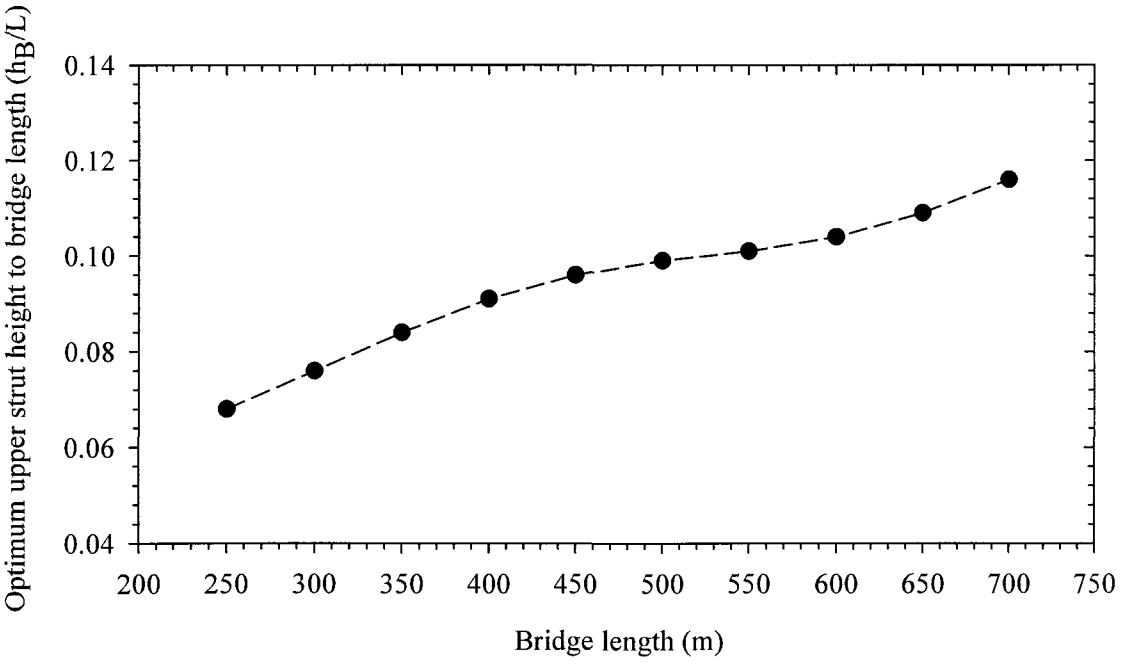

(b) Case (2) "four lanes".

Fig. 5.5 Optimum upper strut beam height to bridge length.

The optimum values for the mid-span lengths obtained from the analyses are normalized with respect to the total length (L). The variations of the ratio ($\gamma_2 = M/L$) with the bridge length (L) are plotted in Figs. 5.6(a) and 5.6(b) for Case (1) and Case (2), respectively. The results show that the optimum solutions lead to a limited variation in the main span to length ratio (γ_2). The optimum values for (γ_2) range between *0.48* and *0.50*. Unless the topography of the site dictates larger main span values, it is recommended to use values within this range for (γ_2).

5.4.5 Optimum Deck and Pylon Dimensions

For each bridge length, the optimum parameters defining the deck and the pylon cross sections are obtained from the analyses. In addition to the thickness of the reinforced concrete slab, the deck parameters include the following components of the two steel main girders: total depth, thickness and width of top flange, thickness and width of bottom flange, and thickness of web. Since the slab constitutes a significant portion of the weight of the deck, the optimization routine directed the search towards the minimum possible value for the slab thickness. As such, all the analyses estimate a value of *150 mm*, which is the lower bound value assumed for the slab thickness.

The variations of the optimum parameters of the steel main girders with the bridge length are provided in Figs. 5.7 to 5.10. The general trend shows an increase in all the girders dimensions with the increase in length. Also as expected, the dimensions obtained for Case (2) are larger than those for Case (1). The girder height and flanges widths vary almost linearly with the bridge length. The most significant variations are shown in the flanges widths, as shown in Fig. 5.8.

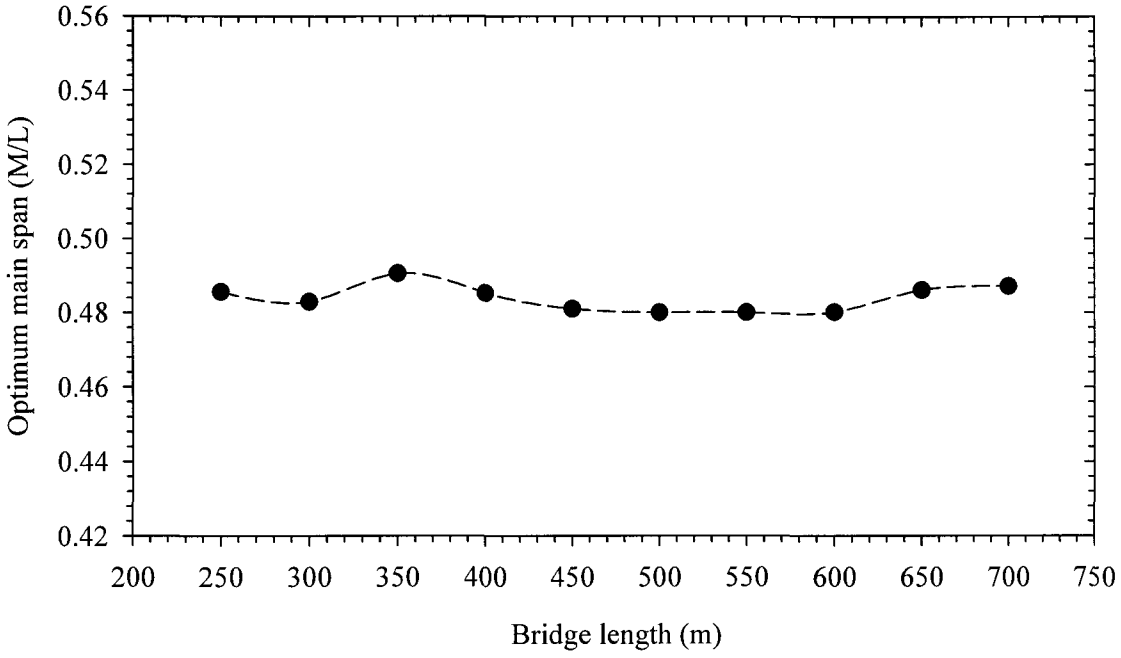

(a) Case (1) "two lanes".

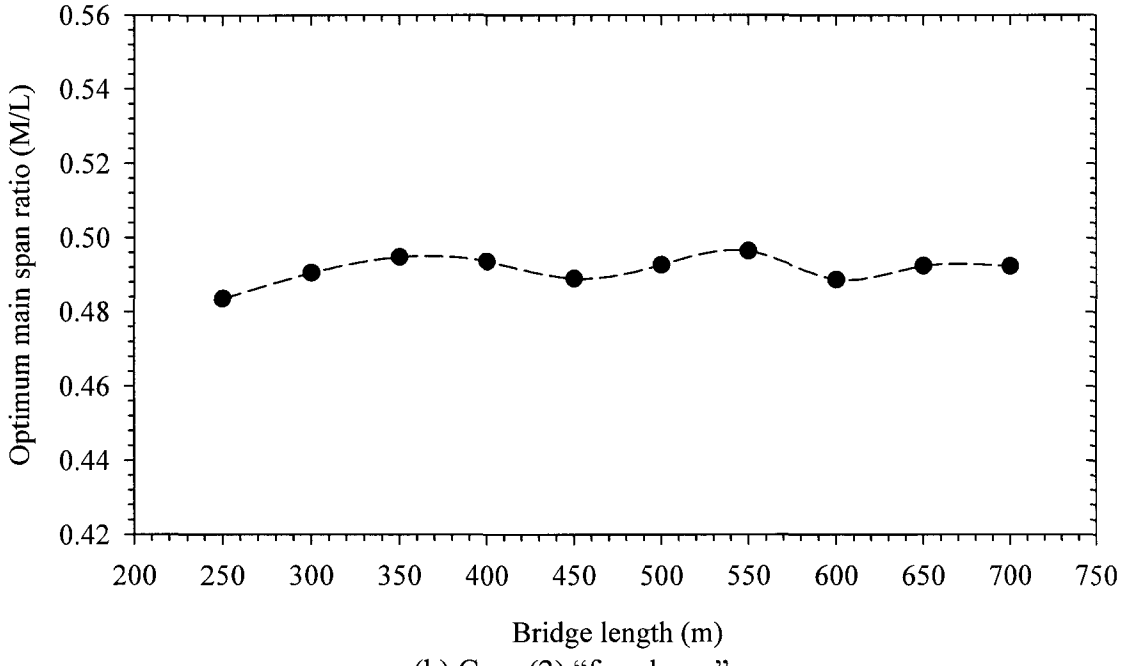

(b) Case (2) "four lanes".

Fig. 5.6 Optimum main span length (M).

The bottom flange dimensions exceed the top flange counterparts because of the existence of the reinforced concrete slab at the top edge of the cross-section. Compared to other dimensions, the least variations are obtained in the flanges thicknesses, as shown in Fig. 5.9.

As discussed earlier, a hollow rectangular cross-section is assumed for the two pylons. The dimensions H_p, B_p and t_p represent the length (along the bridge longitudinal direction), width (along the bridge transverse direction) and the thickness of the pylon cross-section, respectively. The variations of the optimum values of these parameters with the bridge length are given in Fig. 5.10.

The analyses indicate that the buckling capacity of the pylon dictates the values of the cross-section dimensions. Since, the buckling length of the pylons in the longitudinal direction is larger than its counterpart in the transverse direction, the values of the length H_p exceeds those of the width B_p for all cases, as shown in Figs. 5.10(a) and 5.10(b). Although, the general trend shows an increase with the bridge length, the values of H_p and B_p remain constant within some specific ranges. The variations in the thickness values are quite small.

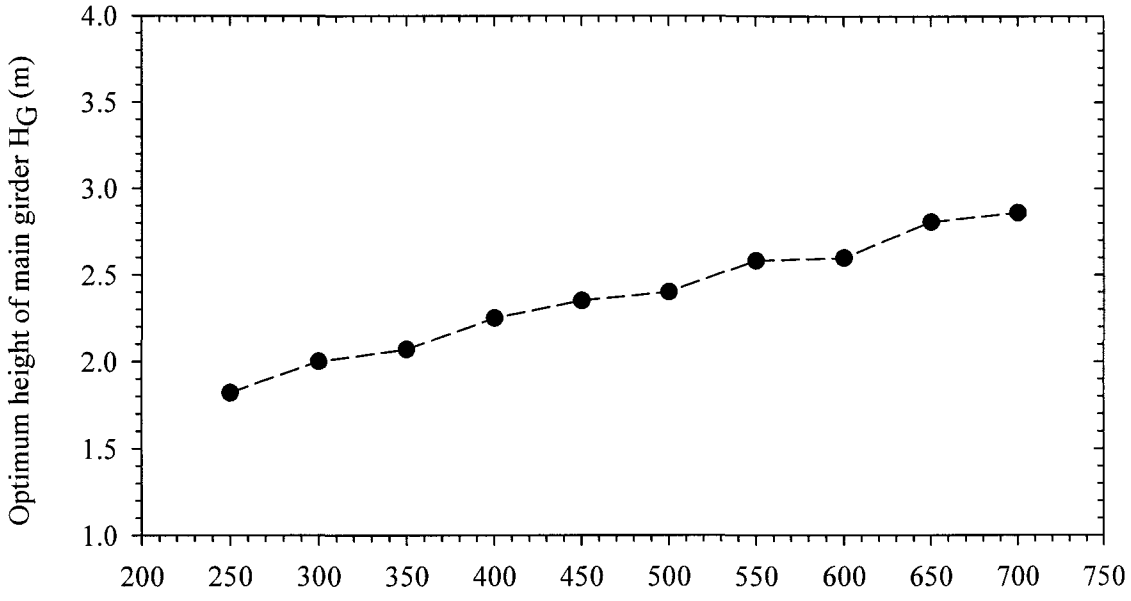

(a) Case (1) "two lanes".

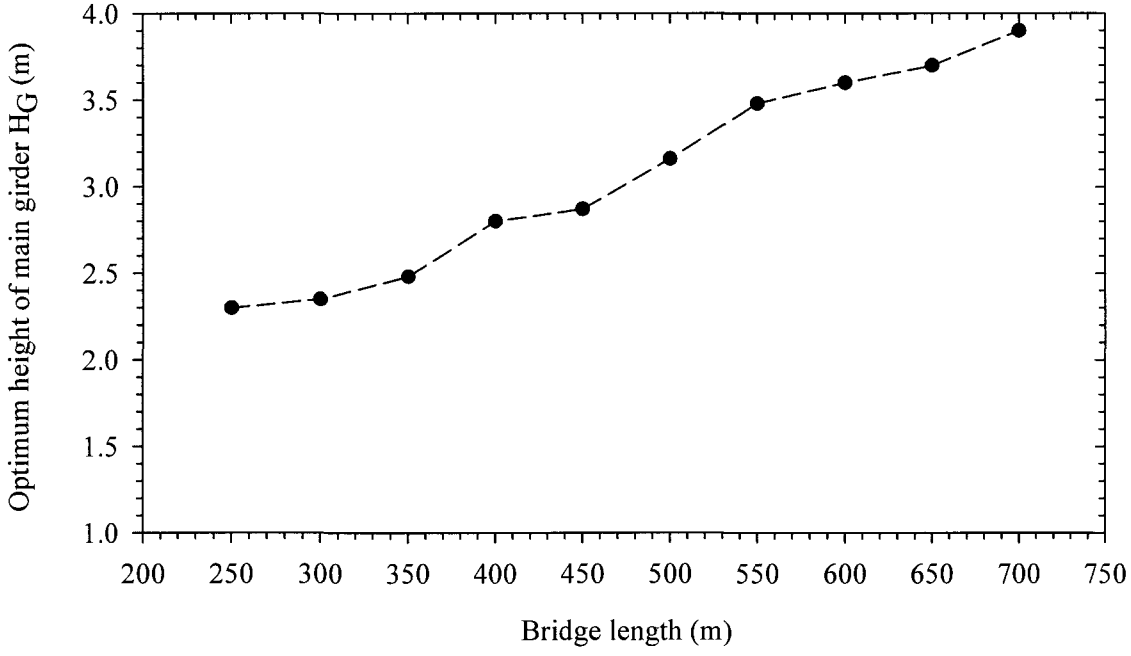

(b) Case (2) "four lanes".

Fig. 5.7 Optimum height of girder height (H_G).

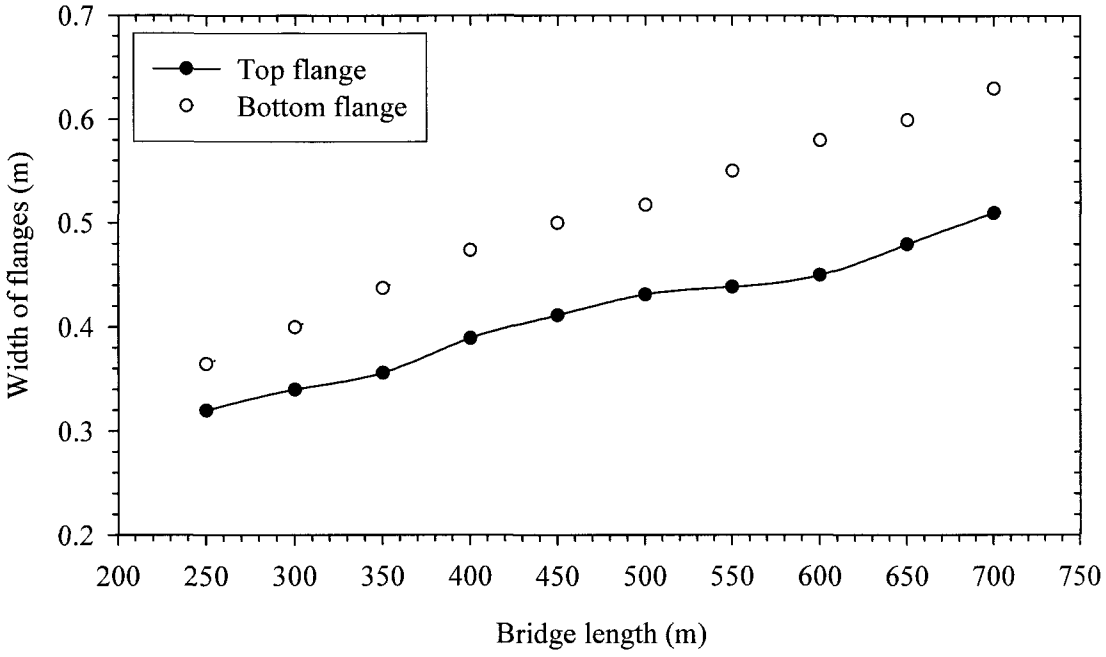

(a) Case (1) "two lanes".

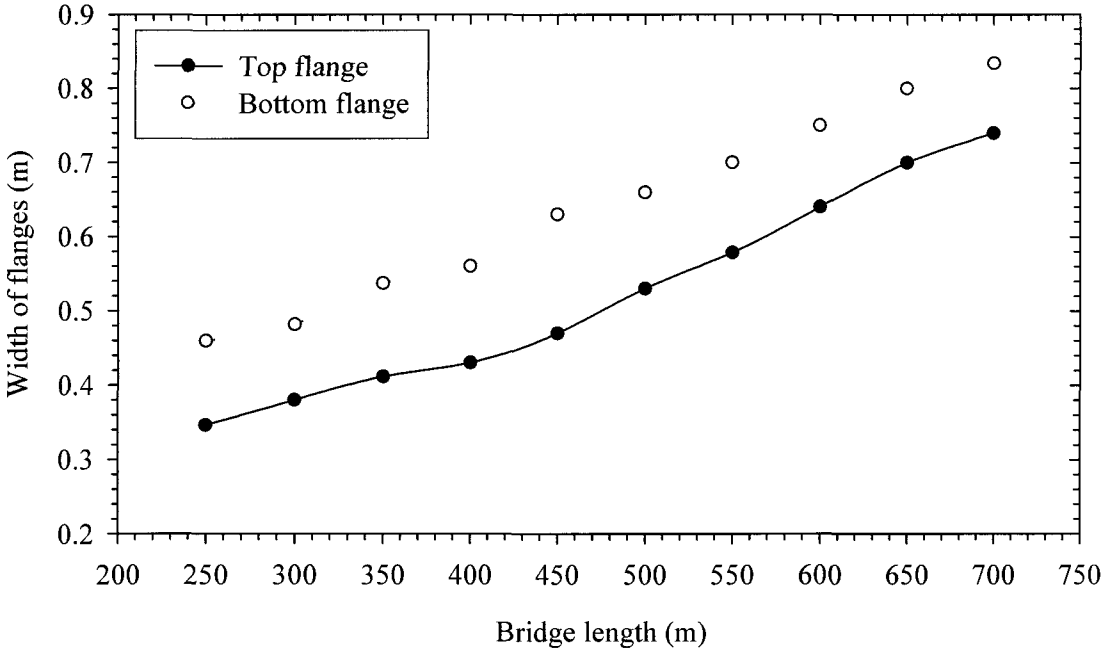

(b) Case (2) "four lanes".

Fig. 5.8 Optimum width of girder flanges.

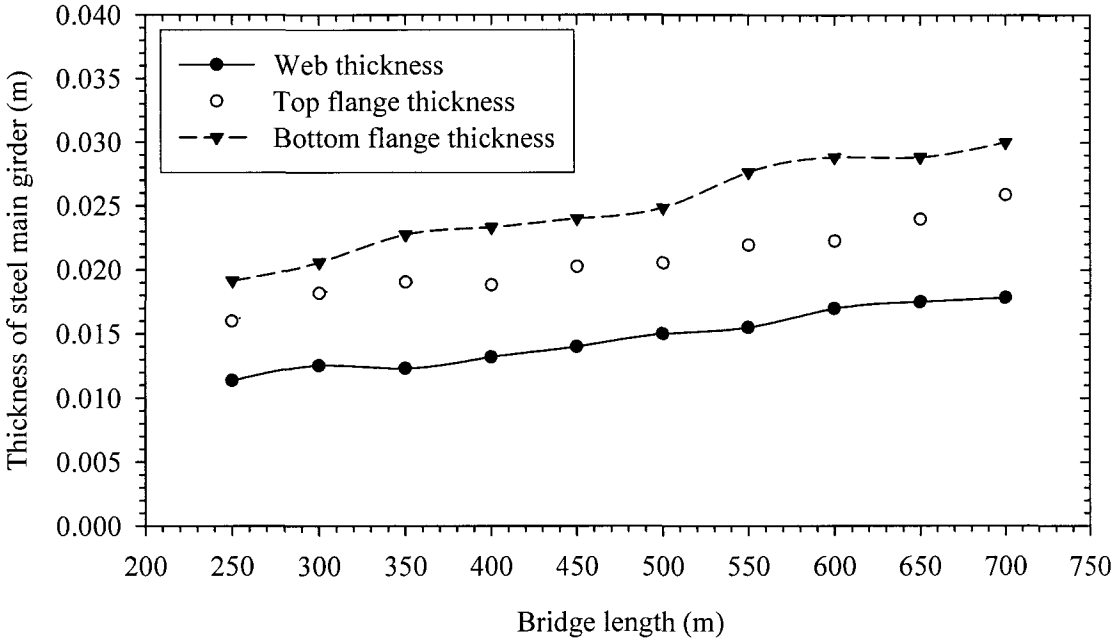

(a) Case (1) "two lanes".

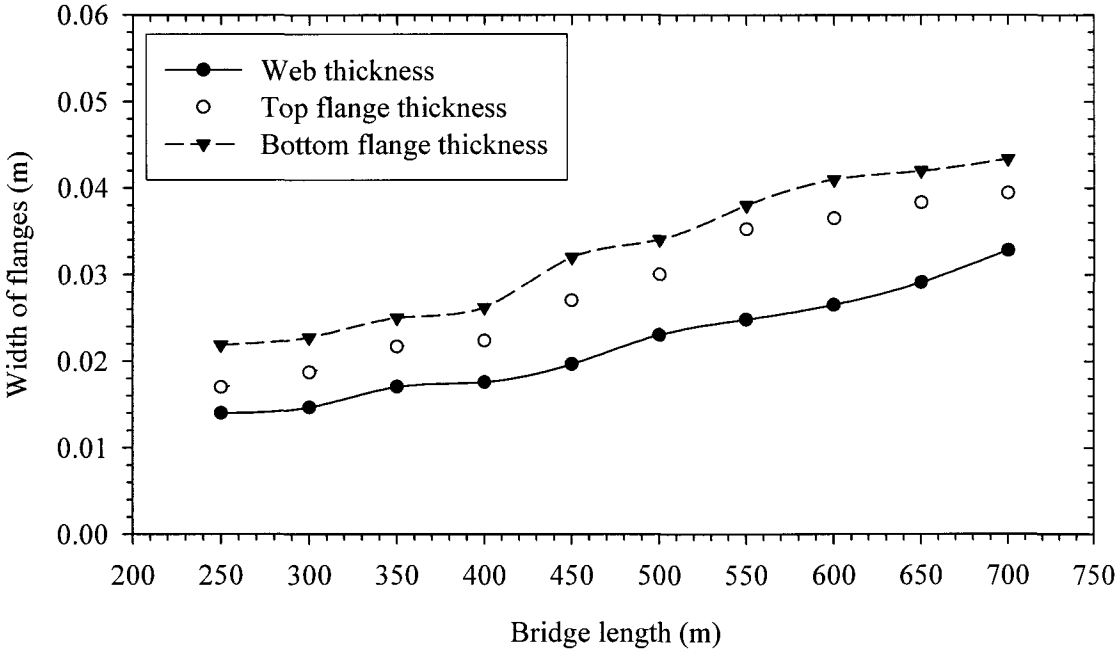

(b) Case (2) "four lanes".

Fig. 5.9 Optimum thicknesses of flanges and web of main girder.

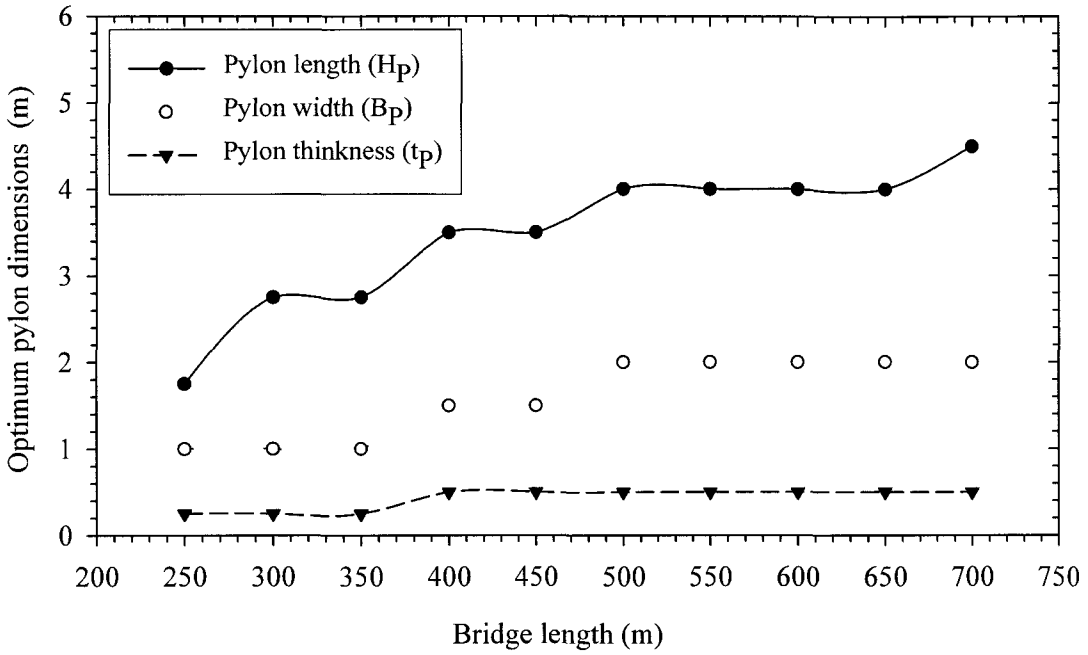

(a) Case (1) "two lanes".

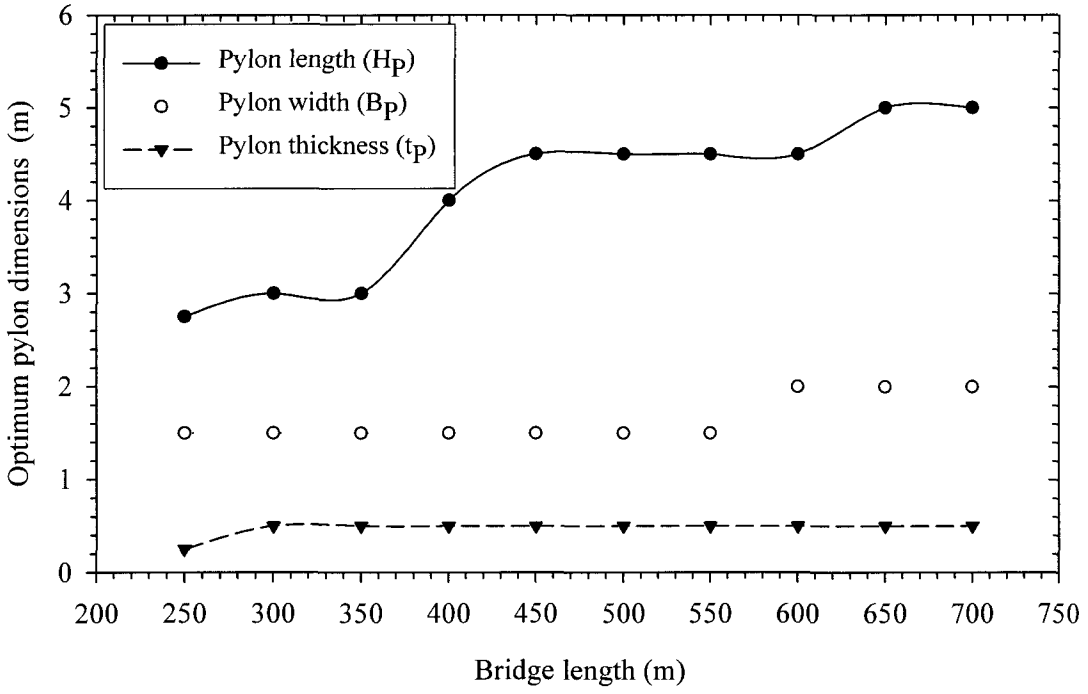

(b) Case (2) "four lanes".

Fig. 5.10 Optimum dimensions of pylon.

5.5. Conclusions

In this study, a database for the optimum design parameters defining the geometric configuration and cross-section dimensions of various components of cable-stayed bridges is developed. The study considers bridges having open-shaped composite steel-concrete decks and semi-fan cable arrangements. The database is conducted using the numerical scheme developed in the previous chapter, which combines finite element analysis, the genetic algorithm technique and design procedures for various components of cable stayed bridges. The numerical scheme incorporates the cables post-tensioning forces proposed in Chapter 3 in order to offset the effect of dead loads. The optimum design parameters obtained from the current study are presented in the form of tables and curves. They are provided as functions of the total length of the bridges. For a specific bridge length, the optimum values for the number of stay cables, main span length, height of the pylons, and cross-section dimensions of the pylons, deck and stay cables can be determined using this database. The database is useful in the preliminary design stage of the considered type of cable stayed bridges. It provides useful information for a preliminary cost estimate of the bridge. The geometric configurations and cross-sections dimensions estimated using this data base can serve as starting values for subsequent detailed analyses. The following specific conclusions can be drawn from the results of the optimization analyses of two-lane (Case 1) and four-lane (Case 2) bridges:

1. The optimum number of stay cables generally increases with the increase in the bridge length.

2. The optimum number of stay cables for the four lane case (Case 2) is generally larger than that for the two lane case (Case 1). This is true with the exception for the bridge lengths equal to *250 m* and *700 m.*
3. The optimum sizes of stay cables for Case (2) are larger than those for Case (1).
4. For Case (1), the optimum height of the pylon increases with the bridge length gradually till reaching an asymptotic value of *0.1* at *L=400 m.* Beyond this value, the ratio remains almost constant.
5. For case (2), the optimum height of the pylon increases almost linearly with the bridge length.
6. The optimum ratios of the main span to the bridge length ($\gamma_2 = M/L$) for both cases range between *0.48* and *0.50.*
7. In all analyses, the thickness of the concrete slab of the deck always reaches its lower bound, since any increase in this thickness significantly increases the total weight of the bridge.
8. The dimensions of the girders and pylon obtained for Case (2) are larger than those for Case (1).
9. The buckling capacity of the pylons for both cases dictates the values of the cross-section dimensions.
10. The pylons cross-section dimensions in the longitudinal direction of the bridge are always larger than the dimensions in the transverse direction of the bridge.

5.6 References

1. Gimsing NJ. Cable Supported Bridges Concept and Design. 2nd edition. New York: John Wiley & Sons Inc.; 1997.
2. Walther R., Houriet B., Isler W., Moia P., Klein JF. Cable-stayed bridges. Thomas Telford Ltd., Thomas Telford House, London; 1988.
3. Nieto F, Hernández S, Jurado J Á. Optimum design of long-span suspension bridges considering aeroelastic and kinematic constraints. J Struct. Multidisc Optim 2009;39:133-151.
4. Nazmy AS, Abdel-Ghaffar A. Three-dimensional nonlinear static analysis of cable-stayed bridges. Computers and Structures 1990;34(2):257-271.
5. Hong NK, Chang SP, Lee SC. Development of ANN-based preliminary structural design systems for cable-stayed bridges. Advanced in Engineering Software 2002;33:85-96.
6. Simões LMC, Negrão JHJO. Sizing and geometry optimization of cable-stayed bridges. J Computer & structure 1994; 52:309-321.
7. Long W, Troitsky, MS, Zielinski ZA. Optimum design of cable stayed bridges, J Structural Engineering and Mechanics 1999; Vol. 7, No. 3, 241-257.
8. Simões LMC, Negrão JHJO. Optimization of cable-stayed bridges with box-girder decks. J Adv. Eng. Software 2000; 31:417-423.
9. Chen DW, Au FTK, Tham LG, Lee PKK. Determination of initial cable forces in prestressed concrete cable-stayed bridges for given design deck profiles using the force equilibrium method. J Comput Struct 2000;74:1–9.

10. Lute V, Upadhyay A, Singh KK. Computationally efficient analysis of cable-stayed bridge for GA-based optimization. Eng Appl Artif Intell 2009;22(4-5):750-8.
11. Canadian Highway Bridge Design Code, (2006), CAN/CSA-S6-06.
12. Svensson HS, Christopher BG, Saul R. Design of a cable-stayed steel composite bridge. Journal of structural engineering New York, N.Y. 1986;112(3):489-504.
13. Troitsky M.S., Cable-stayed bridges: theory and design. 2nd Ed. Oxford: BSP; 1988.
14. Ren WX, Peng, XL. Baseline finite element modeling of a large span cable-stayed bridge through field ambient vibration tests. Comput. Struct 2005; 83(8-9):536-550.
15. AASHTO (2007). *LRFD Bridge Design Specifications*, 4th Edition, Washington, D. C., USA
16. Ernst JH. Der E-Modul von Seilen unter berucksichtigung des Durchhanges. Der Bauingenieur 1965; 40(2):52–5 (in German).
17. Michalewicz Z and Fogel DB. How to solve it: modern heuristics. 2nd Edn New York: Springer, c2004.
18. Agrawal TP. Cable-stayed bridges - parametric study. J.Bridge Eng. 1997;2(2):61-7.

CHAPTER 6

CONCLUSIONS AND RECOMMENDATIONS

6.1 Introduction

The research work conducted and accomplished in this thesis consists of four parts. The first part includes development of a new method to evaluate the optimum post-tensioning cable forces for cable-stayed bridges under the action of dead load. The second part presents surrogate polynomial functions that can be used to evaluate post-tensioning cable forces in semi-cable stayed bridge under the action of the dead load. The third part involved development of an optimization design software that integrates a finite element model, real coded genetic algorithm (RCGA), surrogate polynomial functions for evaluating post-tensioning cable forces, and design methodologies to optimize the design of semi-fan cable-stayed bridges. The fourth part presents a database for the optimum design of three-span composite cable stayed bridges with semi-fan cable arrangement. The general conclusions pertaining to each one of the four research parts are presented below.

6.2 Optimum Post-Tensioning Cable Forces of Cable-Stayed Bridges

This chapter presents a new method that can be used to obtain the optimum post-tensioning cable forces for cable-stayed bridges under the effect of dead load. In this method, the finite element method, B-spline curves, and real coded genetic algorithm (RCGA) are utilized. The B-spline curves are used to model the post-tensioning functions along the bridge deck. The real coded genetic algorithms (RCGA) are employed to

optimize shapes of the post-tensioning functions to achieve minimum deflections along the bridge deck. Positions of the control points are treated as the design variables rather than the cable forces.

This significantly reduces the number of design variables, leading to a decrease in the computational time, and an improvement in the accuracy of the final solution. In addition, such a reduction increases the probability of finding the global optimum post-tensioning cable force. The proposed method is efficient for bridges having large number of stay cables.

One of the advantages of the proposed method compared to previous techniques is that it minimizes transverse deflections for both the deck and the pylon, simultaneously. It also provides the optimal post-tensioning cable forces distribution that minimizes moment distributions along the deck and the pylon. The results shows that the proposed objective function achieves 95 % reduction in the displacement of the pylon's top and 91 % reduction in the moment at the pylon base, with a uniform distribution of the post-tensioning forces among various cables. Therefore, it leads to the optimal structural design of the whole cable-stayed bridge.

The chapter shows that the sag effect is the only source of geometric nonlinearity that slightly affects the determination of the post-tensioning cable forces. Accordingly, from an engineering point of view, a linear analysis is sufficient for the determination of the post-tensioning cable forces.

6.3 Post-Tensioning Cable Forces Functions for Semi-Fan Cable-stayed Bridges

Surrogate polynomial functions that can be used to evaluate post-tensioning cable forces in semi-cable stayed bridges under the action of dead load are developed. The proposed functions depend on the parameters defining the geometric configuration of the bridges as well as the number of stay cables. The proposed sets of post-tensioning forces minimize the deflections of the deck and the pylons of the bridges. The availability of these post-tensioning force functions is very useful since it saves the significant effort required by the bridge designers to estimate such forces. The post-tensioning functions can be stored as a built-in library in the design software of cable-stayed bridges. The accuracy of the post-tensioning functions is assessed by applying the calculated post-tensioning cable forces on several bridges and comparing the results with those obtained from numerical optimization analyses. The optimum geometric configuration that leads to the most uniform post-tensioning cable forces in semi-fan cable-stayed bridges is investigated. The following conclusions can be drawn from this investigation:

1. The values of the ratio γ_1 (the main span length and the total length) ranging between *0.50* and *0.52* are considered the optimum ratios for all cases as they lead to:
   - Minimum lateral deflection and bending moment in the pylon.
   - Uniform distribution for the post-tensioning cable forces.
2. The increase of the pylon height significantly reduces the required post-tensioning cable-forces.
3. Under the combined effect of dead load and post-tensioning forces, the variation of the pylon height has a slight effect on the bending moment at the pylon's base.

4. The geometrical configuration of a cable-stayed bridge plays a very fundamental role in the design and cost of the bridge.

6.4 Optimum Design Technique for Semi-Fan Cable-Stayed Bridges

In this chapter, an implementation of a powerful optimization technique in the design of semi-fan cable-stayed bridge has been introduced. The proposed numerical code integrates a finite element model, real coded genetic algorithm (RCGA), surrogate polynomial functions for evaluating post-tensioning cable forces, and design methodologies based on the Canadian Highway Bridge Design Code CAN/CSA-S6-06. Initially, the problems are solved as unconstrained minimization problems then the constraints are implemented in the form of penalty functions. The effects of the post-tensioning cable forces, the geometrical configuration, and the number of stay cables on the cost design of the bridge have been investigated. Finally, the optimum values of the design variables for a real cable-stayed bridge are provided under different design conditions. The conclusions that can be drawn from this chapter are:

1. By applying the appropriate post-tensioning forces to the stay cables, a reduction of 43.2% is achieved in the cost of the considered cable-stayed bridge. Most of this reduction occurs in the bridge deck. The costs of the pylons and the stay cables remain almost unchanged. This is due to the large reduction of maximum positive and negative bending moments of the deck resulting from the application of the post-tensioning cable forces.

2. The cost design of the cable-stayed bridge is greatly affected by the variations of the height of the pylon above the deck and the main span length. Therefore, these two parameters should be considered within the design variables.
3. Under a fixed value for the number of stay cables, the chapter conducted to asses the effects of the height of the pylon above the deck and the main span length on the cost design reveals that :
    a. The increase in the pylon height decreases the cost of the entire cable-stayed bridge. However, this reduction becomes less significant beyond a ratio of upper strut height to bridge length of 0.092.
    b. The increase in the pylon height reduces the cost of the bridge deck and increases the cost of the pylon.
    c. The increase in the pylon height reduces the cost of stay cables; however, this trend becomes negligible beyond a ratio of upper strut height to bridge length of 0.092. Only for $\gamma_1 = 0.54$ and $\gamma_2 \geq 0.092$, the cost of the stay cables increases with pylon height.
4. The cost design of the stay-cable bridge is notably affected by the selection of the number of stay cables. Accordingly, the number of stay cables should be included within the set of design variables.
5. The chapter conducted to asses the effect of varying the number of stay cables on the design cost, while maintaining the height of the pylon above the deck and the main span length constant reveals that:

a. The increase in the number of stay cables gradually decreases the total cost the cable-stayed bridge up to ten stay cables in each single group (*N=10*). Beyond this limit, the cost of bridge slightly increases and then becomes almost constant.
b. The increase in the number of stay cables increases the cost of the pylon, due to the increase in the pylon height to accommodate the cable anchor positions.
c. The increase in the number of stay cables decreases the cost of the deck; however, this decrease becomes less significant when the number of stay cable in each single group increases beyond a value of twelve (*N=12*).
d. The increase in the number of stay cables decreases the cost of stay cables until the number of stay cables reaches ten (*N=10*). Beyond this number, the stay cables cost increases.

6. The inclusion of all design variables in the optimization routine leads to the best optimum solution.
7. Compared to an optimization solution involving fixed geometric configuration to the values applied in the real bridge, up to *15%* reduction in the total cost of the bridge can be achieved when all design variables are included

6.5 Database for the Optimum Design of Semi-Fan Cable-stayed Bridges

In this chapter, a database for the optimum design parameters defining the geometric configuration and cross-section dimensions of various components of cable-stayed bridges is developed. The chapter considers bridges having open-shaped composite steel-concrete decks and semi-fan cable arrangements. The database is conducted using the numerical scheme developed in the previous chapter, which combines finite element

analysis, the genetic algorithm technique and design procedures for various components of cable stayed bridges. The numerical scheme incorporates the cables post-tensioning forces proposed in Chapter 3 in order to offset the effect of dead loads. The optimum design parameters obtained from the current chapter are presented in the form of tables and curves. They are provided as functions of the total length of the bridges. For a specific bridge length, the optimum values for the number of stay cables, main span length, height of the pylons, and cross-section dimensions of the pylons, deck and stay cables can be determined using this database. The database is useful in the preliminary design stage of the considered type of cable stayed bridges. It provides useful information for a preliminary cost estimate of the bridge. The geometric configurations and cross-sections dimensions estimated using this data base can serve as starting values for subsequent detailed analyses. The following specific conclusions can be drawn from the results of the optimization analyses of two-lane (Case 1) and four-lane (Case 2) bridges:

1. The optimum number of stay cables generally increases with the increase in the bridge length.
2. The optimum number of stay cables for the four lane case (Case 2) is generally larger than that for the two lane case (Case 1). This is true with the exception for the bridge lengths equal to *250 m* and *700 m.*
3. The optimum sizes of stay cables for Case (2) are larger than those for Case (1).
4. For Case (1), the optimum height of the pylon increases with the bridge length gradually till reaching an asymptotic value of *0.1* at *L=400 m.* Beyond this value, the ratio remains almost constant.

5. For case (2), the optimum height of the pylon increases almost linearly with the bridge length.
6. The optimum ratios of the main span to the bridge length ($\gamma_2 = M/L$) for both cases range between *0.48* and *0.50*.
7. In all analyses, the thickness of the concrete slab of the deck always reaches its lower bound, since any increase in this thickness significantly increases the total weight of the bridge.
8. The dimensions of the girders and pylon obtained for Case (2) are larger than those for Case (1).
9. The buckling capacity of the pylons for both cases dictates the values of the cross-section dimensions.
10. The pylons cross-section dimensions in the longitudinal direction of the bridge are always larger than the dimensions in the transverse direction of the bridge.

6.6 Recommendations for Future Research

For future research, the following numerical investigations related to the design of cable-stayed bridges are recommended:

- Conduct intensive parametric studies to developed surrogate post-tensioning polynomial functions for cable-stayed bridges with fan and harp arrangements.
- Conduct optimization studies on cable-stayed bridges with fan and harp arrangements.
- Conduct optimization studies on other types of bridge deck.
- Conduct similar studies for long span suspension bridges.

- Account for the seismic loading in the optimization code.
- Account for the construction stage in the optimization code.

APPENDIX I

COEFFICIENTS OF POST-TENSIONING POLYNOMIAL FUNCTIONS

(1) Number of stay cable (N) = 5

Cable No	(b_o)	(b_1)	(b_2)	(b_3)	(b_{11})	(b_{22})	(b_{33})	(b_{12})	(b_{13})	(b_{23})
Group (1)										
C (1)	-303 63	-774 36	1178 62	4 72	-7445 28	1893 5	-159 01	1014 5	-891 4	3436 53
C (2)	559 33	2730 22	1906 78	0 00	-2716 71	-128 53	-864 49	-2518 72	217 31	1303 76
C (3)	-442 73	-1954 46	3618 54	-1 94	1176 54	-122 88	-859 67	1859 45	202 19	-919 81
C (4)	237 41	310 16	4746 51	7 07	2500 94	29 49	-616 9	-594 18	81 34	-1868 33
C (5)	262 39	1095 34	2482 82	-10 59	-1498 2	-6 98	-345 25	-1056 77	88 84	420 03
Group (2)										
C (1)	5 53	-213 2	455 86	-0 96	1089 77	228 57	-234 31	83 26	-75 68	-481 46
C (2)	482 68	1974 81	1594 41	5 88	708 39	-54 03	-519 99	-1961 94	96 05	-432 79
C (3)	362 09	1571 32	2077 25	12 94	-860 15	158 32	-558 03	-1503 05	-2 83	208 37
C (4)	-704 82	-2695 05	3399 12	8 95	-1318 91	300 56	-676 41	2774 26	-47 21	242 19
C (5)	330 72	1580 05	5065 71	13 89	-979 51	114 73	-1348 57	-1477 76	104 22	179 86

(2) Number of stay cable (N) = 6

Cable No	(b_o)	(b_1)	(b_2)	(b_3)	(b_{11})	(b_{22})	(b_{33})	(b_{12})	(b_{13})	(b_{23})
Group (1)										
C (1)	-344 87	-1044 83	675 48	-9 08	-6005 59	1680 67	-239 52	1208 5	-773 57	2916 24
C (2)	543 16	2268 37	2013 07	5 28	199 01	32 04	-1040 6	-2256 13	126 16	-123 01
C (3)	27 38	24 37	2281 06	5 2	1093 39	-308 67	-737 67	-76 61	277 05	-747 01
C (4)	-121 78	-742 63	670 75	-7 54	2266 66	-243 97	-689 34	595 81	239 51	-1130 94
C (5)	-148 77	-839 22	1729 03	9 08	2270 43	-263 65	-482 45	727 5	209 25	-1348 11
C (6)	-189 86	-931 33	1794 74	12 32	1125 67	-146 65	-475 98	853 24	143 44	-749 46
Group (1)										
C (1)	100 78	414 19	1134 78	15 86	-903 96	226 14	35 24	-388 92	-117 28	291 35
C (2)	-343 31	-1172 76	1984 95	13 89	-2194 2	316 3	-33 5	1302 84	-149 09	810 43
C (3)	6 35	135 45	1755 44	12 52	-1552 46	310 44	-256 66	-65 92	-116 93	568 62
C (4)	-17 64	45 24	1556 01	8 46	-1958 39	434 28	-658 69	2 82	-134 99	914 03
C (5)	47 69	289 06	3505 53	5 9	-1088 02	257 86	-700 77	-237 6	-28 82	193 86
C (6)	-110 08	-207 84	2851 61	15 86	-1654 64	282 9	-817 76	317 06	-36 73	615 31

(3) Number of stay cable (N) = 7

Cable No	(b_o)	(b_1)	(b_2)	(b_3)	(b_{11})	(b_{22})	(b_{33})	(b_{12})	(b_{13})	(b_{23})
Group (1)										
C (1)	-152 01	-631 89	1602 79	12 6	-5309 54	1780 47	-394 65	624 74	-852 86	2568 27
C (2)	579 75	2511 83	1779 12	19 69	-1807 39	216 04	-817	-2444 36	-3 15	888 44
C (3)	253 66	1138 62	1192 2	19 32	-755 61	-194 24	-645 11	-1094 38	191 91	350 58
C (4)	-262 23	-1306 98	2026 95	27 12	1244 76	-85 04	-526 48	1188 35	112 57	-845 89
C (5)	210 27	353	1467 57	14 4	2419 68	-59 75	-325 86	-582 88	88 5	-1426 85
C (6)	489 77	1701 53	1782 24	3 21	717 33	-42 34	-478 84	-1831 24	98 26	-517 11
C (7)	146 37	674 37	723 42	12 46	-801 69	-157 9	-487 45	-635 78	146 14	388 71
Group (2)										
C (1)	95 45	497 47	1514 51	13 34	-789 28	135 1	-72 12	-427 93	-65 13	257 61
C (2)	-118 66	-273 2	1843 24	0 44	-884 62	73 43	-123 26	386 81	-10 24	223 42
C (3)	-274 63	-907 93	1694 68	8 12	-322 66	80 13	-396 63	1004 32	6 36	40 2
C (4)	-310 18	-1013 03	1441 82	9 53	-610 25	104 62	-462 82	1122 12	5 17	226 13
C (5)	-189 53	-454 33	1818 44	5 44	-1863 11	203 14	-589 26	595 98	-21 93	823 42
C (6)	98 02	706 75	2043 48	4 11	-1498 95	66 18	-503 99	-552 07	46 35	554 36
C (7)	-167 34	-615 26	3538 51	7 41	-9 17	89 4	-795 95	637 34	59 22	-293 1

(4) Number of stay cable (N) = 8

Cable No	(b_o)	(b_1)	(b_2)	(b_3)	(b_{11})	(b_{22})	(b_{33})	(b_{12})	(b_{13})	(b_{23})
Group (1)										
C (1)	339 89	1736 16	-164 83	22 38	-6167 83	1497 5	115 18	-1518 35	-747 87	2908 48
C (2)	589 71	2635 05	314 64	7 89	-2583 98	308 9	-551 67	-2522 81	-67 82	1358 07
C (3)	824 32	3307 58	1317 71	7 36	-229 87	-163 93	-582 69	-3320 73	176 19	37 25
C (4)	843 17	3105 11	1412 18	15 76	1359 13	-264 6	-644 68	-3248 88	215 21	-748 86
C (5)	640 41	2232 42	-407 39	-2 85	1695 44	-123 14	-514 05	-2419 27	148 33	-729 93
C (6)	730 24	2656 71	-471 9	-9 33	1082 98	-47 81	-508 58	-2814 7	112 72	-404 14
C (7)	775 48	2914 51	-266 42	-6 54	494 89	-63 9	-513 32	-3033 3	116 42	-121 81
C (8)	941 14	3629 57	572 46	-0 31	106 03	-168 92	-546 09	-3712 58	163 37	-31 73
Group (2)										
C (1)	-316 25	-1216 26	1263 11	13 31	-292 55	234 86	96 05	1261 77	-132	-22 91
C (2)	-543 38	-1982 16	2751 38	9 94	-757 22	153 27	-162 08	2098 86	-65 83	94 83
C (3)	-600 52	-2208 26	2114 33	17 37	-702 5	70 04	-143 94	2325 28	-21 94	110 96
C (4)	-562 11	-2026 9	2934 3	7 12	-609 88	43 11	-308 5	2151 29	20 18	3 24
C (5)	-467 41	-1663 52	2869 39	2 26	-606 48	93 77	-352 39	1775 79	9 72	-2 65
C (6)	-454 32	-1645 41	3392 14	4 54	-719 43	158 44	-470 22	1742 93	-12 6	-6 15
C (7)	-666 54	-2533 78	1980 13	12 73	-838 14	222 5	-581 67	2603 4	-43 09	249 09
C (8)	-517 98	-2004 34	1592 79	16 25	435 16	3 8	-565 55	2028 02	70 96	-299 01

(5) Number of stay cable (N) = 9

Cable No	(b_o)	(b_1)	(b_2)	(b_3)	(b_{11})	(b_{22})	(b_{33})	(b_{12})	(b_{13})	(b_{23})
Group (2)										
C (1)	38 36	275 48	1174 74	17 46	-4130 32	1442 71	-463 42	-225 13	-682 48	2095 21
C (2)	156 23	674 46	-64 4	11 04	-1144 96	362 84	-455 7	-667 92	-114 79	662 48
C (3)	309 78	1217 47	310 07	11 79	598 68	-190 47	-463 56	-1245 09	168 48	-263 52
C (4)	85 87	276 18	1139 65	12 71	1509 31	-331 79	-464 21	-315 81	236 24	-842 34
C (5)	77 1	237 44	827 18	4 62	1158 61	-291 84	-437 65	-282 37	217 87	-623 05
C (6)	144 92	339 3	1354	9 78	1631 12	-194 83	-433 19	-461 31	160 73	-926 97
C (7)	39 41	-113 8	1459 82	11 53	1606 85	-143 07	-459 44	-22 26	131 91	-909 75
C (8)	-106 78	-640 21	1445 38	4 68	1329 72	-79 71	-568 79	528 22	110 93	-738 25
C (9)	-255 73	-1215 03	1638 88	-9 43	1141 76	-99 9	-591 66	1105 72	138 6	-658 99
Group (2)										
C (1)	-46 58	-185 3	1411 58	1 28	-425 12	270 67	130 6	203 31	-141 23	25 98
C (2)	-175 21	-554 34	466 33	5 15	-1451 64	347 62	-59 62	631 67	-167 25	717 3
C (3)	-181 39	-497 75	1949	4 35	-1994 38	299 27	3 58	633 21	-140 51	726 8
C (4)	-101 01	-190 11	3125 3	0 91	-2125 58	311 14	-264 82	308 86	-116 12	726 88
C (5)	-26 39	21 1	1730 28	2 77	-1578 72	310 21	-340 32	41 18	-106 96	646 41
C (6)	-27 79	-7 38	2325 94	4 09	-1199 26	237 47	-414 75	60 15	-61 2	385 58
C (7)	-199 85	-660	2793 61	4 09	-907 12	159 13	-434	734 12	-15 5	160 77
C (8)	-293 3	-1047 75	2878 03	6 36	-911 22	154 33	-432 61	1115 7	-12 35	157 4
C (9)	98 14	651 69	3947 55	7 46	-1398 39	133 71	-683 34	-532 73	21 06	376 29

(6) Number of stay cable (N) = 10

Cable No	(b_0)	(b_1)	(b_2)	(b_3)	(b_{11})	(b_{22})	(b_{33})	(b_{12})	(b_{13})	(b_{23})
Group (1)										
C (1)	490 54	2021 48	1999 09	26 67	-4478 95	1487 08	-254 26	-1976 28	-725 28	2011 21
C (2)	540 78	2383 11	916 22	27 65	-2367 92	338 56	-537 63	-2286 35	-115 77	1204 15
C (3)	579 91	2306 56	908 65	18 45	-2 66	-151 27	-474 52	-2326 45	140 14	-19 11
C (4)	507 24	1885 5	1270 38	18 2	803 86	-220 12	-505 87	-1963 92	174 89	-477 67
C (5)	515 55	1919 36	1948 23	13 62	543 59	-159 65	-535 2	-1995 31	147 32	-415 92
C (6)	474 96	1806 44	1416 79	19 89	212 9	-146 13	-544 46	-1860	132 94	-170 63
C (7)	544 96	2036 59	1562 17	18 5	526 39	-152 31	-504 79	-2111 35	132 92	-367 03
C (8)	544 98	2001 18	1745 21	12 69	886 18	-171 96	-582 21	-2097 29	153 59	-548 64
C (9)	514 68	1823 44	1308 65	8 2	1498 72	-241 39	-454 15	-1942 81	182 96	-867 2
C (10)	483 26	1548 34	1416 15	4 9	2570 4	-254 01	-536 78	-1742 7	195 82	-1403 5
Group (2)										
C (1)	-501 75	-1844 47	-230 57	8 48	-329 13	131 64	-112 37	1930 23	-68 84	249 67
C (2)	-50 02	-73 04	208 91	-4 56	-891 39	230 08	122 27	143 14	-112 23	393 74
C (3)	60 22	327 81	883 7	-9 42	-852 1	265 21	8 95	-280 49	-112 96	317 03
C (4)	139 5	639 81	667 04	-0 54	-1062 97	273 61	-73 55	-596 79	-116 25	465 95
C (5)	125 22	561 96	531 12	1 67	-851 85	258 74	-192 03	-534 17	-99 13	403 57
C (6)	95 98	428 22	669 15	7 18	-869 38	272 33	-233 36	-407 26	-104 75	397 05
C (7)	19 47	133 77	520 98	3 91	-501 34	190 93	-308 91	-113 22	-51 38	248 01
C (8)	21 67	158 89	626 81	4 79	-566 98	155 78	-306 07	-128 99	-31 73	260 15
C (9)	103 53	512 26	588 07	6 25	-424 9	93 74	-397 56	-474 97	8 31	222 02
C (10)	458 39	1660 68	2352 24	5 16	301 87	146 58	-418 27	-1751 59	-11 9	-358 16

(7) Number of stay cable (N) = 11

Cable No	(b_o)	(b_1)	(b_2)	(b_3)	(b_{11})	(b_{22})	(b_{33})	(b_{12})	(b_{13})	(b_{23})
Group (1)										
C (1)	392 74	27 96	1628 33	1789 13	-439 51	1251 08	-5099 81	-1684 69	-596 41	2484 98
C (2)	143 31	15 64	234 32	726 77	-330 33	448 15	-2060 83	-661 69	-179 9	1079 99
C (3)	399 86	12 88	605 12	1702 14	-398 25	-119 3	-405 57	-1664 59	116 91	216 68
C (4)	545 46	16 33	631 46	2328 58	-452 72	-381 76	-342 26	-2270 74	252 2	185 23
C (5)	477 73	18 74	1370 32	2050 28	-418 21	-404 55	-503 27	-1985 11	256 43	152 41
C (6)	334 27	22 65	1190 82	1420 32	-385 31	-331 59	-421	-1378 57	210 42	117 41
C (7)	302 8	20 98	1719 85	1122 48	-360 54	-242 53	244 59	-1160 97	163 67	-290 91
C (8)	275 5	20 66	1801 24	966 56	-360 07	-239 98	514 25	-1026 5	161 83	-443 01
C (9)	282 83	7 17	1353 99	1011 49	-335 25	-279 6	574 84	-1069 56	192 42	-428 8
C (10)	247 8	2 26	3073 4	942 8	-451 93	-348 78	480 96	-960 53	239 13	-558 38
C (11)	182 95	-2 34	4150 17	775 36	-456 17	-474 2	13 52	-740 45	306 17	-464 97
Group (2)										
C (12)	269 46	-3 86	-775 68	1123 89	94 11	220 43	-114 75	-1109 01	-106 36	145 04
C (13)	82 66	9 47	-437 51	321 23	-4 45	316 5	242 81	-325 51	-163 74	-26 91
C (14)	-115 99	-7 06	677 09	-443 85	-14 09	355 95	-321 86	457 43	-161 31	84 55
C (15)	-235 14	-10 2	1031 28	-964 23	-28 81	447 18	-618 23	959 08	-198 81	169 13
C (16)	-389 33	-6 93	1318 98	-1569 12	-84 09	389 49	-538 53	1571 61	-166 09	101 23
C (17)	-441 54	-5 63	1594 82	-1801 7	-123 55	357 18	-329 5	1793 03	-144 29	-41 04
C (18)	-472 77	-3 05	1405 21	-1947 03	-214 61	306 77	-12 54	1922 85	-112 04	-149 04
C (19)	-428 11	1 09	1859	-1797 9	-296 84	246 36	511 51	1758 9	-76 95	-440 81
C (20)	-306 93	-0 02	1228 48	-1303 82	-340 4	138 12	927 62	1260 37	-14 52	-555 37
C (21)	-187 58	2 61	328 15	-815 36	-406 75	94 82	1174 24	767 02	11 36	-538 92
C (22)	-243 17	15 34	1168 43	-988	-242 83	247 11	-657 65	983 53	-89 23	218 88

(8) Number of stay cable (N) = 12

Cable No	(b_o)	(b_1)	(b_2)	(b_3)	(b_{11})	(b_{22})	(b_{33})	(b_{12})	(b_{13})	(b_{23})
Group (1)										
C (1)	416 54	22 36	1045 41	1824 5	-403 74	1318 04	-4489 96	-619 1	-1747 45	2140 17
C (2)	277 74	18 71	789 38	1114 85	-335 98	557 37	-2046 31	-241 29	-1119 73	1013 6
C (3)	354 12	13 02	1669 9	1523 36	-280 95	90 77	-1885 11	-1 24	-1471 52	798 45
C (4)	472 33	29 42	1000 43	1968 11	-313 25	-173 74	-933 81	120 06	-1929 55	400 17
C (5)	548 45	25 85	1376 28	2238 76	-373 34	-329 86	-225 93	208 52	-2217 99	-4 68
C (6)	543 61	19 84	902 87	2081 55	-313 54	-303 04	397 9	193 24	-2129 12	-279 23
C (7)	467 36	25 09	1509 12	1721 28	-343 33	-147 47	-34 89	109 38	-1790 18	-120 33
C (8)	494 57	20 22	1921 86	1785 13	-332 66	-123 2	-13 95	99 64	-1873 7	-185 96
C (9)	561 32	15 54	2041 32	2054 4	-348 77	-194 78	198 65	140 1	-2142 91	-303 21
C (10)	582 41	18 11	1410 86	2195 35	-468 74	-330 06	626 21	213 21	-2264 15	-400 79
C (11)	459 7	6 57	1762 13	1797 02	-389 4	-486 9	727	298 97	-1817 94	-525 48
C (12)	53 07	8 76	2660 72	322 09	-376 32	-722 76	1021 37	415 48	-258 53	-804 53
Group (1)										
C (1)	100 53	-8 13	-357 01	495 04	87 3	178 02	-161 63	-84 1	-450 02	106 4
C (2)	-81 24	-3 89	-586 51	-274 38	22 3	323 15	171 79	-152 5	292 86	4 45
C (3)	-209 01	-4 58	-572 18	-632 33	-25 26	225	-421 35	-101 85	730 51	303 98
C (4)	-279 19	-8 03	-124 46	-966 27	-80 14	246 92	-734 51	-104 62	1039 41	408 54
C (5)	-356 14	-7 35	4 74	-1302 23	-228 85	300 62	-735 68	-117 74	1354 83	437 51
C (6)	-462 02	-7 93	43 28	-1672 11	-348 58	267 47	-762 66	-89 23	1745 41	482 29
C (7)	-506	-1 6	507 8	-1921 24	-289 31	248 75	-469 37	-87 24	1967 63	244 33
C (8)	-477 22	2 78	216 88	-1837 34	-285 24	191 38	68 31	-59 12	1864 36	23 6
C (9)	-384 77	-0 11	1857	-1523 61	-344 46	145 89	439 46	-25 21	1528 02	-355 57
C (10)	-214 18	5 12	2185 41	-975 32	-391 95	66 22	1305 2	15 5	916 57	-834 52
C (11)	-237 64	7 32	706 36	-1014 57	-362 4	79 11	935 73	7 49	975 22	-489 02
C (12)	-401 91	2 96	248 06	-1537 94	-327 25	127 64	-177 51	-15 89	1560 89	135 52

(9) Number of stay cable (N) = 13

Cable No	(b_o)	(b_1)	(b_2)	(b_3)	(b_{11})	(b_{22})	(b_{33})	(b_{12})	(b_{13})	(b_{23})
Group (1)										
C (1)	81 46	248 71	-1484 58	-15 31	-375 74	867 95	6 74	-311 35	-398 9	387 12
C (2)	180 87	795 65	-618 81	9 16	-2227 98	598 27	-230 85	-773 8	-264 28	1250 11
C (3)	232 06	1107 34	-414 13	12 26	-2039 52	156 86	-350 94	-1040 47	-34 09	1194 88
C (4)	298 17	1330 67	-337 49	14 99	-1150 7	-115 97	-349 1	-1280 43	101 13	723 9
C (5)	347 66	1417 6	125 87	18 95	25 79	-297 87	-364 02	-1413 37	189 56	46 28
C (6)	359 9	1441 15	-45 39	16 37	403 4	-369 53	-294	-1446 83	222 15	-155 9
C (7)	341 08	1272 01	-252 76	9 02	704 83	-313 98	-374 54	-1333 58	206 5	-240 92
C (8)	331 19	1242 89	-336 62	5 77	463 86	-267 74	-390 38	-1300 96	186 06	-102 25
C (9)	343 27	1263 86	-282 58	5 49	496 15	-239 99	-364 93	-1332 95	169 76	-137 9
C (10)	384 18	1384 06	302 08	6 77	746 17	-262 15	-401 8	-1473 41	182 52	-315 85
C (11)	445 03	1571 41	768 67	2 94	1277 02	-313 28	-395 66	-1685 36	212 88	-662 43
C (12)	510 81	1736 5	1974 44	10 38	1565 64	-320	-402 2	-1884 56	207 45	-972 65
C (13)	594 99	1960 18	2881 14	16 01	2295 4	-389 48	-447	-2156 56	239 25	-1447 88
Group (2)										
C (1)	297 38	1059 39	-84 51	7 94	473 42	289 46	93 04	-1115 98	-155 76	-246 34
C (2)	142 68	552 24	1019 43	2 9	-260 2	362 81	-10 55	-555 6	-177 99	43 77
C (3)	42 71	234 53	1710 46	3 05	-674 15	336 42	-79 58	-193 92	-161 26	193 93
C (4)	-68 21	-222 92	1483 46	7 47	-773 1	359 48	10 86	261 47	-177 85	209 64
C (5)	-173 83	-593 24	1411 55	7 35	-729 61	301 52	-62 15	655 41	-141 99	208 38
C (6)	-295 75	-1150 36	1069 02	8 8	-619 78	339 76	-92 46	1175 74	-157 33	191 56
C (7)	-348 78	-1333 08	1601 53	-3 32	-373 08	278 24	-218 23	1366 42	-103 26	35 68
C (8)	-378 71	-1469 01	1771 61	7 72	-328 71	217	-172 28	1503 94	-84 07	-44 95
C (9)	-381 73	-1487 31	426 46	11 64	-92 17	212 36	-208 46	1504 58	-80 15	41 92
C (10)	-385 23	-1521 4	1186 67	10 34	235 49	114 29	-243 35	1532 83	-25 59	-218 94
C (11)	-343 16	-1345 81	1627 3	11 02	587 92	73 39	-302 15	1359 92	-0 01	-425 18
C (12)	-178 82	-732 64	1315 23	15 78	819 06	22 15	-380 83	718 47	28 07	-466 75
C (13)	-13 68	-204 48	2045 91	4 87	266 33	119 64	-539 08	114 08	5 31	-226 82

APPENDIX II

DESIGN PROVISIONS PROVIDED BY THE CANADIAN HIGHWAY BRIDGE CODE

- **Notation for material properties**

E_s = Modulus of elasticity of steel.

v_s = Poisson's ratio of steel.

f_y = Yield strength of steel.

f_c' = Compressive strength of concrete.

- **Resistance factors**

According to clause 10.5.7, [CAN/CSA-S6-06], resistance factors shall be taken as follows:

flexure, $\phi_s = 0.95$;

shear, $\phi_s = 0.95$

compression, $\phi_s = 0.90$;

tension, $\phi_s = 0.95$;

tension in cables, $\phi_{tc} = 0.55$;

reinforcing steel in composite construction, $\phi_r = 0.90$;

concrete in composite construction, $\phi_c = 0.75$.

- **Positive bending moment, clause 10.11** [CAN/CSA-S6-06]

The factored moment resistance of the deck section in bending shall be computed using a fully plastic stress distribution, as shown in Figs. II(a) and II(b).

C_{rSlab} = factored compressive resistance of slab = $C_{rConcrete} + C_{rRFT}$

$C_{rConcrete}$ = factored compressive resistance of concrete = $0.85\phi_C b_e t_{Slab} f'_c$

where,

b_e = effective width of concrete slab = $2b\left(1-\left\{1-\frac{L}{15b}\right\}^3\right)+B_{FT}$, clause 5.8.2.1 [CAN/CSA-S6-06].

L = the distance between two stay cables.

b = distance between the two steel main girders.

B_{FT} = the top flange width.

t_{Slab} = thickness of concrete slab.

C_{rRFT} = factored compressive resistance of reinforcement steel $\phi_r A_{RFT} f_y$.

where,

A_{RFT} = area of reinforcing steel within the effective width of a concrete slab.

C_{rMG} = factored compressive resistance of structural steel = $\phi_s A_s F_y$.

A_s = area of steel main girder.

- Case (a)

Plastic neutral axis in concrete

(Class 1, 2 and 3)

When $C_{rSlab} \geq C_{MG}$, the plastic neutral axis in the concrete slab as show in Fig. IIa, and the depth of the compressive stress block, (a), shall be computed from:

$$a = \frac{C_{MG} - \phi_r A_{rRFT} f_y}{0.85 \phi_c b_e f'_c}$$

and the factored moment resistance of the section shall be computed from

$$M_{rDeck} = C_{rConcrete} e_c + C_{rRFT} e_r$$

where

$$C_{rConcrete} = 0.85 \phi_c b_e a f'_c$$

$$C_{rRFT} = \phi_r A_{RFT} f_y$$

- Case (b)

Plastic neutral axis in steel

Class (1 and 2) and Class (3) if the compression portion of the web of the steel section $\leq$ $\left(850 t_{web} / \sqrt{F_y}\right)$

When $C_{rSalb} < C_{rMG}$, the plastic axis is in the web as shown in Fig. II(b), and the depth of the compressive stress block, a, shall be taken as equal to t_{Slab} and the factored moment resistance shall be computed from:

$$M_{rDeck} = C_{rConcrete} e_c + C_{rRFT} e_r + C_s e_s$$

where

$$C_{rConcrete} = 0.85 \phi_c b_e t_{Salb} f'_c$$

$$C_{rRFT} = \phi_r A_{RFT} f_y$$

$$C_s = 0.5 (C_{rMG} - C_{rSlab})$$

$$C_{rMG} = \phi_s A_s F_y$$

$$C_{rSlab} = C_{rConcrete} + C_{rRFT}$$

$$C_{rRFT} = \phi_r A_{RFT} f_y$$

(Class 3)

if the compression portion of the web of the steel section $> \left(850 t_{web} / \sqrt{F_y}\right)$, Fig. II(c).

$$M_{rDeck} = C_{rConcrete} e_c + C_{rRFT} e_r + C_s e_s$$

where

$$C_{rConcrete} = 0.85 \phi_c b_e t_{Salb} f'_c$$

$$C_{rRFT} = \phi_r A_{RFT} f_y$$

$$C_s = \varphi_s A'_{sc} F_y$$

$$A'_{sc} = \frac{C_{rConcrete} + C_{RFT} + C_s}{\varphi_s F_y}$$

- **Negative bending moment**

Class (1 and 2), Fig. II(d).

$$M_{rDeck} = T_{rRFT} e_r + T_s e_s$$

where

$$T_{rRFT} = \phi_r A_{rRFT} f_y$$

$$T_s = 0.5(C_{rMG} - T_{rRFT})$$

$$C_{rMG} = \phi_s A_s F_y$$

Class (3), Fig. II(e).

$M_{rDeck} = T_{rRFT} e_r + T_s e_s$

- **Axial tensile force**

$T_{rDeck} = T_{rRFT} + T_{rMG}$

T_{rRFT} = factored tensile resistance of slab reinforcement = $\phi_r A_{RFT} f_y$

T_{rMG} = factored tensile resistance of structural steel = $\phi_s A_s F_y$

A_{RFT} = area of reinforcing steel within the effective width of a concrete slab.

As = area of the steel main girders

- **Axial compression force**

The upper compression flanges are supported laterally by the deck slab.

The lower compression flanges are supported laterally by a horizontal bracing.

The design of the lower bracing is not included in the current study, but its own weight is considered.

Class (1)

C_{rDeck} = factored compressive resistance of the deck = $C_{rSlab} + C_{rMGStrength}$

C_{rSlab} = factored compressive resistance of slab = $C_{rConcrete} + C_{rRFT}$

$C_{rMGStrength}$ = factored over all compressive resistance of structural steel

$= \phi_s A_s F_y (1 + \lambda^{2n})^{-1/n}$, clause 10.9.3.1 [CAN/CSA-S6-06]

where

$$\lambda = \frac{KL}{r}\sqrt{\frac{F_Y}{\pi^2 E_s}}$$

$n = 2.24$

K = effective length factor.

L = Length.

r = radius of gyration $\sqrt{I/A}$

$U_{1x} = \dfrac{0.85\omega_{1x}}{1 - \dfrac{C_{fDeck}}{C_{ex}}}$, clause 10.9.4.2 [CAN/CSA-S6-06].

where,

$\omega_1 = 1.0$

C_{ex} = Euler buckling load.

Class (2 and 3)

C_{rDeck} = factored compressive resistance of the deck = $C_{rSlab} + C_{rMGStrength}$.

C_{rSlab} = factored compressive resistance of slab = $C_{rConcrete} + C_{rRFT}$.

$C_{rMGStrength}$ = factored over all compressive resistance of structural steel

$$= \phi_s A_s F_y (1 + \lambda^{2n})^{-1\ n}$$

where

$$\lambda = \frac{KL}{r}\sqrt{\frac{F_Y}{\pi^2 E_s}}$$

$n = 2.24$

K = effective length factor

L = Length

r = radius of gyration= $\sqrt{I/A}$

$$U_{1x} = \frac{\omega_{1x}}{1 - \frac{C_{fDeck}}{C_{ex}}}$$

where,

$\omega_1 = 1.0$

C_{ex} = Euler buckling load.

- **Interaction Diagram**

The interaction diagram is computed using a fully plastic stress distribution [CAN/CSA-S6-06], Fig. II(f).

- **Shear force,** clause 10.10.5 [CAN/CSA-S6-06]

V_{rDeck} = factored shear resistance of the web steel main girder = $\phi_s A_w F_s$

A_w = web area = $h_w t_w$

h_w and t_w are the height and the thinness of the main girder web

F_s = shear stress = $F_{cr} + F_t$

The spacing between transverse stiffeners (a) is assumed equal to height of main girders webs (h_w)

$k_v = 9.3$

Case (1)

$$\frac{h_w}{t_w} \le 502\sqrt{\frac{k_v}{F_y}}$$

$F_{cr} = 0.577\,F_y$ and $F_t = 0$

Case (2)

$$502\sqrt{\frac{k_v}{F_y}} \le \frac{h_w}{t_w} \le 621\sqrt{\frac{k_v}{F_y}}$$

$$F_{cr} = \frac{290\sqrt{F_y k_v}}{h_w / t_w} \text{ and } \mathrm{F_t} = (0.5\mathrm{F_y} - 0.866\mathrm{F_{cr}})\left(\frac{1}{\sqrt{1+(\mathrm{a}/\mathrm{h_w})^2}}\right)$$

Case (3)

$$\frac{h_w}{t_w} \le 621\sqrt{\frac{k_v}{F_y}}$$

$$F_{cr} = \frac{180000k_v}{(h_w / t_w)^2} \text{ and } \mathrm{F_t} = (0.5\mathrm{F_y} - 0.866\mathrm{F_{cr}})\left(\frac{1}{\sqrt{1+(\mathrm{a}/\mathrm{h_w})^2}}\right)$$

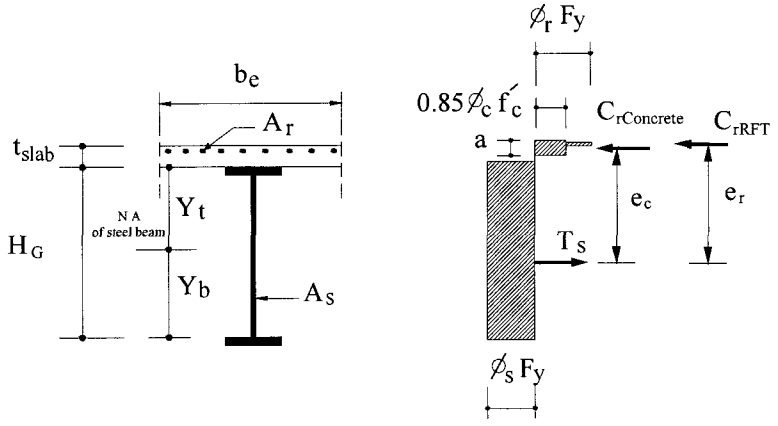

Fig. II(a) Plastic neutral axis in the concrete slab.

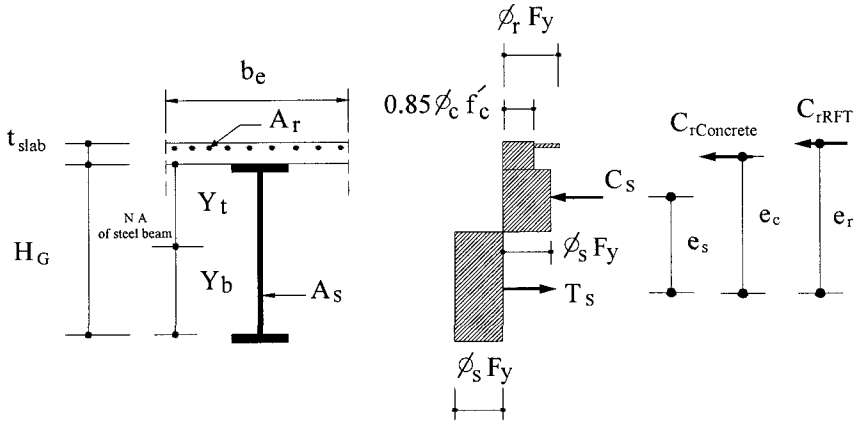

Fig. II(b) Plastic neutral axis in the steel section.

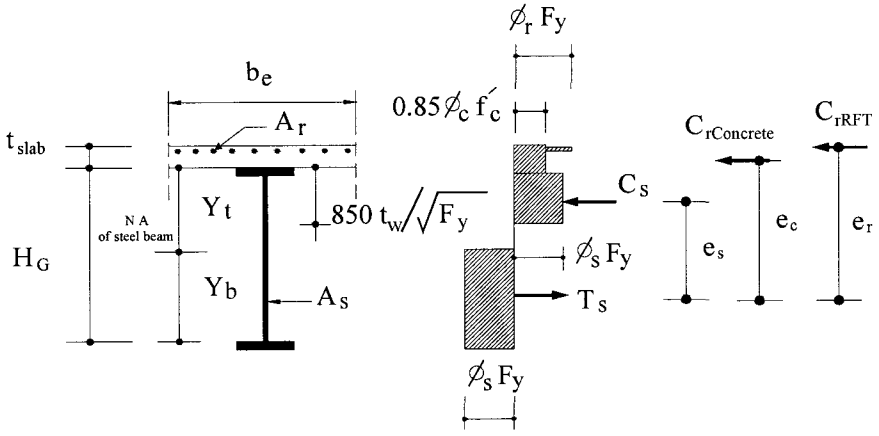

Fig. II(c) Positive bending moment (class 3).

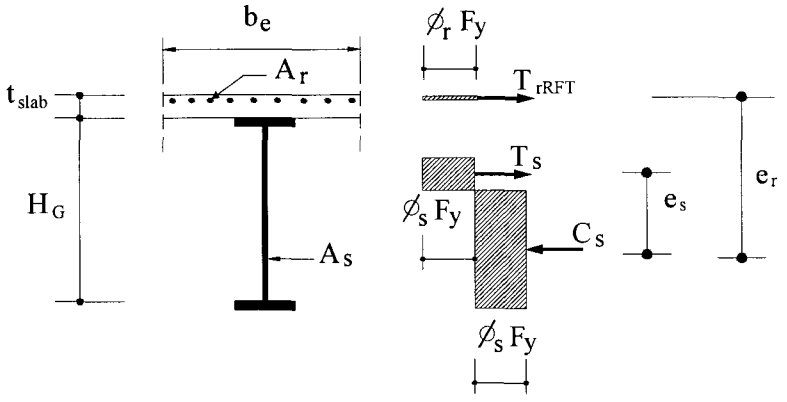

Fig. II(d) Negative bending moment.

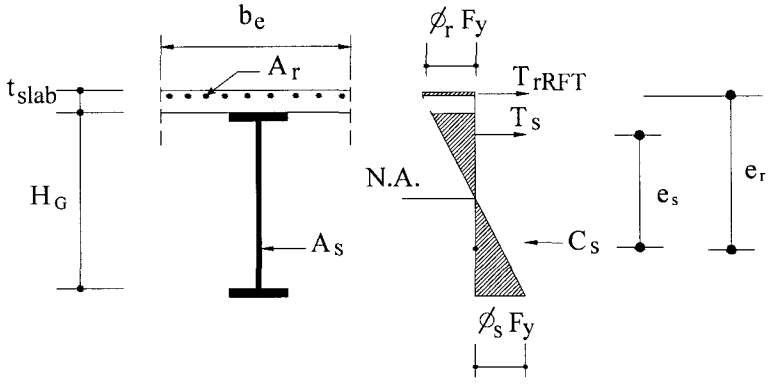

Fig. II(e) Negative bending moment (class 3).

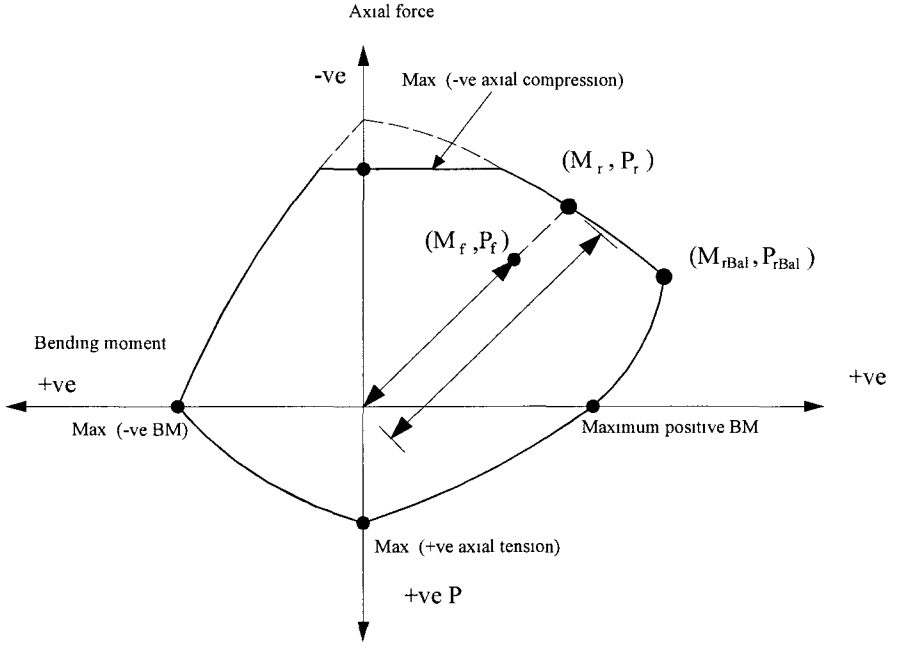

Fig. II(f). Interaction diagram of deck.

CURRICULUM VITAE

Name:	Mahmoud Mohamed Ibrahim Hassan
Place of birth:	Port-Said, Egypt
Year of birth:	July 26, 1975
Post-secondary Education and Degrees:	B.Sc. 1993-1998 Civil Engineering Department, Structural Division Suez Canal University, Port-Said, Egypt M.Sc. 1999-2002 Civil Engineering Department, Structural Division Suez Canal University, Port-Said, Egypt Ph.D. 2006-2010 The University of Western Ontario London, Ontario, Canada
Honours And Awards:	Governmental Scholarship - 2006 to 2010 Graduate Merit fellowship - 1999 to 2002 Undergraduate Merit scholarship - 1993 to 1998
Academic Appointments:	Teaching and Research Assistant Civil and Environmental Engineering Department The University of Western Ontario, London, Ontario, Canada May 2006 to July 2010 Teaching and Research Assistant Faculty of Engineering Suez Canal University, Port-Said, Egypt January 1999 to April 2006

Professional Appointments:

Part-time design engineer
O/A Engineering Analysis and Dynamics, London, Ontario, Canada

Part-time design engineer
O/A Value Engineering Association, London, Ontario, Canada

Part-time design engineer
El Arabi Engineering Consultants, Port Said, Egypt.

Publications:

Refereed Journals

Hassan, M, El Arabi, I., El Gendy, M. and Ibrahim, F.K.,"Stability of Frames Considering Soil-Structure Interaction", *Engineering Research Bulletin, Faculty of Engineering and Tech., Helwan University, Matarya, Cairo, Vol.79, 2002.*

Hassan, M., Ibrahim, F.K., El Arabi, I. and El Gendy, M., "Stability of Cracked Frames Resting on Perfect Elastic Foundations", *Port Said Engineering Research Journal (PSERJ), Faculty of Engineering, Suez Canal University, Vol.6, No. 1, 2002.*

Conference Proceedings

Hassan, M., Nassef, A. and El Damatty, A. A., "A Coupled Optimization/Finite Element Model for the Design of Cable Stayed Bridges", *Proceedings of the 37th Annual General Conference of the Canadian Society for Civil Engineering*, CSCE, Quebec City, Quebec, Canada, 2008.

Hassan, M., Ibrahim, F.K., El Gendy, M. and El Arabi, I, "Stability of Frames with Cracked Foundation Elements and Resting on Elastic Soil", *2nd Minia International Conference for Advanced Trends in Engineering, 2002.*